

INFORMATION TO USERS

This was produced from a copy of a document sent to us for microfilming. While the most advanced technological means to photograph and reproduce this document have been used, the quality is heavily dependent upon the quality of the material submitted.

The following explanation of techniques is provided to help you understand markings or notations which may appear on this reproduction.

1. The sign or "target" for pages apparently lacking from the document photographed is "Missing Page(s)". If it was possible to obtain the missing page(s) or section, they are spliced into the film along with adjacent pages. This may have necessitated cutting through an image and duplicating adjacent pages to assure you of complete continuity.
2. When an image on the film is obliterated with a round black mark it is an indication that the film inspector noticed either blurred copy because of movement during exposure, or duplicate copy. Unless we meant to delete copyrighted materials that should not have been filmed, you will find a good image of the page in the adjacent frame.
3. When a map, drawing or chart, etc., is part of the material being photographed the photographer has followed a definite method in "sectioning" the material. It is customary to begin filming at the upper left hand corner of a large sheet and to continue from left to right in equal sections with small overlaps. If necessary, sectioning is continued again—beginning below the first row and continuing on until complete.
4. For any illustrations that cannot be reproduced satisfactorily by xerography, photographic prints can be purchased at additional cost and tipped into your xerographic copy. Requests can be made to our Dissertations Customer Services Department.
5. Some pages in any document may have indistinct print. In all cases we have filmed the best available copy.

University
Microfilms
International

300 N. ZEEB ROAD, ANN ARBOR, MI 48106
18 BEDFORD ROW, LONDON WC1R 4EJ, ENGLAND

HSU, CHUN-CHIN

PROPYLENE METATHESIS WITH RHENIUM-OXIDE SUPPORTED BY
GAMMA-ALUMINA AS CATALYST, INCLUDING KINETIC AND INITIAL
REACTION STUDIES

The University of Oklahoma

PH.D.

1980

University
Microfilms
International

300 N. Zeeb Road, Ann Arbor, MI 48106

18 Bedford Row, London WC1R 4EJ, England

THE UNIVERSITY OF OKLAHOMA
GRADUATE COLLEGE

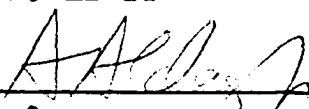
PROPYLENE METATHESIS WITH RHENIUM OXIDE SUPPORTED
BY γ -ALUMINA AS CATALYST, INCLUDING KINETIC
AND INITIAL REACTION STUDIES

A DISSERTATION
SUBMITTED TO THE GRADUATE FACULTY
in partial fulfillment of the requirement for the
degree of
DOCTOR OF PHILOSOPHY

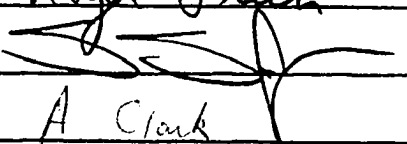
BY
CHUN-CHIN HSU
Norman, Oklahoma
1980

PROPYLENE METATHESIS WITH RHENIUM OXIDE SUPPORTED
BY γ -ALUMINA AS CATALYST, INCLUDING KINETIC
AND INITIAL REACTION STUDIES

APPROVED BY



Roger Fresh


A Clark

DISSERTATION COMMITTEE

ABSTRACT

The most stable activity of the $\text{NH}_4\text{ReO}_4/\gamma\text{Al}_2\text{O}_3$ catalyst is obtained at about 50°C reaction temperature, and the highest activity is obtained at about 100°C reaction temperature. The break-in period observed at 0°C is due to the reduction of the catalyst by propene and the formation of organometallic complex, and this break-in period will probably be observed below 8°C . The reaction, and deactivation rates are first order with respect to the active site density. The break-in rate is first order with respect to the adsorption active site density.

There are seven catalysts studied, i.e., $\text{NH}_4\text{ReO}_4/\gamma\text{Al}_2\text{O}_3$, $\text{NH}_4\text{ReO}_4/\text{TiO}_2$, $\text{NaReO}_4/\gamma\text{Al}_2\text{O}_3$, $\text{NH}_4\text{ReO}_4/3\text{A(K) zeolite}$, $\text{NH}_4\text{ReO}_4/3\text{A(Ca) zeolite}$, $\text{NH}_4\text{ReO}_4/13\text{X(Na) zeolite}$, and $\text{NH}_4\text{ReO}_4/13\text{X(Ca) zeolite}$. The standard catalyst, $\text{NH}_4\text{ReO}_4/\gamma\text{Al}_2\text{O}_3$, has the highest activity among these seven catalysts. The sodium and potassium ions have negative effect on the activity if zeolite is used as support or NaReO_4 is used as promoter. Bronsted acids adjacent to the adsorption site have a promotion effect on the activity.

The result of surface titration study with ethylene, the high ratio of ethylene to butenes at the beginning, and

the temperature programmed desorption effect on reaction suggest that the carbene mechanism is more reasonable for describing the metathesis reaction. When trans-2-butene is used as the reactant, the result also suggests that carbene mechanism is more reasonable; otherwise the product distribution can not be interpreted.

Temperature programmed desorption studies indicate that both the overall catalyst and the individual adsorption sites are energetically heterogeneous. Due to the adsorption of a mixture, readsorption during TPD run, and migration during TPD run, exact quantitative data are difficult to obtain from the TPD technique. For example, only the rough average value of the heat of desorption may be obtained instead of the exact value.

ACKNOWLEDGMENT

The author would like to express his sincere gratitude and appreciation to Dr. A.W. Aldag for his advice, guidance, and encouragement throughout this research.

The author is also grateful to the committee members, Dr. A. Clark, Dr. S.S. Sofer, and Dr. R.E. Frech, for their interest in this research and review of the work.

Thanks are due to Dr. J.C. Hsu for his assistance throughout this research and Mr. K. Hudson for his technical assistance.

The financial support by the National Science Foundation is gratefully acknowledged.

The author also wishes to thank his parents and wife for their encouragement.

CONTENTS

	Page
LIST OF TABLES.....	viii
LIST OF FIGURES.....	xi
 CHAPTER	
I. INTRODUCTION.....	1
II. EXPERIMENTAL.....	16
III. RESULTS.....	22
I. Effect of Reaction Temperature.....	22
II. Effect of Sources for Support and Promoter	36
III. Study of Mechanism Via Pulse Technique....	46
IV. Temperature Programmed Desorption Study...	86
V. Specific Poison by CO ₂ and NH ₃	102
IV. DISCUSSION.....	107
I. Rate Equations of The Kinetic Study.....	107
II. Break-in and Deactivation.....	112
III. Effect of Sources for Support and Promoter	114
IV. The Effect of Bronsted Acid.....	117
V. Temperature Programmed Desorption Studies.	120
VI. Mass Transfer Effect.....	123

VII.	Reaction Mechanism.....	129
VIII.	Determination of Kinetic Parameters from Pulse Study.....	141
V.	CONCLUSION.....	147
VI.	BIBLIOGRAPHY.....	151

TABLES

1. Illustration of Time Dependent Conversion at Different Reaction Temperature.....	31
2. Result of Correlation.....	34
3. TPD Results Obtained After Flow System Kinetic Study.....	35
4. Comparison of Activities with Different Sources for Support and Promoter.....	39
5. Mass Balance Table for Injection of 5 Pulses P at 24°C, 34ml/min, 0.2 cm Bed, 7.76 micro-gmole/ pulse.....	50
6. Mass Balance Table for 5 Pulses P at 24°C, 34ml/ min, 0.2 cm Bed, 14.8 micro-gmole/pulse.....	53
7. Mass Balance for 5 Pulses P at 24°C, 13 ml/min, 0.2 cm Bed, 7.76 micro-gmole/pulse.....	55
8. Mass Balance for 5 Pulses P at 0°C, 34 ml/min, 0.2 cm Bed, 7.76 micro-gmole/pulse.....	59
9. Mass Balance for 5 Pulses P at 0°C, 13 ml/min, 0.2 cm Bed, 7.76 micro-gmole/pulse.....	61
10. Mass Balance for 5 Pulses P at 24°C, 34 ml/min, 0.55 cm Bed, 7.76 micro-gmole/pulse.....	64

11.	Mass Balance for 5 Pulses P at 24°C, 34 ml/min, 0.55 cm Bed, 14.8 micro-gmole/pulse.....	66
12.	Mass Balance for 5 Pulses TB2 at 24°C, 34 ml/min, 0.2 cm Bed, 7.76 micro-gmole/pulse.....	69
13.	Mass Balance for 5 Pulses at 0°C, 34 ml/min, 0.2 cm Bed, 7.76 micro-gmole/pulse.....	71
14.	One Pulse Study with P at 24°C.....	73
15.	One Pulse Study with P at 0°C.....	74
16.	One Pulse Study with P at 24°C, and 0.55 cm Bed....	75
17.	One Pulse Study with TB2 at 24°C, 34 ml/min.....	77
18.	Surface Titration Study with 1P-5E at 24°C.....	79
19.	Surface Titration Study with 1P-5E-1P at 24°C.....	82
20.	Surface Titration Study with 2P-7E-2P at 0°C.....	84
21.	Comparison of TPD Results with Different Pre- adsorption and TPD Conditions.....	88
22.	Comparison of Peak Maximum Temperature Obtained from TPD with Different Preadsorption Conditions...	92
23.	Effect of Temperature Increasing Rate on The Desorbed Species.....	94
24.	Comparison of Desorbed Species when TPD Stops at Different Temperatures	97
25.	Comparison of Peak Maximum Temperature and Heat of Desorption at Different Bed Thicknesses.....	99
26.	CO ₂ Adsorption Amount.....	101
27.	Effect of CO ₂ Pretreatment at 24°C on Reaction at 24°C.....	104

28.	Effect of CO ₂ Pretreatment at 24°C on Reaction at 0°C.....	105
29.	Rate Equations Obtained from Kinetic Data.....	110

FIGURES

1. Flow Diagram of The Equipment.....	18
2. Kinetic Study at 0°C.....	23
3. Kinetic Study at 25°C.....	24
4. Kinetic Study at 50°C.....	25
5. Kinetic Study at 103°C.....	26
6. Kinetic Study at 203°C.....	27
7. Comparison of The Kinetic Data on The Same Scale...	32
8. Comparison of Activity at Different Reaction Temperature and Time.....	37
9. Activity Comparison of $\text{NH}_4\text{ReO}_4/\text{TiO}_2$ and $\text{NH}_4\text{ReO}_4/13\text{X}(\text{Ca})$ zeolite.....	43
10. Activity Comparison of $\text{NH}_4\text{ReO}_4/3\text{A}(\text{Ca})$ at Different Activation and Reaction Temperatures.....	44
11. Activity Comparison of $\text{NH}_4\text{ReO}_4/\text{Al}_2\text{O}_3$, $\text{NH}_4\text{ReO}_4/3\text{A}(\text{Ca})$ and $\text{NH}_4\text{ReO}_4/13\text{X}(\text{Ca})$ at Different Activation and Reaction Temperatures.....	45
12. Pulse Study with 0.2 cm Bed at 24°C, 7.76 micro- gmole/pulse, 34 ml/min.....	49
13. Pulse Study with 0.2 cm Bed at 24°C, 34 ml/min, 14.8 micro-gmole/pulse.....	52

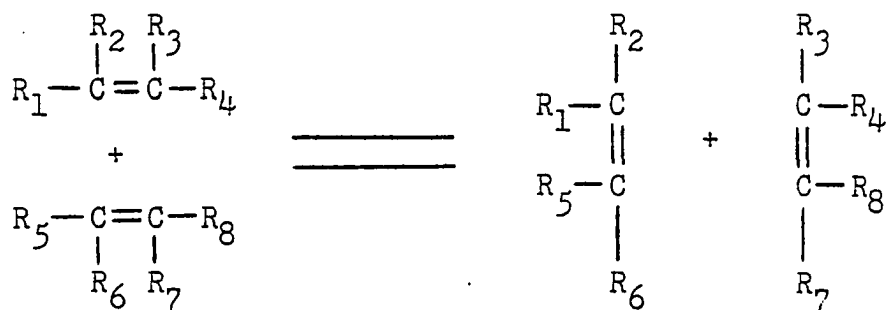
14.	Pulse Study with 0.2 cm Bed at 24°C, 13 ml/min and 7.76 micro-gmole/pulse.....	54
15.	Pulse Study with 0.2 cm Bed at 0°C, 34 ml/min, 7.76 micro-gmole/pulse.....	58
16.	Pulse Study with 0.2 cm Bed at 0°C, 13 ml/min, 7.76 micro-gmole/pulse.....	60
17.	Pulse Study with 0.55 cm Bed at 24°C, 34 ml/min, 7.76 micro-gmole/pulse.....	63
18.	Pulse Study with 0.55 cm Bed at 24°C, 34 ml/min, 14.8 micro-gmole/pulse.....	65
19.	Pulse Study with 0.2 cm Bed at 24°C, 34 ml/min, 7.76 micro-gmole TB2/pulse.....	68
20.	Pulse Study with 0.2 cm Bed at 0°C, 34 ml/min, 7.76 micro-gmole TB2/pulse.....	70
21.	Illustration of TPD Chromatogram.....	91
22.	Illustration of Migration During TPD Run.....	95
23.	TPD Chromatogram of CO ₂ Desorption.....	100
24.	Effect of TPD on The Next Pulse Reaction.....	103
25.	Superimposition Effect on The Deactivation.....	111
26.	Critical Active Site Concentration Effect on The Production of TB2.....	132
27.	Superimposition Effect of Active Sites Generated By Oxygen Regeneration and By Reduction.....	133

PROPYLENE METATHESIS WITH RHENIUM OXIDE SUPPORTED
BY γ -ALUMINA AS CATALYST, INCLUDING KINETIC
AND INITIAL REACTION STUDIES

CHAPTER I

INTRODUCTION

Banks and Bailey(1) applied molybdenum hexacarbonyl, tungsten hexacarbonyl, and molybdenum oxide supported by alumina as catalysts to the olefin reaction system and found the disproportionation reaction. By this reaction, linear olefins were converted into equal amounts of shorter and longer chains of olefins and may be characterized as:



where R_1 to R_8 represent hydrogen or hydrocarbon groups. Olefin dismutation(2) and olefin metathesis(3) are terms also commonly used by other researchers.

There are homogeneous and heterogeneous metathesis reactions and the latter is of more interest to this study. The catalysts for heterogeneous metathesis are mainly transition metal oxides, carbonyls, and sulfides deposited on high surface area supports like silica and alumina. (4) Some of the heterogeneous metathesis studies have been carried out with WO_3/SiO_2 (5), $\text{MoO}_3/\text{Al}_2\text{O}_3$ (6), and $\text{Mo}(\text{CO})_6/\text{Al}_2\text{O}_3$ (7) catalysts. Recently there has been an increasing interest in the $\text{Re}_2\text{O}_7/\text{Al}_2\text{O}_3$ catalyst. The $\text{Re}_2\text{O}_7/\text{Al}_2\text{O}_3$ catalyst is well known for its selectivity and activity even at ambient temperature and subatmospheric pressure (4). The rhenium containing catalyst has also been used in hydrogenation reactions (8) and automobile exhaust system (9).

There are three kinds of mass transfer effects, interphase, intraparticle, and site-localized diffusion effects, proposed for the olefin metathesis (10). The interphase mass transfer effects have been observed in propene disproportionation with WO_3/SiO_2 catalyst. (10) If the mass transfer effects exist, the reaction rate will be a function of the amount of the catalyst used, the particle size of the catalyst, and the concentration of the promoter. Usually, the interphase and the intraparticle mass transfer effects may be tested by changing the amount of the catalyst used and the particle size respectively, while keeping the space velocity at a constant value. Lin et al. (11) found that the reaction on a 20% $\text{Re-Al}_2\text{O}_3$ catalyst was mass transfer

limited, but the mass transfer effect was not observed with 10% Re-Al₂O₃ catalyst.

The heterogeneous metathesis reactions show a maximum in rate with respect to the reaction temperature (12,13). Clark and Moffat (12) ascribed this rate-temperature maximum to the result of superimposition of reversible deactivation of sites and the irreversible poisoning of sites. They also found that the criterion for the existence of such maxima is that the absolute value of the heat of adsorption must be greater than 1/2 of the Arrhenius activation energy.

The time on stream activity of an activated catalyst usually contains three periods: break-in, steady state, and deactivation (5). The break-in may be due to the reduction of the catalyst by olefin and the formation of organometallic complex between the olefin and catalyst. The deactivation may be ascribed to poisoning by impurities, poisoning by high molecular weight products and coke, loss of surface area, sintering, and structure changes of the catalyst. Wills and Luckner (5) proposed that within the steady state region the catalyst was WO_{2.9} compared with the WO₃ of the activated catalyst. Therefore, the catalyst was reduced during the break-in period. However, the break-in was still observed on the prereduced catalyst and was ascribed to the irreversible adsorption and the formation of an organometallic complex. Banks and Pennella (14) proposed that the olefin metathesis over the WO₃/SiO₂ catalyst occurs through the pro-

motion of electrons from olefin π -orbital to the level of olefin anti-bonding π^* -orbital. Therefore, the catalytic activity may be a function of the energy level of the metal which may be adjusted by changing the oxidation state of the metal ion or by changing the number and geometry of the ligands. They suggested that the number of active sites may be increased through modification by the polyolefins of the energy level distribution. Furthermore, adding a small amount of polyolefin may shorten the break-in period. Castellano et al. (15) proposed that the metathesis activity was related to the presence of Mo(V) species originating from reduction of the catalyst when $\text{MoO}_3/\text{Al}_2\text{O}_3$ was used. Andreev (16) proposed that the reduction occurred when the $\text{Re}_2\text{O}_7/\text{Al}_2\text{O}_3$ catalyst contacted propene and the reflectance spectra showed the existence of Re(VI).

It is believed that after calcination of the catalyst some kind of reaction occurs between the promoter and the support. Fridman et al. (17) showed that NH_4ReO_4 decomposes in the temperature interval 580-750°K, while no apparent change was observed with pure $\gamma\text{-Al}_2\text{O}_3$ except loss. The method applied was the differential thermal analysis. However, a peak was observed above 1120°K instead of between 580-750°K if $\text{NH}_4\text{ReO}_4/\text{Al}_2\text{O}_3$ was used as a sample. This may suggest a strong interaction between the rhenium and the support. Based on XPS studies, Minachev et al. (18) proposed that it is more difficult to reduce $\text{HReO}_4/\gamma\text{-Al}_2\text{O}_3$ than to

reduce $\text{HReO}_4/\text{SiO}_2$. They attributed this difference to the strong interaction of Re^{+7} to the alumina surface. LeRoy and Johnson (19) concluded from X-ray diffraction, IR, and ESR studies that the rhenium in Pt/Re/alumina may only be reduced to Re^{+4} instead of Re^0 . Echigoya and Nakamura (20) suggested that there are three types of active sites on the catalyst (K, L, and M) and the activity is enhanced by a doubly-promoting effect of Re ions. They classified the compositions of the K, L, and M sites as: $\text{Re}/\text{Al} < 1/99$, $1/99 \leq \text{Re}/\text{Al} \leq 3/97$, and $\text{Re}/\text{Al} > 3/97$ respectively. The activity for olefin metathesis increased in the order: $\text{M} > \text{L} > \text{K}$. X-ray spectrum suggested that the active sites in the M region was comprized of Re-O-Re bonds which were so weak that they could be easily converted to active sites by activation at elevated temperature and the reduction and complexation with olefins. The L region was comprized of Re-O-Al bonds without doubly-promoting effect. The activity of the K region could be enhanced only when reduced with hydrogen. Martinotti et al. (21) found that the catalyst structure differed from the bulk MoO_3 structure if the catalyst was supported by Al_2O_3 . They also proposed that the structure depended on the promoter concentration and the acidity of the catalyst. The structure changed from tetrahedral oxomolybdenum to mixed tetrahedral-octahedral to the formation of $\text{Al}_2(\text{MoO}_4)_3$ with increasing concentration of MoO_3 .

The metathesis reaction is always accompanied by the

isomerization reaction (2). By suitably choosing the reaction conditions and/or adjusting the catalyst acidity, the isomerization activity may be suppressed (2,22). Using a deuterated acid catalyst such as silica-alumina to study the isomerization of 1-butene, Kimura and Ozaki (23) found that the concentration of deuterated 2-butenes was much higher than that of the deuterated 1-butene when the evacuation temperature was near 100°C. The concentration of deuterated 2-butenes decreased with increasing evacuation temperature, although the conversion increased with increasing evacuation temperature. On the other hand, if the reaction was carried out with a non-deuterated acid catalyst and 1-butene in the presence of deuteropropene then the concentration of deuterated 2-butenes predominated again even if the evacuation temperature was 500°C. Thus, this reaction proceeded, at least partly, through a proton donor-acceptor mechanism with either a Bronsted acid on the surface or the carbonium ions formed by adsorption of olefins on Lewis acids. Brouwer (24) studied the double-bond isomerization of olefins on acid catalysts and concluded that cis-olefins usually were formed in preference over trans-olefins. He also proposed that the product distribution depended upon the property of the catalyst and both the cis- and trans-olefins were primary products.

With rhenium, Anion vacancies were formed upon reduction by hydrogen or carbon monoxide (16,26) or upon the evacuation at high temperature (23). Andreev et al. (16) proposed an

an F-center for a shuttle mechanism in which the production of Re^{+7} -F center and the production of Re^{+6} -anion vacancy became a cyclic process to generate metathesis activity. In this mechanism the anion vacancy served as an electron trap. Hall et al. (26) demonstrated that the catalytic activity for cyclopropane decomposition increased with anion vacancy concentration and the Bronsted sites of alumina OH groups were close to that of the anion vacancy. Engelhardt (25) found that the activity of $\text{MoO}_3/\text{Al}_2\text{O}_3$ for metathesis increased with hydrogen reduction. However, the activity was negligible if the catalyst was reduced at high temperature (550°C). He attributed this observation to the different types of adsorbed hydrogen.

Turner et al. (2) demonstrated that the metathesis of 1-butene over $\text{CoO}/\text{MoO}_3/\text{Al}_2\text{O}_3$ catalyst may be made highly selective to ethylene plus hexene-3 or propene plus pentene by suitable choice of reaction conditions or by poisoning the catalyst with controlled amounts of sodium ion. They also found that the selectivity increased with increasing NaHCO_3 concentrations, but that the metathesis conversion decreased. Swift et al. (22) showed that the addition of thallium to alumina reduced the surface acidity and inhibited the double bond isomerization. They also showed that the addition of thallium to $\text{MoO}_3/\text{Al}_2\text{O}_3$ resulted in a high selectivity for olefin metathesis. There was a relationship between this selectivity and the ionic radius of monovalent thallium and

group Ia ions which was $\text{Cs} > \text{Rb} > \text{Tl} > \text{K} > \text{Na} > \text{Li}$. These results suggest the idea of using NaReO_4 for the promoter instead of NH_4ReO_4 .

Garten et al.(27) found that TiO_2 was a better support than Al_2O_3 and SiO_2 for the Ni catalyst in CO/H_2 synthesis reactions. They showed that this substitution resulted in high activity, high selectivity to high molecular weight products, and a slow deactivation rate. Clark et al. (11) indicated that a SiO_2 supported rhenium oxide catalyst was easier to be reduced than an Al_2O_3 supported catalyst and the SiO_2 supported catalyst needed higher reaction temperature. Pott(28) showed the catalyst life was five times longer if the catalyst was mixed with 3A molecular sieve at the ratio of one gram catalyst and four grams molecular sieve. These results propose the idea of using TiO_2 or molecular sieve as support instead of Al_2O_3 or SiO_2 .

There are two types of metathesis reaction: the first one is transalkylation, the second is transalkylidenation (29). The transalkylation type reaction was first proposed by Mol et al.(31). The transalkylation type reaction was first proposed by Turner et al.(2) and a quasi-cyclobutane intermediate was suggested. The transalkylidenation type reaction was proven as the correct one.

Based on the transalkylidenation reaction, three reaction mechanisms were proposed: pairwise concerted, pairwise nonconcerted, and carbene mechanism. A pairwise con-

certed mechanism was first shown by Turner et al. (2) with a quasi-cyclobutane as an intermediate. A pairwise nonconcerted mechanism was found by Brunck and Grubbs (33) which had a metallocyclopentane complex as an intermediate (30). Burk et al. (34) demonstrated the carbene mechanism through experimental result. The carbene mechanism contains initiation and propagation steps which is similar to a polymerization reaction. A metal hydride may play an important role in the initiation step (35) and the carbene serves as a chain carrier.

Based on the transalkylidenation type reaction, four kinetic models were proposed (30, 31): Rideal model, Langmuir-Hinshelwood one site model, Langmuir-Hinshelwood two sites model, and the model for the carbene mechanism. Begley and Wilson (36) studied the propylene disproportionation using tungsten-silica catalyst. The correlation of the pilot plant kinetic data with Rideal and Langmuir-Hinshelwood models showed that the former adequately correlated the data. Kemball et al. (7), Wills et al. (37), and Wills et al. (38) studied the propylene metathesis using $\text{Mo(CO)}_6/\text{Al}_2\text{O}_3$, WO_3/SiO_2 and $\text{CoO/MoO}_3/\text{Al}_2\text{O}_3$ as catalysts respectively. They all found that the Langmuir-Hinshelwood two-site model adequately correlated the initial rate data. If the models other than the carbene, are used to explain the metathesis reaction, the homologs of shorter and longer chains produced via metathesis must be of equal amount.

The pulse technique may be used as a perturbation method to describe the transient behavior of a process (39). The particular value of this technique is to study the elementary steps of a reaction. The reaction rate measured by flow technique is the measurement of overall reaction, whereas the pulse technique may study the initial steps. Murakami et al. (40) applied the pulse technique to measure the rate constants of the adsorption and desorption of benzene on HY and CaY zeolite. This measurement was based on the retention time and the half width of the chromatographic peak with an assumption that there was no reaction. They also measured the surface reaction rate constant and the desorption rate constant of the reactant when there was a product adsorbed only sparingly on the surface. Murakami et al. (41,42,43, 44,45) studied the pulse technique to derive equations for the conversion by assuming some reaction models and different adsorption strength. They also showed that the conversions for pulse and flow systems were the same only when the reaction was first order and the shape of pulse was rectangular. However, it is still difficult to draw definite conclusion about kinetic data from the pulse technique especially when higher order reaction and side reactions are considered.

The temperature programmed desorption(TPD) technique is a very efficient method for the study of catalyst surfaces. In the temperature programmed desorption technique the temperature is usually continuously varied. An analysis of this

process can be carried out only if the variation of the temperature with time is of a simple function form (46,47). Based on the linear heating schedule, Cvetanovic et al. (47) made the material balance of a single component within the fixed bed. The derivation included the assumptions of first order desorption, steady state conditions, and negligible mass transfer effects. Furthermore, they assumed that the particular adsorption site was homogeneous so that the rate constant of desorption was not a function of the surface coverage but a function only of temperature which may be expressed by the Arrhenius equation. If the individual adsorption site is homogeneous and readsorption does not occur then the activation energy of desorption is obtained from the temperatures corresponding to the peak height by varying the temperature increasing rate. If the individual adsorption site is homogeneous and readsorption occurs then the heat of desorption is obtained instead of the activation energy of desorption. If the site is homogeneous and the desorption is diffusion controlled then the structure and size of the pore are needed in order to calculate the heat of desorption. However, it is still difficult to handle the problem of heterogeneous adsorption sites. Carter and Grant (48) analyzed this problem by assuming that the trapping sites formed a continuous energy spectrum and had a uniform population density. Yoneda(49) analyzed the distribution of the activation energy of desorption by assuming only a single

adsorbed state and that no readsorption occurred. By varying the carrier gas flow rate over a wide range, it can be determined if readsorption occurs(46,47).

Cvetanovic et al.(50,51,52) studied the adsorption of ethylene, propylene, and trans-2-butene on alumina and found two different sites no matter what material was adsorbed. They also found that the sites were heterogeneous with a linear distribution of the activation energy.

The TPD technique may also be applied to the study of a reaction mechanism. Munuera(53) studied the formic acid dehydration on TiO_2 and found two mechanisms depending on the reaction temperature. Cvetanovic et al.(54) found two reaction sites for ethylene on alumina. The weaker sites were responsible for hydrogenation, whereas the stronger sites were responsible for dimerization. The specific activity of the weaker sites increased with the evacuation temperature while the specific activity of the stronger sites was not changed by the evacuation temperature.

The catalysis research group at the department of chemical engineering, University of Oklahoma has had the following achievements:(55,30)

1. The adsorption of ethylene on $\text{NH}_4\text{ReO}_4/\text{SiO}_2$ and $\text{NH}_4\text{ReO}_4/\text{Al}_2\text{O}_3$ were reversible. If the catalyst was partially reduced by hydrogen, the adsorption became slower and partially irreversible. For a high extent of hydrogen reduction, the adsorption on silica supported catalyst became reversible

again, but that on alumina supported catalyst always had a significant amount adsorbed irreversibly.

2. There was interaction between rhenium oxide and alumina. The alumina supported rhenium oxide was more difficult to reduce. The silica supported rhenium oxide was inactive for propene metathesis up to 180°C.

3. The reduced catalyst had a higher initial rate, while the deactivation rate was also higher. It was believed that the irreversibly adsorbed reactant and product caused the rapid deactivation.

4. The mass transfer effect was negligible for the 10% $\text{Re}_2\text{O}_7/\text{Al}_2\text{O}_3$ catalyst, but not negligible over the 21.3% catalyst. The propene metathesis rate data were better correlated by the Langmuir-Hinshelwood mechanism.

5. A break-in was observed for the propene metathesis at 0°C. The kinetic data may be correlated by a model based on the active site concentration. The orders, with respect to the active site concentration, of the break-in and deactivation rates were two and between one and two respectively.

6. The catalyst activity increased with increasing oxygen-regeneration temperature especially above 500°C. Oxygen regeneration may maintain a mesoperrhenate like structure, while the oxygen-free helium may destroy this structure at 500°C and create more metathesis sites.

7. The break-in period was not observed when the evacuation temperature was below 320°C, while it was observed

again when the evacuation temperature was greater than 320°C.

8. If the catalyst was reduced by hydrogen at 24°C, the break-in disappeared and the deactivation rate was higher. If the catalyst was reduced by hydrogen at 500°C, the break-in with a lower initial rate was observed. When reduced at temperatures between 244°C and 335°C, the catalyst was inactive.

9. The activity was not affected if the catalyst was pretreated with ethylene. However, the activity was lowered if the catalyst was pretreated with propene or cis-2-butene and the break-in period disappeared.

The present research work includes the following objectives:

(1) The effect of reaction temperature using a flow system kinetic study method.

(2) The effect of sources for support and promoter on the activity.

(3) A study of the mechanism via the pulse and TPD methods.

(4) The property study of the catalyst surface by the use of TPD and specific poison method.

Unless particularly specified, the following abbreviation will be used in this thesis:

CB2 : cis-2-butene

C(%) : conversion, defined as (moles of reactant input - moles of unreacted reactant output) / (moles of reactant input)

1-B : 1-butene

E : ethylene
P : propylene
P⁺ : olefin with carbon number more than 4
R : reactant
TB2 : trans-2-butene
TPD : temperature programmed desorption
T_M : temperature recorded corresponding to the
time when the peak maximum appear on the TPD
chromatogram
Y(%) : yield, defined as (moles of product other than
reactant)/(moles of reactant input)
B : butene, including 1-B, TB2, and CB2

CHAPTER II

EXPERIMENTAL

A. Material

NH_4ReO_4 ---- 99.0% purity, supplied by Apache Chemicals

$\gamma\text{-Al}_2\text{O}_3$ ---- 99.9% purity, supplied by Harshaw Chemical
Co., Type 0104 (grind to 40-60 mesh)

NaReO_4 ---- 99.95% purity, supplied by Alfa Division
Ventron Corporation

TiO_2 ---- 99.9% purity, supplied by Degauss Co.

Zeolite ---- Type 3A, 4A, 5A, and 13X, supplied by Union
Carbide (grind to 40-60 mesh)

CaCl_2 ---- anhydrous, supplied by Fisher Scientific Co.

CO_2 ---- bone dry grade, supplied by Union Carbide

NH_3 ---- anhydrous 99.99% purity, supplied by Matheson
Co.

CuO ---- reagent grade, supplied by Mallinckrodt Co.

Ethylene --- 99.79% purity research grade, supplied by
Phillips Petroleum Co.

Propene --- 99.79% purity research grade, supplied by
Phillips Petroleum Co.

Trans-2-butene ---- 99.79% purity research grade

B. Catalyst Preparation

Each catalyst used is 9.00w% Re_2O_7 for each support and promoter. The mixture of the support (Al_2O_3 or TiO_2 or zeolite) and the aqueous solution of the promoter (NH_4ReO_4 or NaReO_4) was stirred in excess distilled water at a temperature below the boiling point of water for one day and the water was evaporated. The product was dried in an oven at 150°C for one day.

C. Apparatus for Flow System Kinetic Study

The apparatus used in this study is the same as that used by Hsu(30). The inlet propene and oxygen are dried separately with 3A and 4A molecular sieve. The molecular sieve driers are wrapped with heating tape for regeneration at a high temperature. An on-line sample valve is used to inject the effluent to an F&M Model 810 Gas-Liquid Chromatograph to analyze the gas phase composition. A Keithley Instrument Model 147 nanovolt null detector and Model 260 nanovolt source are used for measuring the thermal emf. A 14 ft long 1/8 inch stainless steel column packed with 20% bis-2-methoxyethyl adipate on Chromosorb P is used for the GLC column.

D. Apparatus for Pulse and TPD Studies

The apparatus used in these studies is shown in Figure 1. The inlet hydrocarbon and oxygen are dried by 3A and

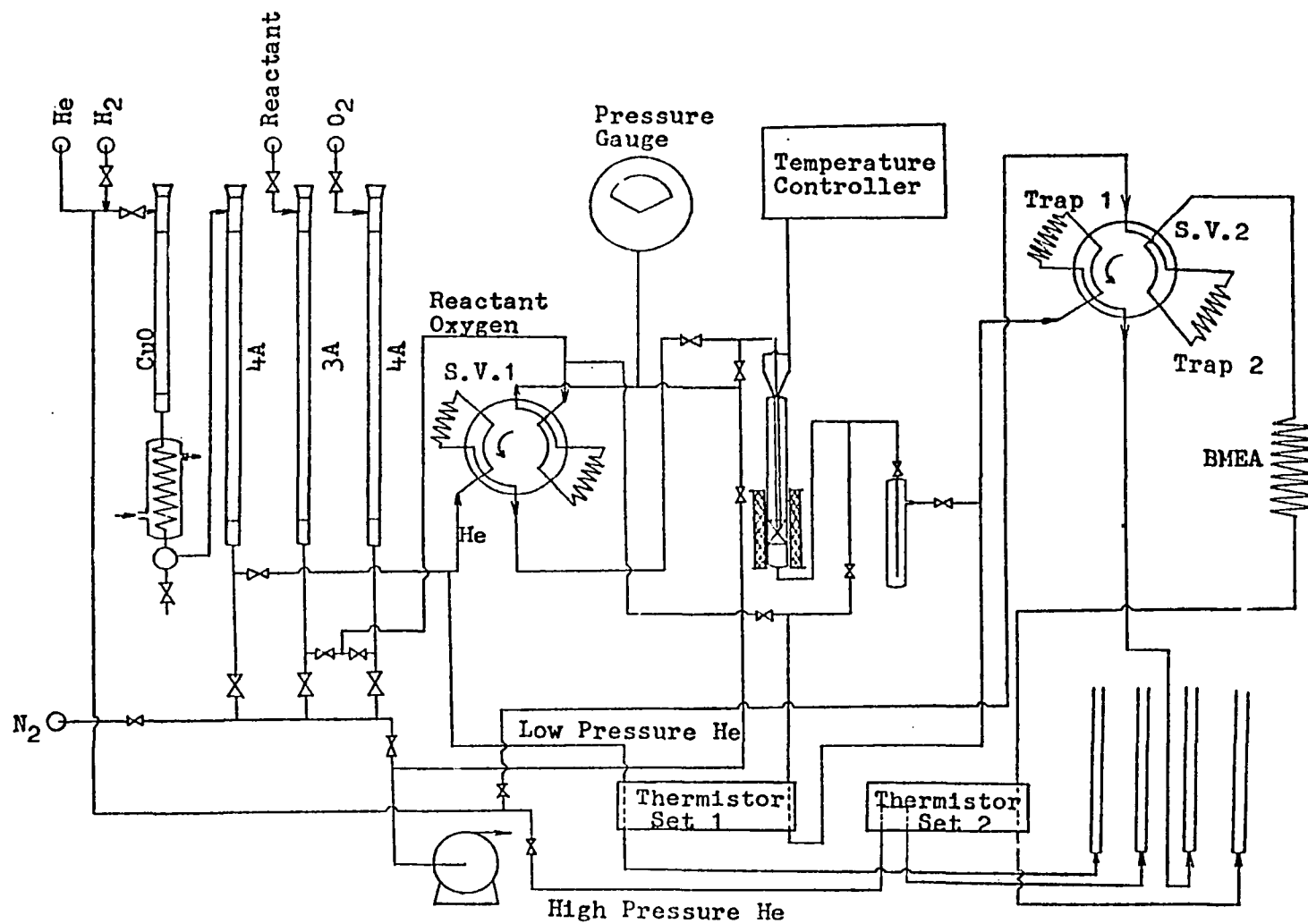


Fig. 1 Flow Diagram for Pulse and TPD Studies

4A molecular sieve columns respectively. The carrier gas (He) goes through the hydrogen reduced cupric oxide and the 4A molecular sieve so that the oxygen and water can be removed. The molecular sieve and cupric oxide columns are operated at room temperature and at 350°C respectively. The molecular sieve columns are regenerated at 350°C with nitrogen. The cupric oxide column is regenerated with helium diluted hydrogen at 220°C. The system includes a temperature controller to control the reactor temperature at a constant value or to raise the temperature linearly. The switch valve 1 (S.V. 1) is used to inject a constant amount of reactant to the reactor carried by He. The traps for switch valve 2 (S.V. 2) are used to trap the gas effluent with liquid nitrogen for further analysis by the thermistor. The thermistor (Set 1) is used for detecting the breakthrough curve when the pulse is injected or for recording the TPD chromatogram. The thermistor (Set 2) is used for analyzing the gas phase product. An Alumel-chromel thermocouple is used for detecting the temperature.

A Gow-Mac Model 40-002 power supply unit supplies power to the thermistors. A Keithley Instrument Model 147 nanovolt null detector and Model 260 nanovolt source are used to measure thermal emf. A Sargent Instrument Model SR recorder is used to record the analysis result by thermistor. An F. L. Moseley Co. Model 135A X-Y recorder records the TPD chromatogram.

E. Procedure for Kinetic Study

The catalyst is activated according to the standard procedure: with dry oxygen at 5 ml/sec for about 14 hours and about 500°C. The catalyst is then cooled to the reaction temperature in static oxygen. This procedure is expressed as follows: 500°C; 5 ml/sec; 14 hr // Rxn @ ***°C.

After activation the whole system, except for the reactor, is evacuated and purged with the mechanical pump and reactant respectively to avoid contamination by oxygen. The bulk oxygen in the reactor is then pumped out from downstream before the injection of reactant. The space velocity of the reactant, propylene, is fixed at 6.75±5% g/hr-g catalyst. Use the on line sampling valve, the product can be analyzed after a certain time interval.

F. Procedure for Pulse and TPD Studies

The catalyst is activated according to the standard procedure which is the same as that for the kinetic study. The helium and propene are checked to determine if they are free of oxygen before being introduced to the reactor. The catalyst is cooled in static oxygen to the reaction temperature after activation. Then the bulk oxygen is pumped out followed by the introduction of the carrier gas. The whole system is then purged with oxygen free helium for a half hour

followed by injections of a known amount of propene at a constant time intervals. The gas phase effluent is trapped by liquid nitrogen for analysis by thermistor.

The TPD study is carried out right after the pulse study by raising the reactor temperature linearly in time. The desorbed material goes through the thermistor first and then through the liquid nitrogen trap, so that the TPD chromatogram can be recorded and the desorbed material can be analyzed. Finally, oxygen is injected pulse by pulse to burn the coke away so that an overall mass balance can be made.

CHAPTER III

RESULTS

I. EFFECT OF REACTION TEMPERATURE

Figure 2 illustrates the time-dependence kinetic curve and the product distribution of propylene metathesis carried out over the $\text{NH}_4\text{ReO}_4/\gamma\text{Al}_2\text{O}_3$ catalyst at 0°C . 0.5119 g catalyst is used with flow system study. Figures 3 to 6 illustrate the kinetic curve and product distribution at different reaction temperature, i.e. 25°C , 50°C , 103°C , and 203°C .

The olefin metathesis rate of the vapor phase may be calculated with the following equation which was suggested by DeMourgunes et al.(56):

$$R = X(V/22400)(273/T)(P/760)(3600/W) \quad (1)$$

$$= XF(3600/W) \quad \text{at } 0^\circ\text{C and 1 atm} \quad (2)$$

where, R = reaction rate (gmole/g catalyst-hr)

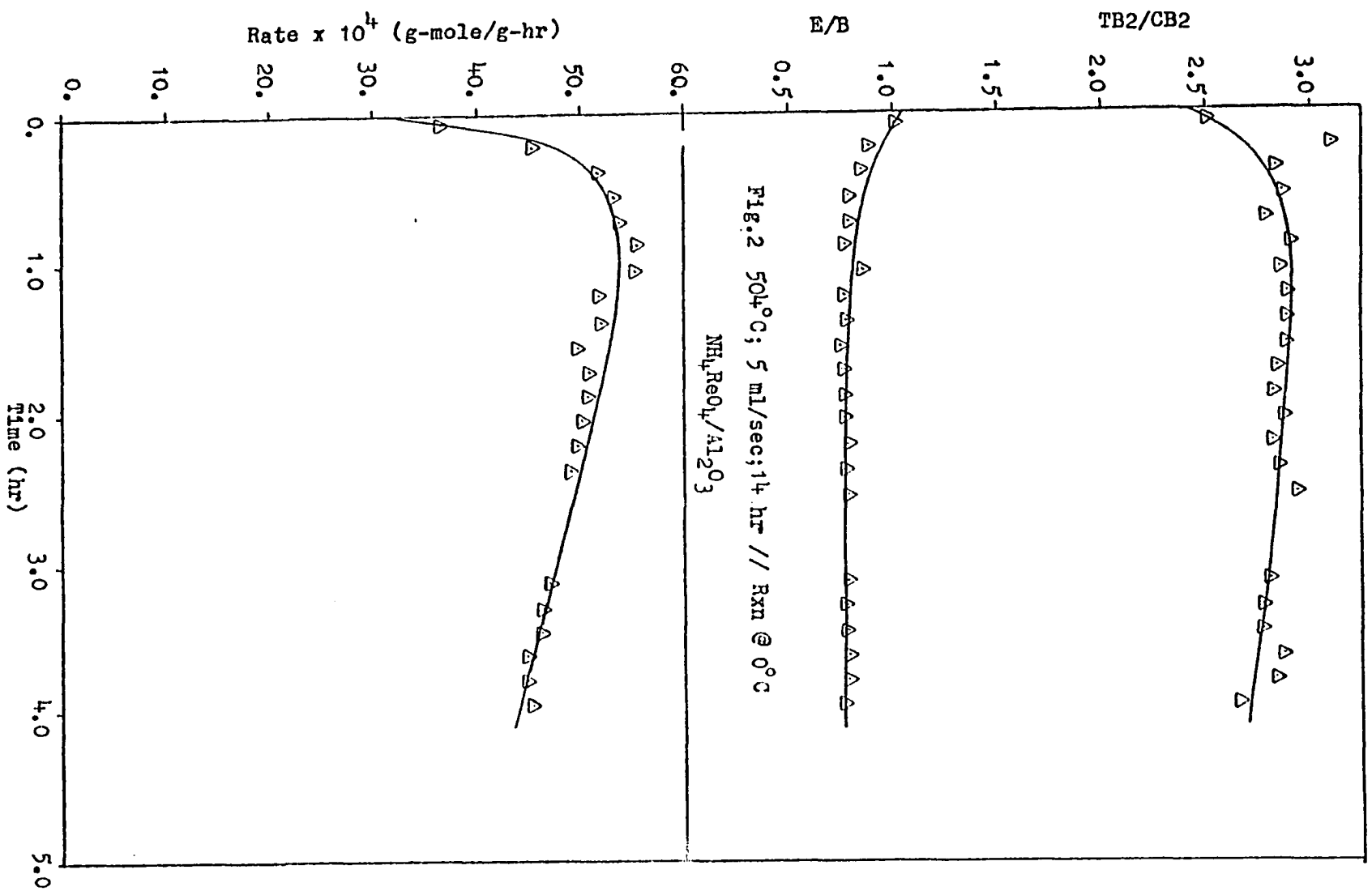
X = fractional conversion

V = volume flow rate of the gas at experimental condition (ml/sec)

T = absolute reaction temperature ($^\circ\text{K}$)

P = partial pressure of the reactant (torr)

W = catalyst mass (g)



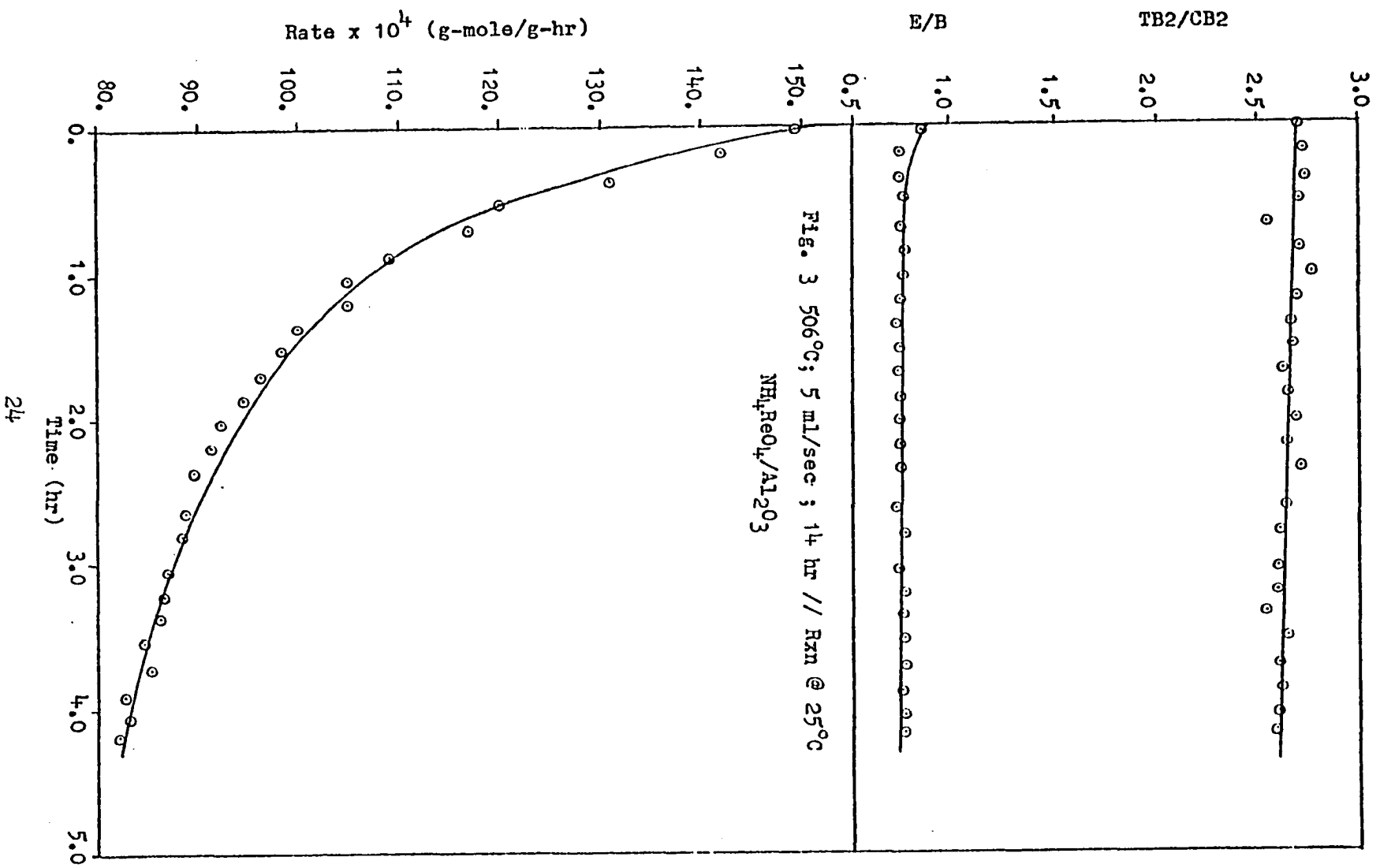
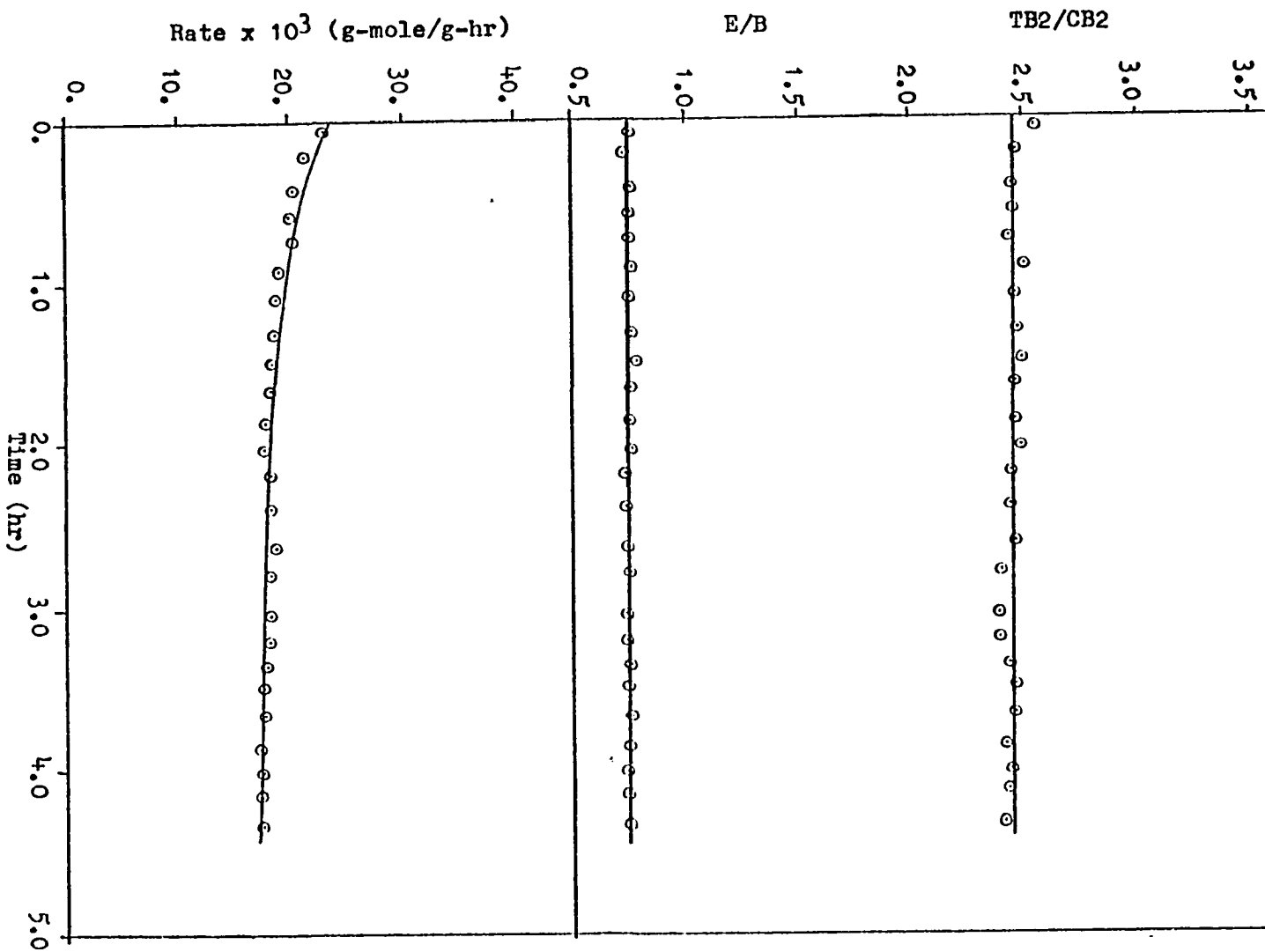
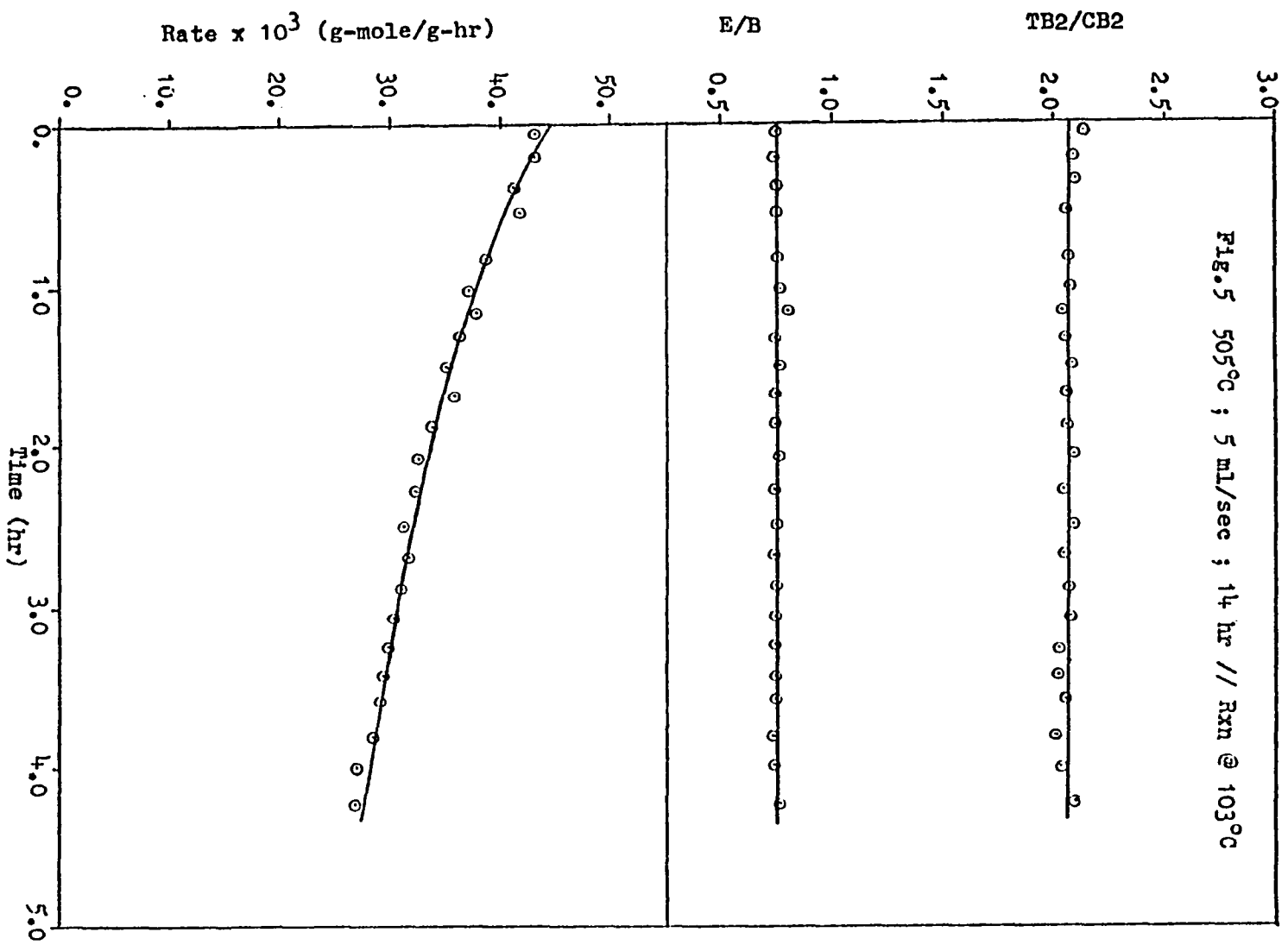


Fig. 4 505°C ; 5 ml/sec ; 14 hr // Rxn @ 50°C
 $\text{NH}_4\text{ReO}_4/\text{Al}_2\text{O}_3$





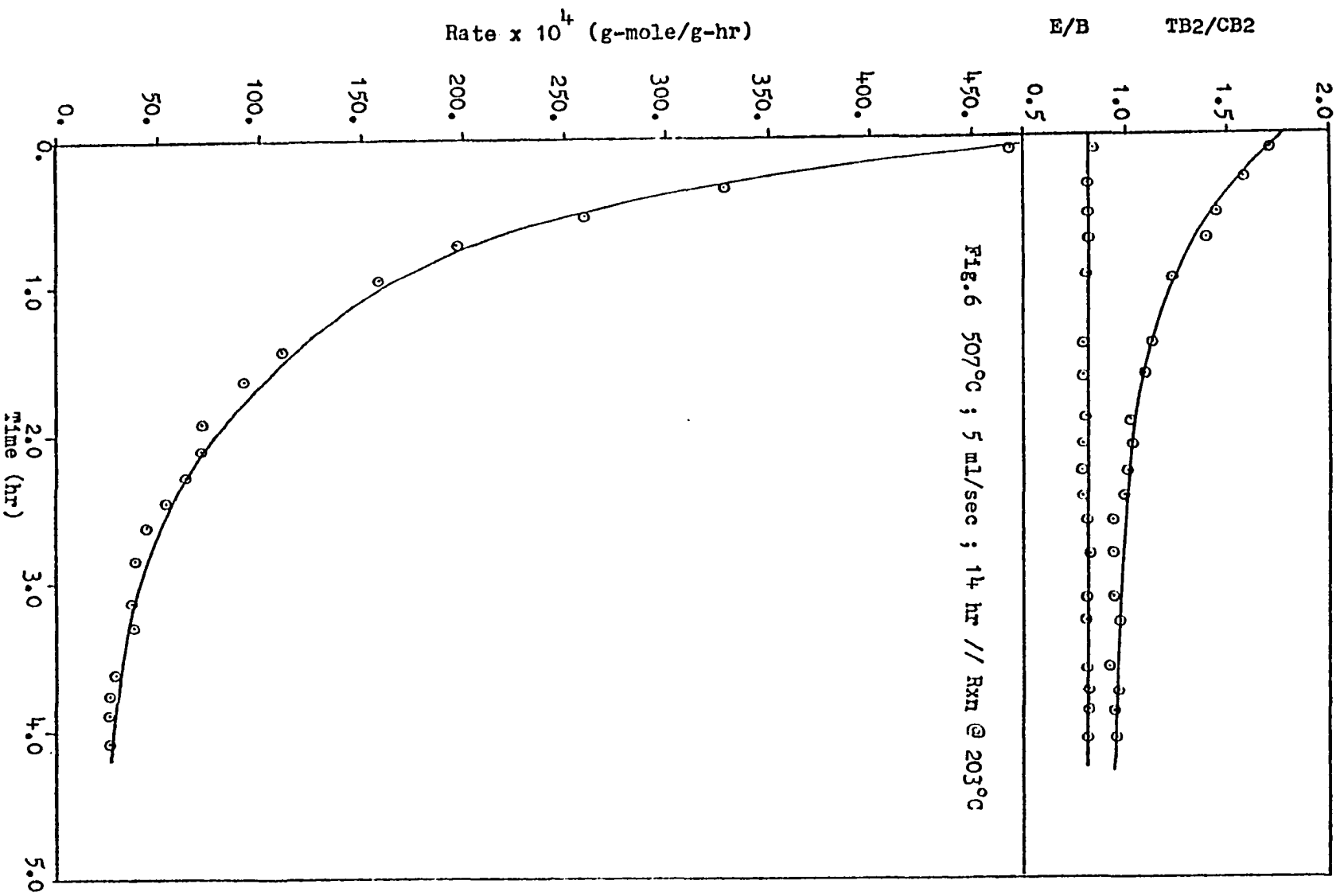


Fig. 6 507°C ; 5 ml/sec ; 14 hr // Rxn @ 203°C

F = gas molar flow rate at 1 atm and 0°C (gmole/sec)

During the study of the reaction temperature effect, the space velocity is fixed at a constant value, i.e. 6.75g/hr-g catalyst. The space velocity may be calculated from the ideal gas law as shown below where the time factor is added to the volume term:

$$N = (PV)/(RT) \quad (\text{gmole/sec}) \quad (3)$$

$$= (PV)(3600)/(82.06T) \quad (\text{gmole/hr}) \quad (4)$$

$$= (PV)(3600)(M/W)/(82.06T) \quad (\text{g/hr-g catalyst}) \quad (5)$$

$$= 43.87(PVM)/(WT) \quad (\text{g/hr-g catalyst}) \quad (6)$$

$$= \text{WHSV} \quad (7)$$

where P = partial pressure of the reactant (atm)

V = volume flow rate of the gas at experimental condition (ml/sec)

R = gas constant (82.06 atm-ml/gmole- $^{\circ}\text{K}$)

T = reaction temperature ($^{\circ}\text{K}$)

M = molecular weight of the reactant

W = catalyst weight (g)

By comparing these derivations, an implicit relationship between rate and space velocity may be found as:

$$\text{WHSV} = 3600(F/W)M \quad (8)$$

The break-in is observed only when the reaction is carried out at ice temperature. It takes about 50 minutes

to reach the maximum reaction rate before the deactivation starts. Only the deactivation period is observed when the reaction is carried out at temperatures higher than 0°C .

Figure 2 indicates that the ratio of ethylene to butenes is higher than the stoichiometric value (i.e. 1) at the beginning (57,58) then decreases to a constant value which is less than one. The same tendency is observed if the reaction is carried out at 25°C , although the initial value is less than one (Fig. 3). A constant value, smaller than one, for the ratio of ethylene to butenes is observed if the reaction temperature is higher than 25°C (Figures 4, 5, and 6).

Figure 2 shows that the ratio of trans-2-butene to cis-2-butene increases with time then decreases after reaching a maximum and the value is always smaller than the thermodynamic equilibrium value (i.e. 3.92 at 0°C). At higher reaction temperatures (Figures 3, 4, 5, and 6) this value is a constant except at 203°C where it decreases with time.

Figure 2 shows that the ratio of E to B is higher than one at the beginning then decreases to a value which is less than one. This result may give some suggestions: (1) more B is adsorbed at the beginning and/or (2) the production of E and B follow different routes and/or (3) the produced E may have a further reaction depending on the concentration of the adsorbed material on the surface.

At higher reaction temperatures (Figures 4, 5, and 6), it seems that the reaction rate to produce butenes is

enhanced and the extent is higher than that for ethylene so that the ratio of ethylene to butenes becomes a constant which is less than one. Such result may also be resulted from the possibility that both the productions of E and B are enhanced by higher reaction temperature, but E has further reaction. The production of cis-2-butene is thermodynamically favored at higher reaction temperature so that the ratio of trans-2-butene to cis-2-butene decreases with increasing reaction temperature(Figures 3, 4, and 5). That the trans-2-butene to cis-2-butene ratio decreases with time may be due to the poisoning of sites producing trans-2-butene or the steric effect upon the formation of trans-2-butene(Fig. 6).

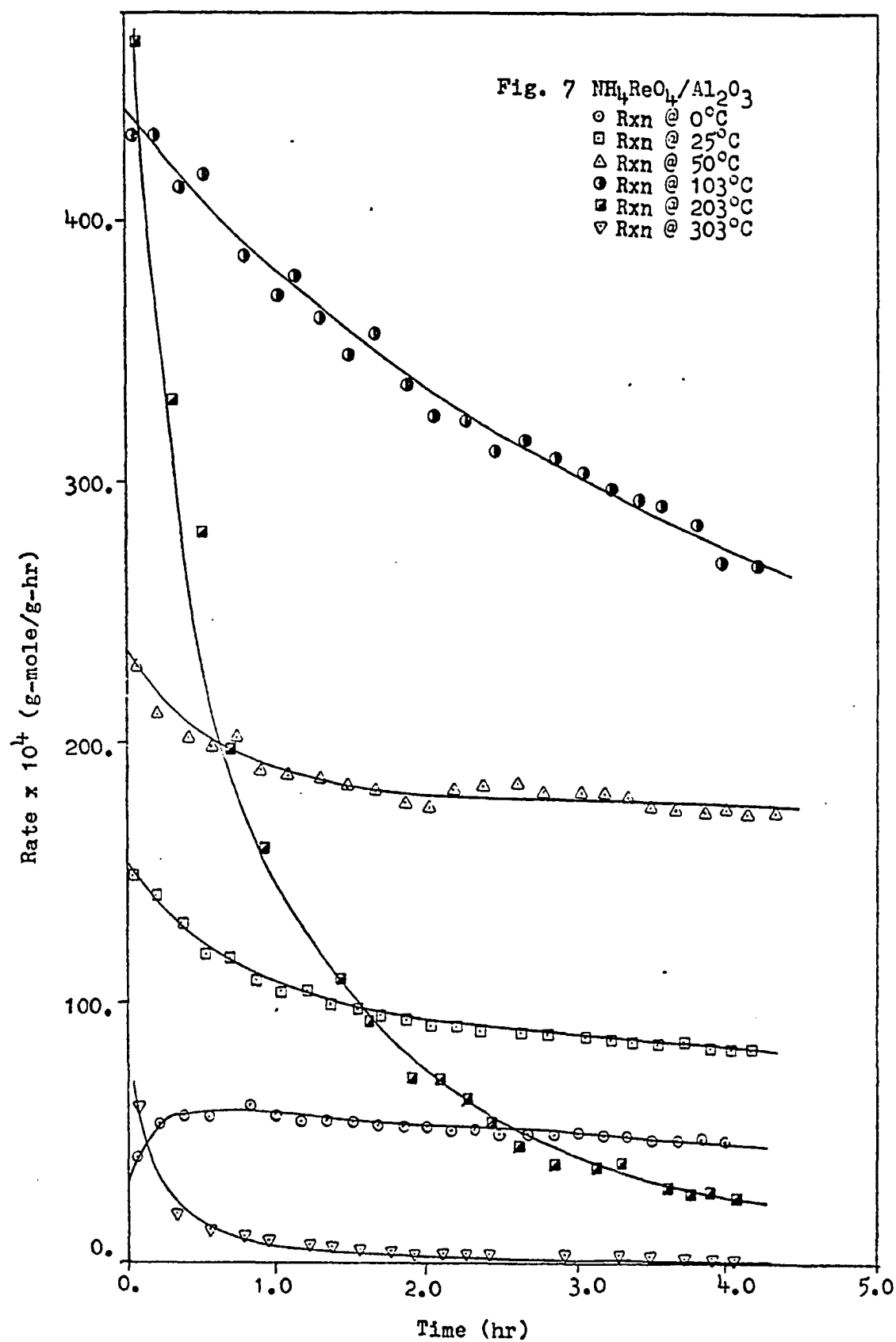
The selectivity of propylene metathesis to ethylene and butenes over the $\text{NH}_4\text{ReO}_4/\text{Al}_2\text{O}_3$ catalyst is 100%. However, at 203°C a trace of 1-butene is observed amounting to about 2% of the total conversion.

Table 1 illustrates the time-dependence of the conversion. The conversion increases with increasing reaction temperature but then decreases rapidly after a certain temperature due to site poisoning.

Figure 7 compares the reaction rate on the same scale. Apparently, the deactivation rate is very fast when the reaction temperature is higher than 103°C. An interesting result is found, i.e., the rate profile at 50°C has the slowest deactivation rate. A correlation of these time-on-stream rate data with the mathematical model proposed by Hsu

	<u>Initial</u>		<u>Maximum</u>		<u>Final</u>	
	<u>Time(min)</u>	<u>C(%)</u>	<u>Time(min)</u>	<u>C(%)</u>	<u>Time(min)</u>	<u>C(%)</u>
0°C	3.0	2.64	50.0	3.87	240.0	3.03
25°C	1.5	9.41	----	----	240.0	5.34
50°C	4.5	14.5	----	----	260.0	11.23
103°C	3.5	28.1	----	----	253.0	17.2
203°C	5.5	31.05	----	----	244.5	1.59

Table 1 Illustration of Time-dependence Conversion at
Different Reaction Temperature



(30) shows that this observation is consistent with the deactivation rate constants obtained from the correlation. Table 2 shows the break-in rate and deactivation rate are first order with respect to the adsorption active site density and the active site density.

The observation of the most stable reaction at 50°C is of value for further study since it is important to the practical application. To maintain a stable activity and to minimize the activity difference between the initial and steady state periods are important for practical use. Since the reaction temperature may affect the adsorption amount and the production of high molecular weight products and coke, it is proposed that the dependence of the deactivation rate upon the reaction temperature can be attributed to the superposition of these two factors. It is well known that the lower temperature the higher adsorption amount while the higher temperature the more high molecular weight products and coke produced.

The flow system kinetic study is carried out again followed by purging the whole system with oxygen free helium to get rid of the gas phase hydrocarbon and the physically adsorbed residue. After this step TPD is used to desorb the chemically adsorbed residue and this is followed by an injection of oxygen to burn the coke away. The same procedure has been carried out at three reaction temperatures and the results are shown in Table 3. Table 3 shows that the adsorp-

Part A:

$$\begin{aligned}
 2-B \ \& \ 1-D: & K(1-(1+Bt)^{-1})\exp(-Gt) \\
 2-B \ \& \ 2-D: & K(1-(1+Bt)^{-1})(1+Gt)^{-1} \\
 1-B \ \& \ 1-D: & K(1-\exp(-Bt))\exp(-Gt) \\
 1-B \ \& \ 2-D: & K(1-\exp(-Bt))(1+Gt)^{-1} \\
 2-B \ \& \ m-D: & K(1-(1+Bt)^{-1})(1+Gt)^{-N}
 \end{aligned}$$

Part B: (at 0 °C)

Order		Dev. (%)
B	D	
2	1	1.34
2	2	1.32
1	1	2.00
1	2	2.06
2	6.32	1.68

Part C: (first order deactivation rate constant)

Rxn. Temp. (°C)	k (hr ⁻¹)
25.0	0.118
50.0	0.0432
103.0	0.114
203.0	0.692*
303.0	0.576

* the deactivation is too fast to be well measured

Table 2 The Result of Correlation

Part A: rate equations of some special cases
 Part B: break-in and deactivation orders at 0°C
 Part C: deactivation rate constant of first order deactivation

	<u>25°C</u>	<u>50°C</u>	<u>103°C</u>
E	1.299E-7	7.934E-8	2.653E-7
P	4.541E-6	3.215E-6	7.009E-6
1-B	1.251E-7	6.102E-8	8.557E-8
TB2	1.796E-6	5.142E-7	1.126E-6
CB2	6.477E-7	2.385E-7	4.779E-7
P ⁺	1.647E-7	5.601E-8	4.597E-8
Total	<u>7.404E-6</u>	<u>4.164E-6</u>	<u>9.009E-6</u>
CO ₂	2.285E-6	1.409E-6	4.343E-6

Table 3 TPD Results Obtained After the Catalyst
Has Been Used for Kinetic Study for
Half Hour
0.5119 g catalyst; 11.68°C/min
(all values are gmole)

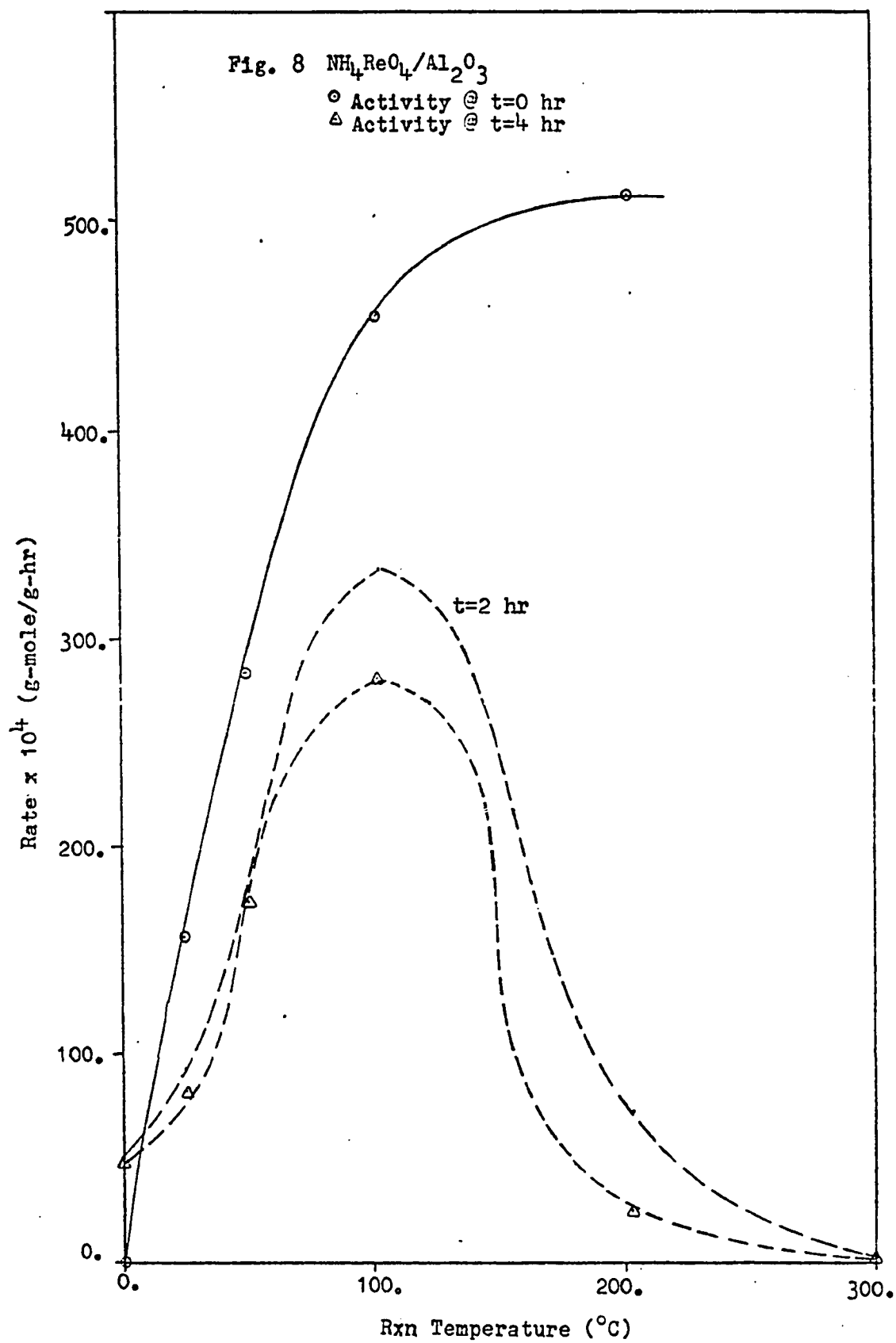
tion amount at 50°C, no matter if hydrocarbon or carbon dioxide is counted, is less than that at 25°C and 103°C. This can partially prove the superposition effect proposed above.

Figure 8 demonstrates the dependence of activity upon the reaction temperature after a certain reaction time. From this figure some observation may be drawn: (1) The initial activity increases with reaction temperature and then reaches a constant value (2) The most stable reaction temperature is around 50°C because the activities are about the same after 2 and 4 hours reaction time (3) The highest activity is around 100°C (4) The break-in period will possibly be observed below 8°C.

II. EFFECT OF SOURCES FOR SUPPORT AND PROMOTER

As mentioned in chapter I, isomerization reaction always accompanies the metathesis reaction(2). By adding Ia or IIa group metal ions the surface acidity may be changed and the isomerization may be depressed(2,22). Therefore, using NaReO_4 as a promoter is proposed instead of NH_4ReO_4 to study the metal effect. Some reviews related to the use of TiO_2 as a support(27) to change the catalyst properties and related to the use of zeolite to improve the catalyst life (28) are given. These reviews also suggest the use of TiO_2 or zeolite as the support instead of Al_2O_3 .

$\text{NaReO}_4/\text{Al}_2\text{O}_3$ is made by adding Al_2O_3 (40-60 mesh) to



the NaReO_4 solution then follow the preparation procedure mentioned in chapter II.

$\text{NH}_4\text{ReO}_4/\text{TiO}_2$, $\text{NH}_4\text{ReO}_4/3\text{A zeolite}$, and $\text{NH}_4\text{ReO}_4/13\text{X zeolite}$ are made by adding TiO_2 , 3A zeolite, and 13X zeolite to the NH_4ReO_4 solution respectively. About 0.5 g catalyst is used for study. Except for $\text{NH}_4\text{ReO}_4/\text{TiO}_2$ the particle size of 40-60 mesh are used because TiO_2 is powder.

II-A Result of $\text{NaReO}_4/\text{Al}_2\text{O}_3$

The activity of this catalyst is almost negligible. Table 4 shows that the initial activity is two order less than the initial activity of $\text{NH}_4\text{ReO}_4/\text{Al}_2\text{O}_3$ even when the reaction temperature is raised to 200°C . There are two possible reasons for this result: (1) the presence of sodium may result in a structure not suitable for the formation of mesoperrhenate structure (2) the concentration of sodium may result in different acidity for reaction.

II-B Result of $\text{NH}_4\text{ReO}_4/\text{TiO}_2$

Table 4 shows that some loss of rhenium is observed when the catalyst is activated at 500°C although it is not known exactly what the dark blue vapor is. Usually the catalyst activity increases with increasing activation temperature(30), but Table 4 shows that the initial activity is higher when activated at 304°C than that activated at 500°C . This may also partially prove that the extent of loss is

Catalyst	Act T/t	Rxn T	ΔT	R_i	color after Rxn	phenomena
$\text{NH}_4\text{ReO}_4/\text{Al}_2\text{O}_3$	509/14	0.0	9.0	0.	gray	-----
	506/14	25.0	6.5	1.568×10^{-2}	gray	-----
	505/14	50.0	1.5	2.837×10^{-2}	gray	-----
	505/14	103.0	-5.0	4.544×10^{-2}	gray	-----
	507/14	203.0	-10.0	5.110×10^{-2}	gray	-----
	508/14	300.0	-11.0	-----	black	-----
$\text{NH}_4\text{ReO}_4/\text{TiO}_2$	505/14	0.0	4.0	-----	-----	much dark blue vapor no more than above
	507/14	154.0	-4.0	-----	-----	
	511/14	203.0	-10.0	-----	gray	same
	505/15	303.0	-15.0	5.023×10^{-4}	gray	same
	509/17	403.0	-25.0	5.184×10^{-4}	black	same
	304/13	204.0	-17.0	2.162×10^{-3}	gray	dark blue vapor
$\text{NaReO}_4/\text{Al}_2\text{O}_3$	510/12	201.0	-6.0	1.921×10^{-4}	gray	-----
$\text{NH}_4\text{ReO}_4/13\text{X}$ (Na)	506/13	0.0	20.0	-----	-----	-----
	505/15	201.0	-5.0	-----	gray	-----
	506/14.5	301.0	-10.0	2.671×10^{-4}	black	-----
$\text{NH}_4\text{ReO}_4/13\text{X}$ (Ca)	506/16.5	0.0	36.0	-----	-----	-----
	508/16	202.0	4.0	1.391×10^{-3}	gray	-----
$\text{NH}_4\text{ReO}_4/3\text{A}$ (K)	535/15	0.0	4.0	-----	-----	dark blue vapor
$\text{NH}_4\text{ReO}_4/3\text{A}$ (Ca)	317/16	204.0	-11.0	6.691×10^{-3}	gray	-----
	308/16	302.0	-16.0	6.161×10^{-3}	black	-----
	506/16	0.0	14.0	-----	-----	dark blue vapor
	506/16	202.0	-10.0	2.871×10^{-3}	gray	no more change

zeolite A: $\text{Na}_{12}((\text{Al}_2\text{O}_3)_{12}(\text{SiO}_2)_{12}) \cdot 27\text{H}_2\text{O}$ with major metal ion K
 zeolite X: $\text{Na}_{86}((\text{Al}_2\text{O}_3)_{86}(\text{SiO}_2)_{106}) \cdot 264\text{H}_2\text{O}$

Table 4 Comparison of Temperature Change When Propylene is Introduced to the Reactor, Initial Activity, and Activation Phenomena with Different Catalyst at Different Activation Temperature

larger when activated at 500°C. The activity of this catalyst is lower than that of $\text{NH}_4\text{ReO}_4/\text{Al}_2\text{O}_3$ can be explained by the fact that the interaction between NH_4ReO_4 and TiO_2 is not strong enough to hold the promoter on the support so that loss is observed.

II-C Result of $\text{NH}_4\text{ReO}_4/13\text{X}$ zeolite

The activity of this catalyst is also negligible. Table 4 shows that no loss is observed during the activation and the temperature change in response to the injection of propylene is higher than that of $\text{NH}_4\text{ReO}_4/\text{Al}_2\text{O}_3$. The higher temperature change may be attributed to the higher extent of adsorption due to the larger pore size. The activity is not observed until 301°C can be due to the presence of SiO_2 in the support which was proposed by Lin(55). The presence of sodium in the support may also play an important role in affecting the acidity and structure of the catalyst.

II-D Result of $\text{NH}_4\text{ReO}_4/13\text{X}$ zeolite(Ca)

Since the presence of sodium in the catalyst has a negative effect on the activity, ion exchange method is applied to replace the sodium by calcium. This idea is from the fact that calcium containing zeolite is good for the catalytic cracking reaction(60). In addition, the electric field(61), surface area(62), and acidity(63) may be affected

by such a change. The result in Table 4 shows that the temperature change becomes larger and the activity is observed at a lower reaction temperature(202°C). Therefore, the substitution of sodium by calcium has a positive effect on the activity. If the change of temperature represents the extent of adsorption then this catalyst should have a lower activity due to higher temperature change. This is, however, not the case. Therefore, the temperature change may also include the heat of reaction or the temperature change only stands for the extent of adsorption but both the adsorption and reaction are enhanced by ion exchange.

II-E Result of $\text{NH}_4\text{ReO}_4/3\text{A(K)}$ zeolite

The result shown in Table 4 indicates there is no activity at 0°C and rhenium loss is observed during the activation. The low activity may be explained by (1) the presence of potassium (2) the presence of SiO_2 in the support (3) loss of rhenium (4) low adsorption capability because the temperature change upon the introduction of propylene is small.

II-F Result of $\text{NH}_4\text{ReO}_4/3\text{A(Ca)}$ zeolite

For the same reason as discussed in Section II-D, the ion exchange method is applied to substitute potassium by calcium. The result in Table 4 shows that the activity at lower activation temperature is higher than that at a higher

activation temperature. This result is due to the loss of promoter. A comparison of the temperature change with that of Section II-E suggests that the ion exchange changes either the structure, or the electric field, or surface area or the combination of these factors of the catalyst.

II-G Cross Comparison of The Effect of Sources

Figure 9 shows that the $\text{NH}_4\text{ReO}_4/\text{TiO}_2$ catalyst activated at 304°C has a higher initial activity than the $\text{NH}_4\text{ReO}_4/13\text{X zeolite}(\text{Ca})$ catalyst if the reaction is carried out around 200°C . However, the former has higher deactivation rate than the latter. Since the $\text{NH}_4\text{ReO}_4/13\text{X zeolite}$ and the $\text{NH}_4\text{ReO}_4/3\text{A zeolite}$ catalysts have lower activities than those of the ion exchanged catalysts, they will not be discussed further in the following.

Figure 10 shows that due to loss the $\text{NH}_4\text{ReO}_4/3\text{A}(\text{Ca})$ zeolite catalyst has higher activity activated at 317°C than activated at 506°C . This catalyst has higher deactivation rate when the reaction is carried out at 302°C than at 204°C . This may be attributed to poisoning resulting from cracking and coking.

Figure 11 shows that the following relationship of activities exists: $\text{NH}_4\text{ReO}_4/\text{Al}_2\text{O}_3 > \text{NH}_4\text{ReO}_4/3\text{A}(\text{Ca}) \text{ zeolite} > \text{NH}_4\text{ReO}_4/13\text{X}(\text{Ca}) \text{ zeolite}$. Furthermore, the catalysts supported by zeolites have lower deactivation rate than that supported by Al_2O_3 . This observation may be explained by

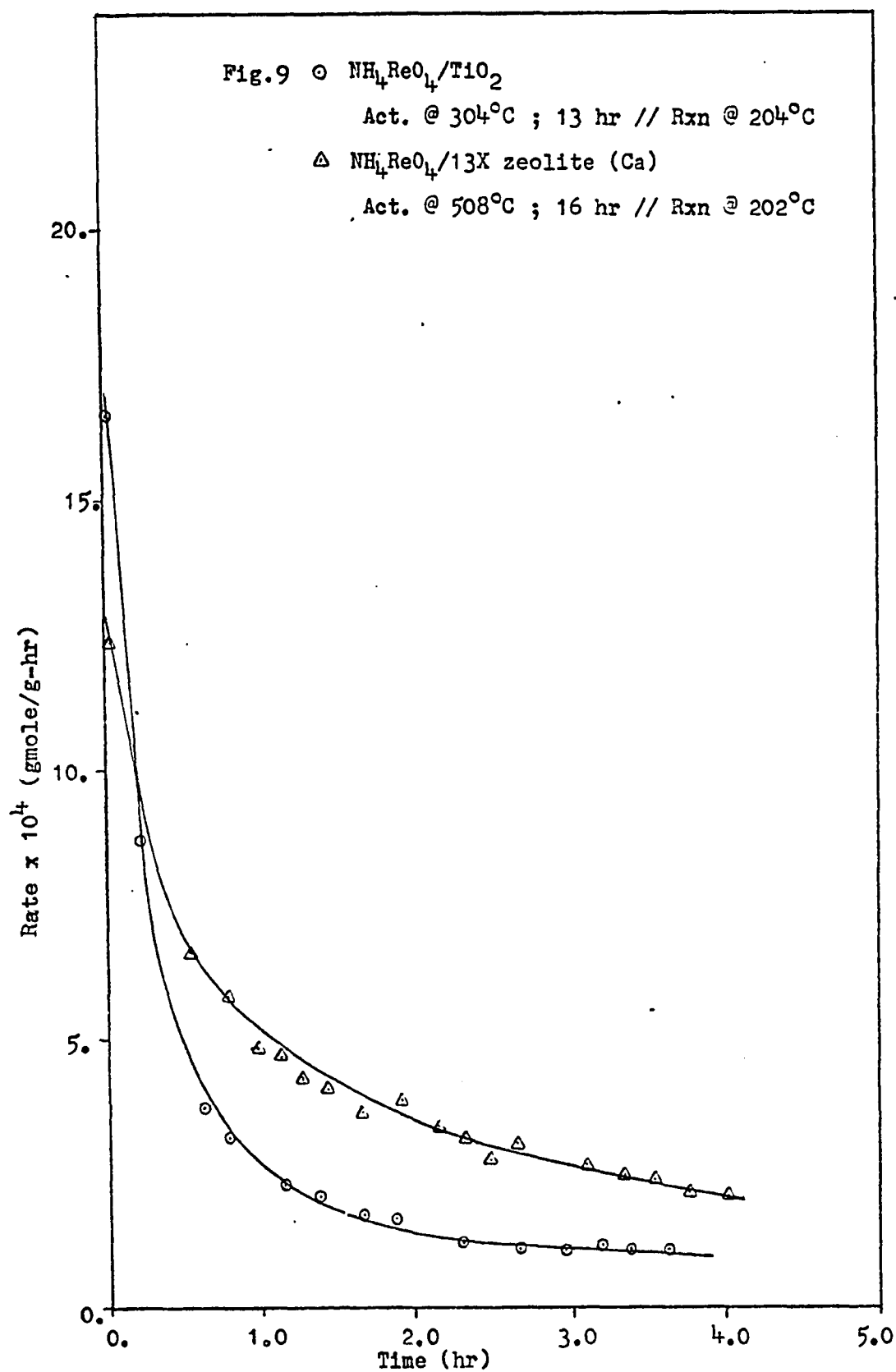


Fig.10 ○ $\text{NH}_4\text{ReO}_4/\text{3A zeolite (Ca)}$

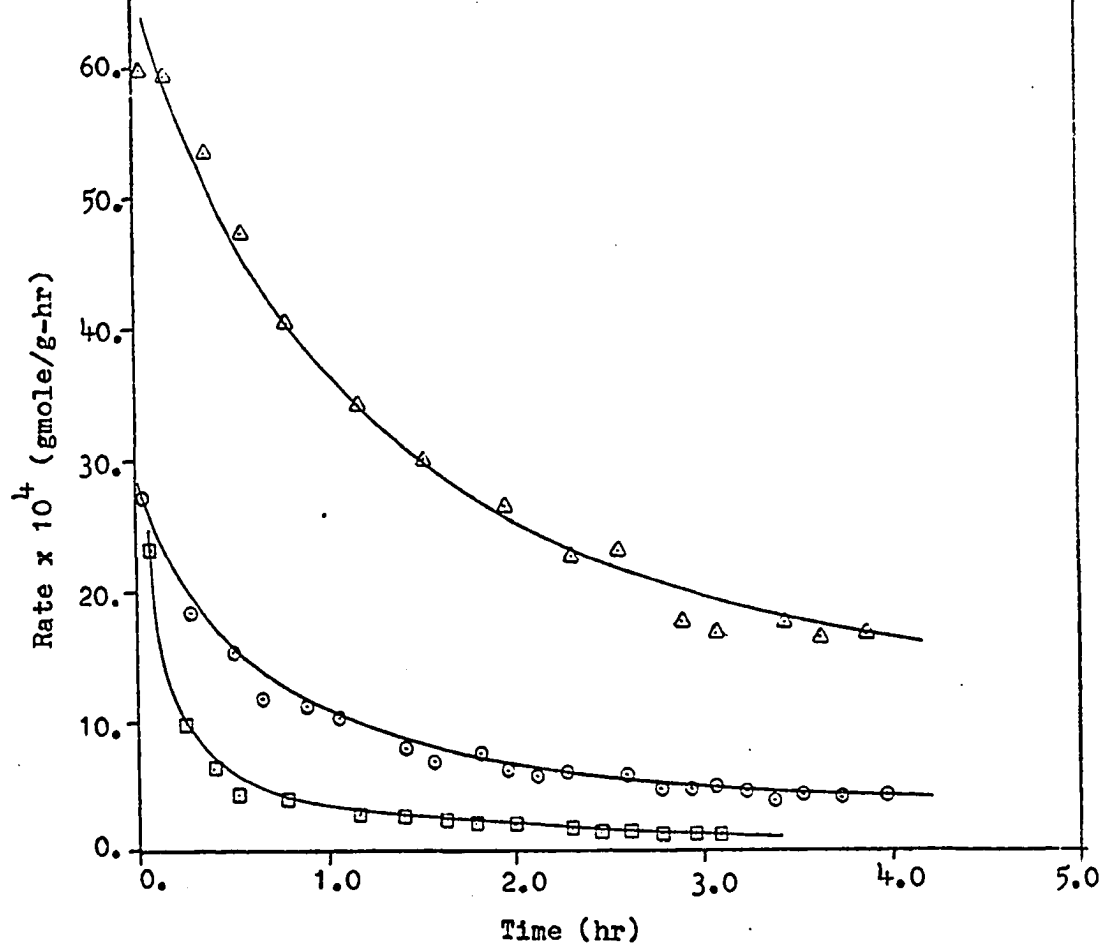
Act. @ 506°C ; 16 hr // Rxn @ 202°C

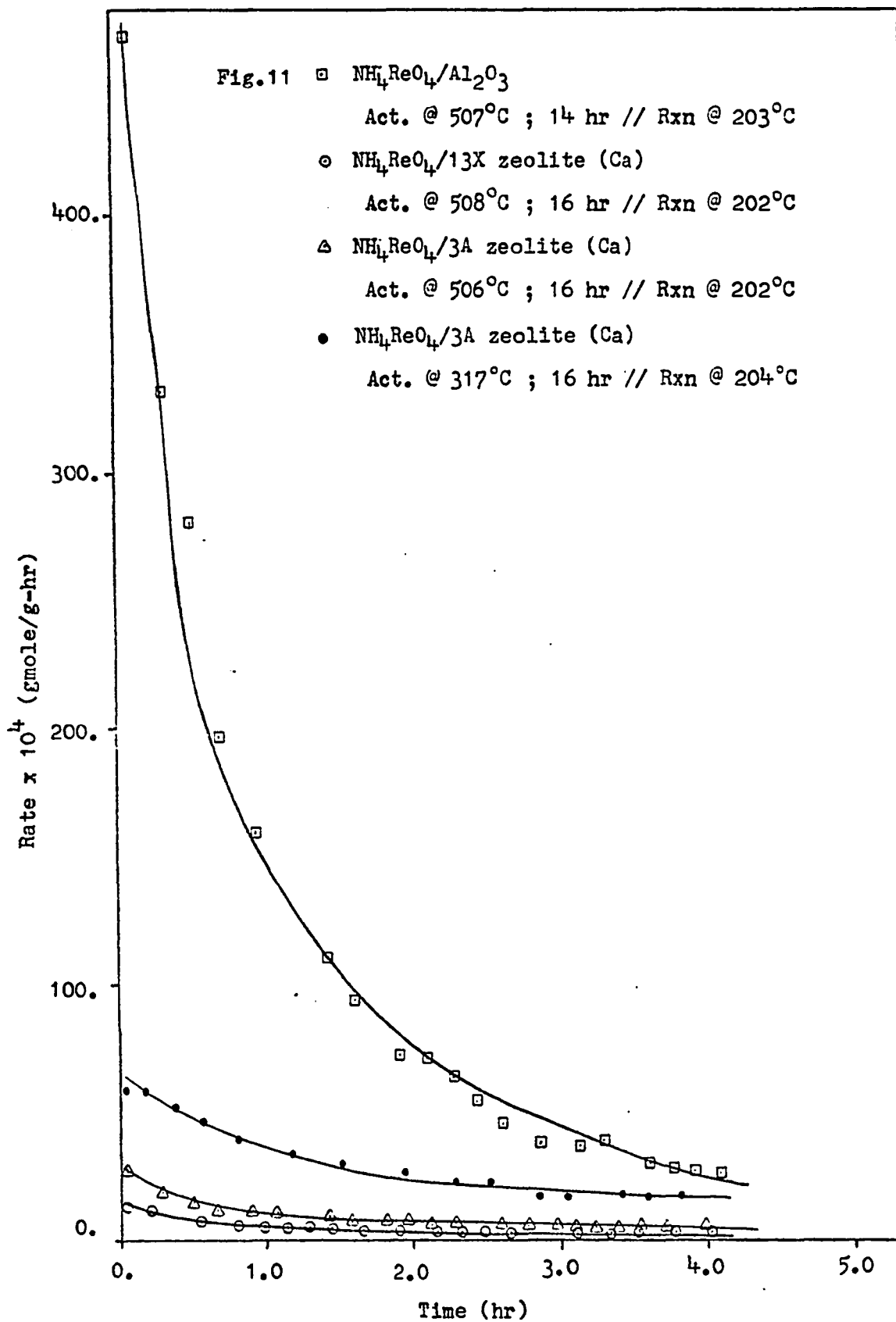
△ $\text{NH}_4\text{ReO}_4/\text{3A zeolite (Ca)}$

Act. @ 317°C ; 16 hr // Rxn @ 204°C

□ $\text{NH}_4\text{ReO}_4/\text{3A zeolite (Ca)}$

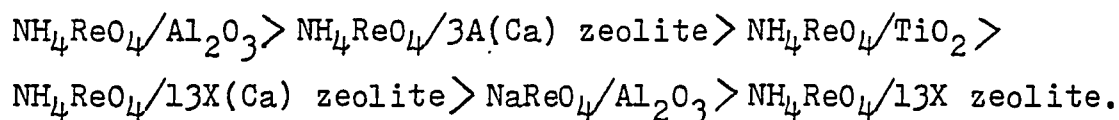
Act. @ 308°C ; 16 hr // Rxn @ 302°C





the existence of SiO_2 in the support. The catalyst supported by 3A(Ca) zeolite has a higher activity than that supported by 13X(Ca) zeolite. This may be due to the higher concentration of Al_2O_3 in the 3A(Ca) zeolite than in the 13X(Ca) zeolite. Therefore, it seems that there is some kind of relationship between the concentrations of alumina and silica, although it is unknown, which causes different activity.

From Table 4 and Figures 9, 10, and 11 the following relationship may be drawn about the relative activity:



III STUDY OF MECHANISM VIA PULSE TECHNIQUE

Begley and Wilson(36) studied the propylene metathesis using tungsten oxide-silica catalyst. They correlated the data with Rideal and Langmuir-Hinshelwood models and found that the Rideal model fitted the experimental data. Kemball et al.(7), and Wills et al.(37,38) studied the propylene metathesis using different catalysts and found that the Langmuir-Hinshelwood two-site model adequately correlated the experimental data. They used a flow system for their kinetic studies. However, according to the author's experience, it takes about two minutes to adjust the flow rate to the desired value if a flow system study is applied. Thus, if the reaction is similar to the polymerization reaction, i.e. including the initiation and propagation steps, then it

is likely that they missed the initiation step especially when the initiation step is a fast reaction. Accordingly, the pulse technique is suggested so that the elementary step may be investigated although it is still difficult to draw definite conclusion about the kinetic parameters from the pulse technique. The analysis of the experimental result herein is based on the material balance, so a good calibration of the equipment is necessary.

The reactant used in this study was mainly propylene, but trans-2-butene was also used. The reactor used was mainly a 3/4" glass sealing tube with fritted disk, but sometimes a 3/8" reactor was also used. The catalyst used was about 0.5 g $\text{NH}_4\text{ReO}_4/\text{Al}_2\text{O}_3$, and the exact amount is shown on the figures and tables. To check the material balance, each figure is followed by a table. There are two rows on the table corresponding to every olefin, the first row represents the number of moles of that olefin and the second row represents the number of carbon atoms. Sometimes, however, the second row is skipped.

III-A General Study with Pulse Technique

In this section the studies with different reaction temperatures, bed thicknesses, carrier gas flow rates, and pulse sizes are described. The equipment is shown in Figure 1. The catalyst was first activated with water-free oxygen for overnight at 500°C, then cooled to the reaction temperature

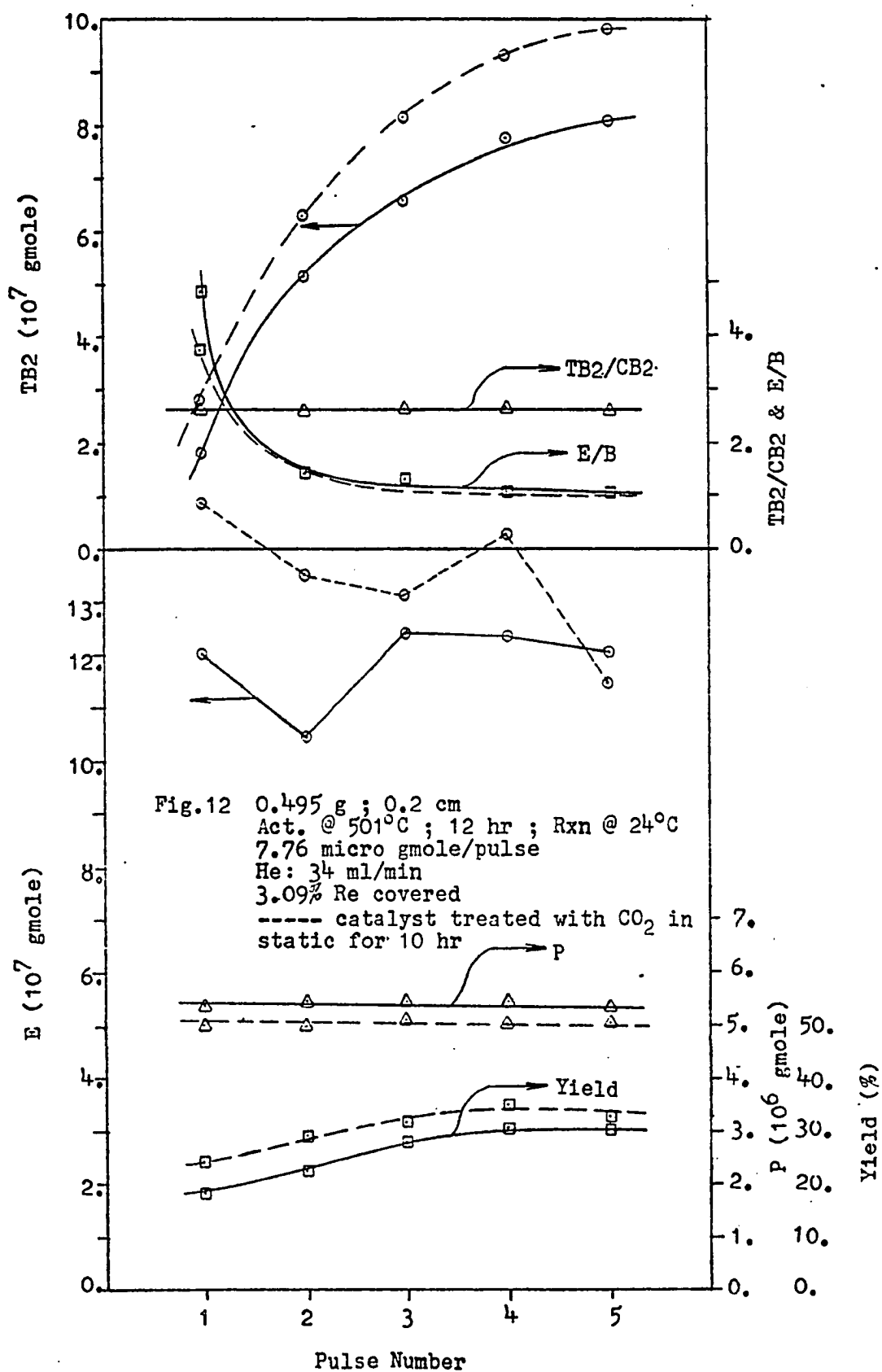
in isolated oxygen. Before introducing the oxygen free helium as the carrier gas to the reactor, the catalyst was evacuated for 5 minutes at the reaction temperature to remove the bulk phase oxygen. A pulse of constant amount, oxygen-free reactant was injected into the carrier gas every 45 minutes and the effluent gas was trapped by liquid nitrogen for further analysis by the thermistor. After the injection and analysis of 5 pulses, the TPD was applied to desorb the chemically adsorbed olefins, followed by the injection of oxygen to burn away the coke so the material balance could be made. The TPD applied was at the rate of $11.68^{\circ}\text{C}/\text{min}$.

Figure 12, a typical result of pulse study, shows product distribution as a function of pulse number. The following table, Table 5, shows the material balance of this study. From these figure and table the following results can be observed:

(1) The production of TB2 increases with pulse number. This fact may be attributed to the extent of surface saturation which increases with pulse number so that TB2 is not as easily adsorbed and/or to the number of active sites for producing TB2 which also increases with pulse number.

(2) TB2/CB2 is always a constant, although it is less than the equilibrium value. This fact may suggest that some kind of thermodynamic equilibrium has been reached between TB2 and CB2.

(3) The production of E is not monotonic.



	Pulse 1	Pulse 2	Pulse 3	Pulse 4	Pulse 5	Flush	TPD
-ΔP	2.367E-6	2.292E-6	2.348E-6	2.324E-6	2.423E-6		
C(%)	30.5	29.5	30.2	29.9	31.2		
E/B	4.867	1.433	1.313	1.089	1.038		
TB2/CB2	2.61	2.62	2.62	2.66	2.60		
Y(%)	18.7	22.9	28.2	30.1	30.5		
E	1.201E-6	1.046E-6	1.241E-6	1.227E-6	1.201E-6	-----	-----
CO ₂	-----	-----	-----	-----	-----	-----	8.782E-7
P	5.393E-6	5.468E-6	5.412E-6	5.437E-6	5.337E-6	7.207E-8	3.071E-7
1-B	3.490E-9	1.930E-8	3.292E-8	4.108E-8	4.477E-8	3.620E-9	4.985E-8
TB2	1.819E-7	5.142E-7	6.577E-7	7.717E-7	8.026E-7	9.435E-8	4.874E-7
CB2	6.958E-8	1.962E-7	2.512E-7	2.897E-7	3.088E-7	3.574E-8	2.177E-7
P ⁺	7.344E-10	4.123E-9	6.127E-9	8.492E-9	9.006E-9	2.993E-9	6.462E-8
Carbon	1.965E-5	2.143E-5	2.250E-5	2.322E-5	2.308E-5	7.936E-7	5.143E-6
Carbon Loss	3.680E-6	1.850E-6	7.730E-7	5.800E-8	2.000E-7	5.964E-6	
Total Loss= 6.560E-6							Deviation= 9.9%
TPD Carbon/Rhenium= 3.09%							

Table 5 0.495 g(0.2cm) ; He: 34 ml/min
 Act. @ 501°C ; 12 hr ; Rxn @ 24°C
 Reactant: 5P ; 7.76 micro gmole/pulse
 (all values are gmole unless specified)

A comparison of the production curves for TB2 and E seems to show that the reaction does not follow the Rideal or Langmuir-Hinshelwood models at the beginning.

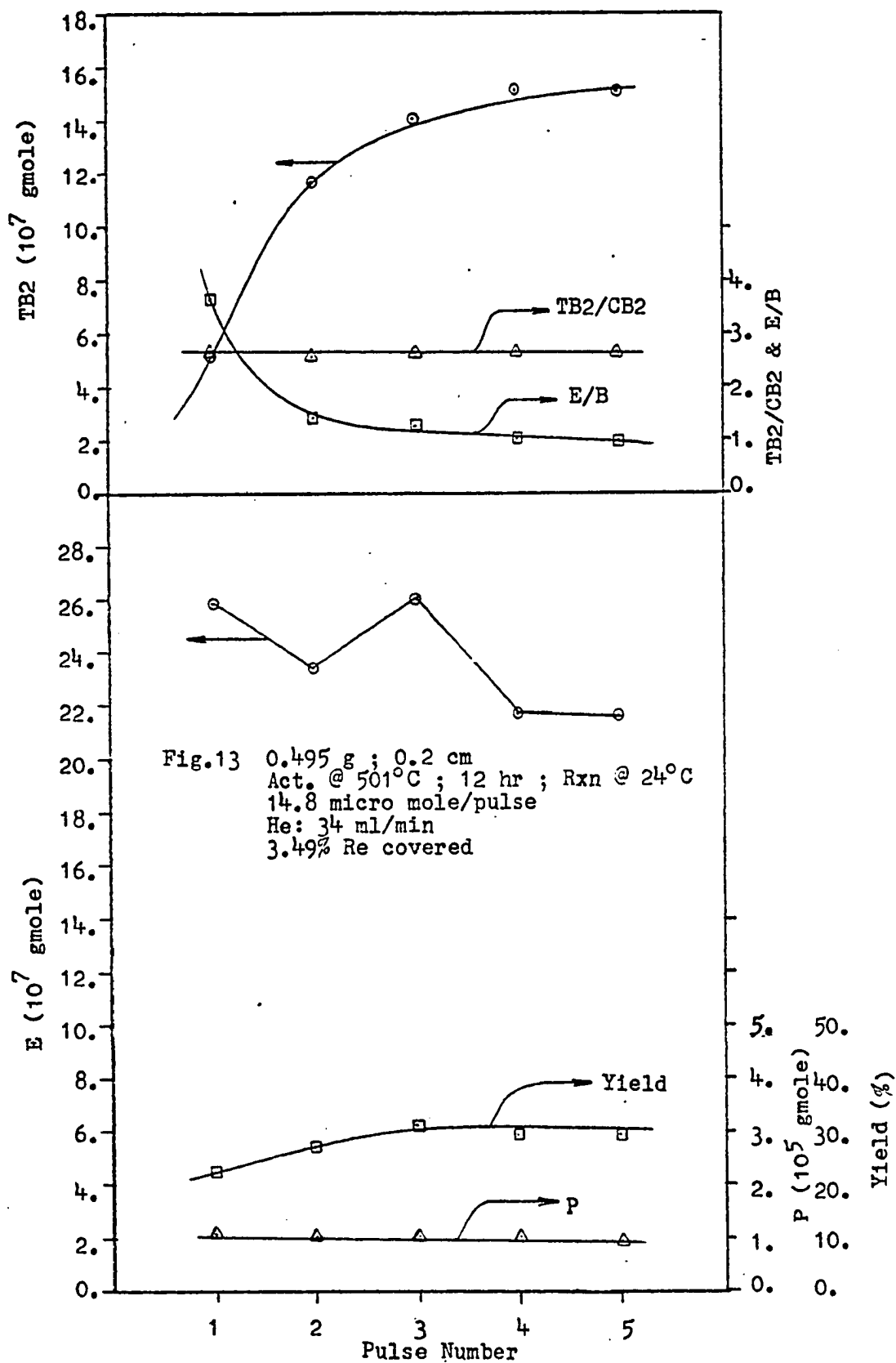
(4) The abnormally high ratio of E/B at the beginning may also support this suggestion that the reaction does not follow the Rideal or Langmuir-Hinshelwood models at the beginning. The ratio of E to B would be unity if the reaction did follow one of these models.

(5) The amount of propylene in the effluent stream is a constant value. Two factors may explain this observation. First, the amount of propylene adsorbed decreases with increasing pulse number, so the amount of propylene in the effluent stream increases with increasing pulse number if the adsorption alone is considered. Secondly, however, the yield increases with increasing pulse number and this may depress the increasing amount of propylene in the effluent. Eventually, the combination of the adsorption and reaction factors gives the constant amount of propylene.

(6) The yield increases with pulse number. This result may be used to support the suggestion that the number of active sites increases upon the reduction of the catalyst by olefins(64,65).

(7) Table 5 shows that after injection of three pulses the surface is likely to be saturated because the carbon loss becomes small and approaches a constant value.

Figure 13, Table 6 and Figure 14, Table 7 demonstrate



	<u>Pulse 1</u>	<u>Pulse 2</u>	<u>Pulse 3</u>	<u>Pulse 4</u>	<u>Pulse 5</u>	<u>Flush</u>	<u>TPD</u>
-ΔP	4.000E-6	4.330E-6	4.500E-6	4.590E-6	4.869E-6		
C(%)	27.0	29.2	30.4	31.0	32.9		
E/B	3.64	1.408	1.282	1.004	0.995		
TB2/CB2	2.63	2.59	2.62	2.66	2.64		
Y(%)	22.3	27.1	31.3	29.4	29.4		
E	2.585E-6	2.345E-6	2.603E-6	2.170E-6	2.164E-6	1.267E-8	-----
CO ₂	-----	-----	-----	-----	-----	-----	1.129E-6
P	1.080E-5	1.047E-5	1.030E-5	1.021E-5	9.931E-6	7.024E-8	3.021E-7
1-B	1.051E-8	4.740E-8	8.086E-8	8.780E-8	1.016E-7	4.079E-9	5.792E-8
TB2	5.111E-7	1.167E-6	1.401E-6	1.508E-6	1.503E-6	1.127E-7	5.331E-7
CB2	1.941E-7	4.509E-7	5.350E-7	5.662E-7	5.702E-7	4.464E-8	2.437E-7
P ⁺	2.839E-9	1.127E-8	1.675E-8	2.267E-8	2.404E-8	5.151E-9	8.279E-8
Carbon	<u>4.044E-5</u>	<u>4.282E-5</u>	<u>4.425E-5</u>	<u>4.373E-5</u>	<u>4.294E-5</u>	<u>9.075E-7</u>	<u>5.788E-6</u>
						6.695E-6	
Carbon Loss	3.953E-6	1.582E-6	1.429E-7	6.685E-7	1.462E-6		

Total Loss= 7.808E-6
 TPD Carbon/Rhenium= 3.49%

Deviation= 16.6%

Table 6 0.495 g(0.2 cm) ; He: 34 ml/min
 Act. @ 501°C ; 12 hr ; Rxn @ 24°C
 Reactant: 5P ; 14.8 micro gmole/pulse
 (all values are gmole unless specified)

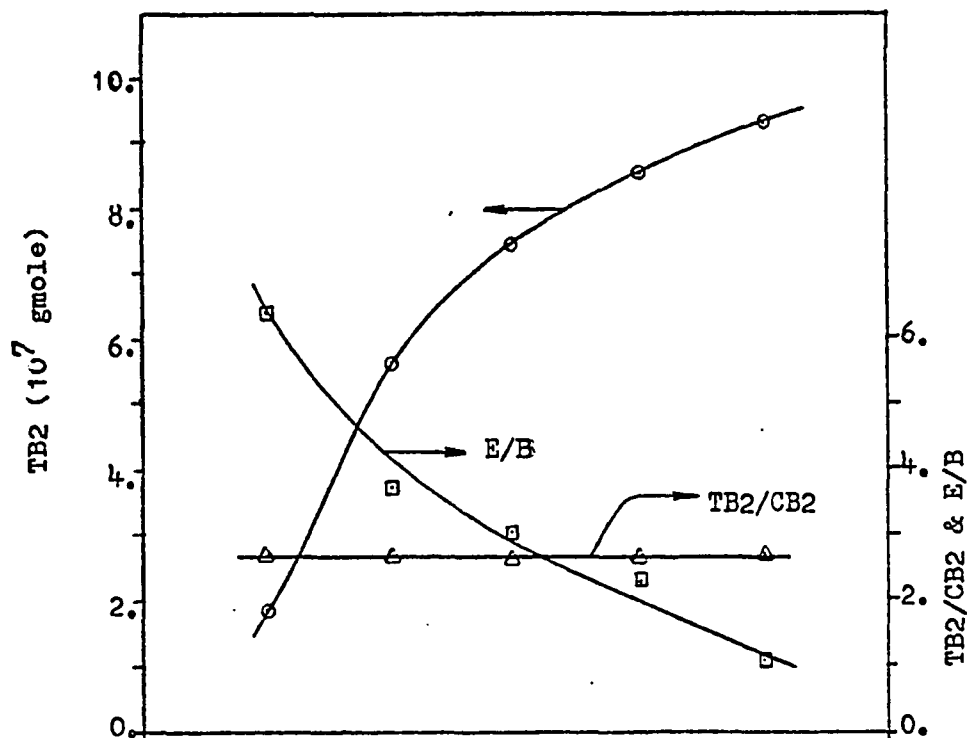
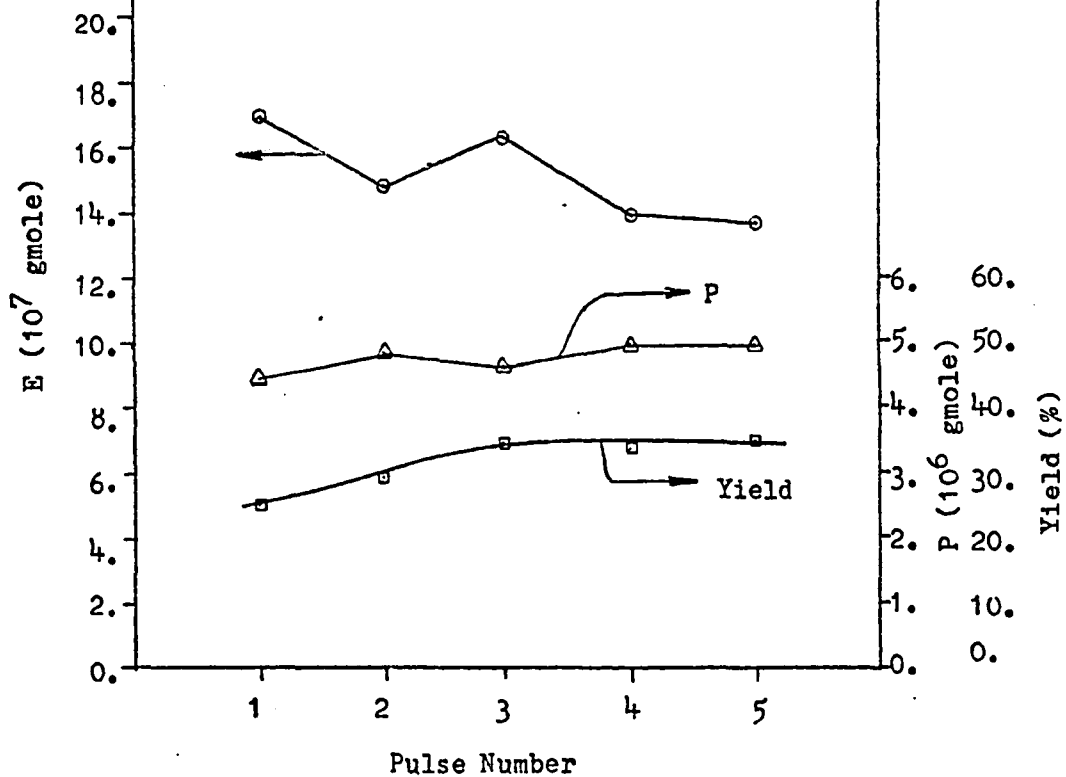


Fig.14 0.495 g ; 0.2 cm
 Act. @ 502°C ; 12 hr ; Rzn @ 24°C
 7.76 micro gmole/pulse
 He: 13 ml/min
 4.0 % Re covered



	<u>Pulse 1</u>	<u>Pulse 2</u>	<u>Pulse 3</u>	<u>Pulse 4</u>	<u>Pulse 5</u>	<u>Flush</u>	<u>TPD</u>
-ΔP	3.337E-6	2.927E-6	3.154E-6	2.777E-6	2.793E-6		
C(%)	43.0	37.7	40.6	35.8	36.0		
E/B	6.4	3.72	3.07	2.29	1.03		
TB2/CB2	2.68	2.68	2.64	2.65	2.66		
Y(%)	25.3	29.3	34.9	33.7	34.7		
E	1.697E-6	1.479E-6	1.636E-6	1.393E-6	1.364E-6	-----	-----
CO ₂	-----	-----	-----	-----	-----	-----	1.113E-6
P	4.423E-6	4.833E-6	4.606E-6	4.983E-6	4.967E-6	2.875E-7	3.823E-7
1-B	7.992E-9	2.176E-8	3.495E-8	3.842E-8	4.190E-8	1.066E-8	6.550E-8
TB2	1.873E-7	5.627E-7	7.470E-7	8.535E-7	9.300E-7	3.280E-7	6.395E-7
CB2	6.987E-8	2.100E-7	2.830E-7	3.220E-7	4.390E-7	1.325E-7	2.860E-7
P ⁺	-----	4.554E-9	6.332E-9	8.703E-9	1.131E-8	1.024E-8	8.944E-8
Carbon	<u>1.773E-5</u>	<u>2.066E-5</u>	<u>2.138E-5</u>	<u>2.263E-5</u>	<u>2.296E-5</u>	<u>2.833E-6</u>	<u>6.672E-6</u>
						9.505E-6	
Carbon Loss	5.550E-6	2.620E-6	1.900E-6	6.520E-7	3.180E-7		

Total Loss= 1.104E-5 Deviation= 13.9%
 TPD Carbon/Rhenium= 4.0%

Table 7 0.495 g (0.2cm) ; He : 13 ml/min
 Act. @ 502°C ; 12 hr ; Rxn @ 24°C
 Reactant: 5P ; 7.76 micro gmole/pulse
 (all values are gmole unless specified)

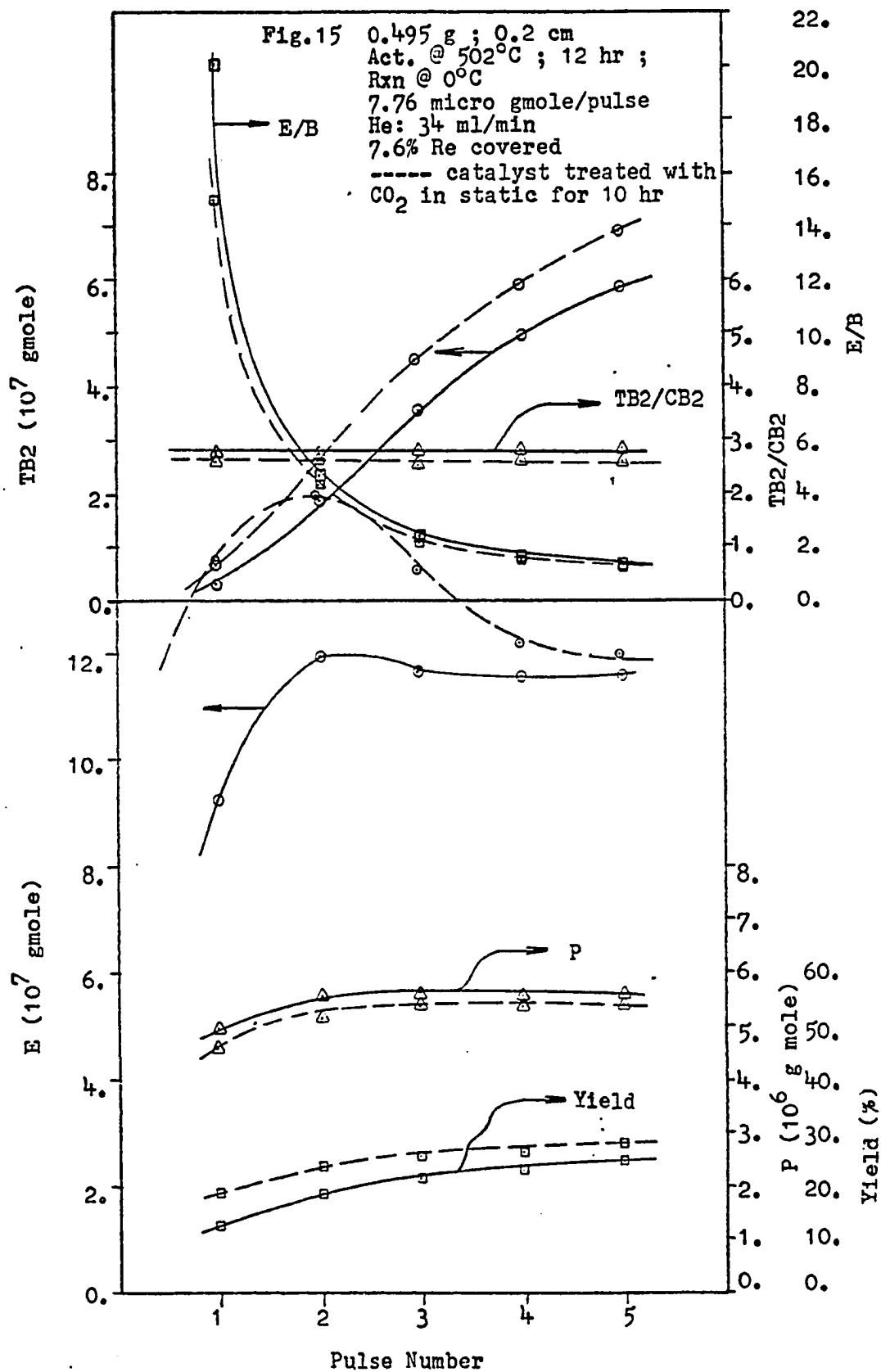
the results using different pulse sizes and carrier gas flow rates from Figure 12, Table 5 respectively. A comparison of Figure 13 with Figure 12 shows a similar product distribution except for the following items: (1) Ethylene drops very quickly after the third pulse. This fact might suggest that the ethylene reacts further and that the extent of the reaction is larger with larger pulse size; (2) The ratio of E/B of the first pulse is slightly lower than that with small pulse size. This fact can be attributed to the double promoting effect caused by the increasing number of active sites for producing B and the increasing amount of reactant.

A greater deviation occurs between Figure 14 and Figure 12: (1) As expected the yield increases because of the slow flow rate; (2) The propylene is less in the effluent stream at the smaller flow rate because of a higher yield and/or more adsorption due to the slower flow rate; (3) Ethylene produced is about one and half times greater than that produced at the higher flow rate. The increasing amount of product because of the slower flow rate is an expected result, but curiously the amount of trans-2-butene does not increase proportionally. This fact suggests that the production of ethylene and trans-2-butene can be through different active sites or different reaction routes. Therefore, the insensitive response of the production of TB2 to the flow rate change results in the slow decrease of the E/B curve; (4) The TB2's in both flow rates of the first pulse are about the

same, which can suggest that a critical concentration of the active sites exists for the production of TB2.

Figure 15 and Table 8 show the result of propylene metathesis at 0°C. Some major observations are as follows: (1) The yield is slightly lower than that shown in Figure 12 because of the lower reaction temperature; (2) More propylene is adsorbed at the first pulse so the propylene curve is not a straight line as was found in Figure 12; (3) The TB2/CB2 is slightly higher than that in Figure 12. This result is reasonable based on the thermodynamic equilibrium conversion; (4) The ethylene production curve is different from that in Figure 12 which can indicate that some kind of reaction occurs between the propylene and the surface and that this reaction is temperature dependent. The surface reduction process can also be a temperature dependent reaction, so the final portion of ethylene curve is also different from that in Figure 12; (5) The TB2 is less than that in Figure 12, which can be attributed to a large adsorption amount at low temperature and/or the slow reduction of the surface at low temperature; (6) The E/B is much larger than that in Figure 12 because of a large adsorption amount of B at low temperature and/or the fact that the productions of E and B follow different paths which can be functions of reaction temperature.

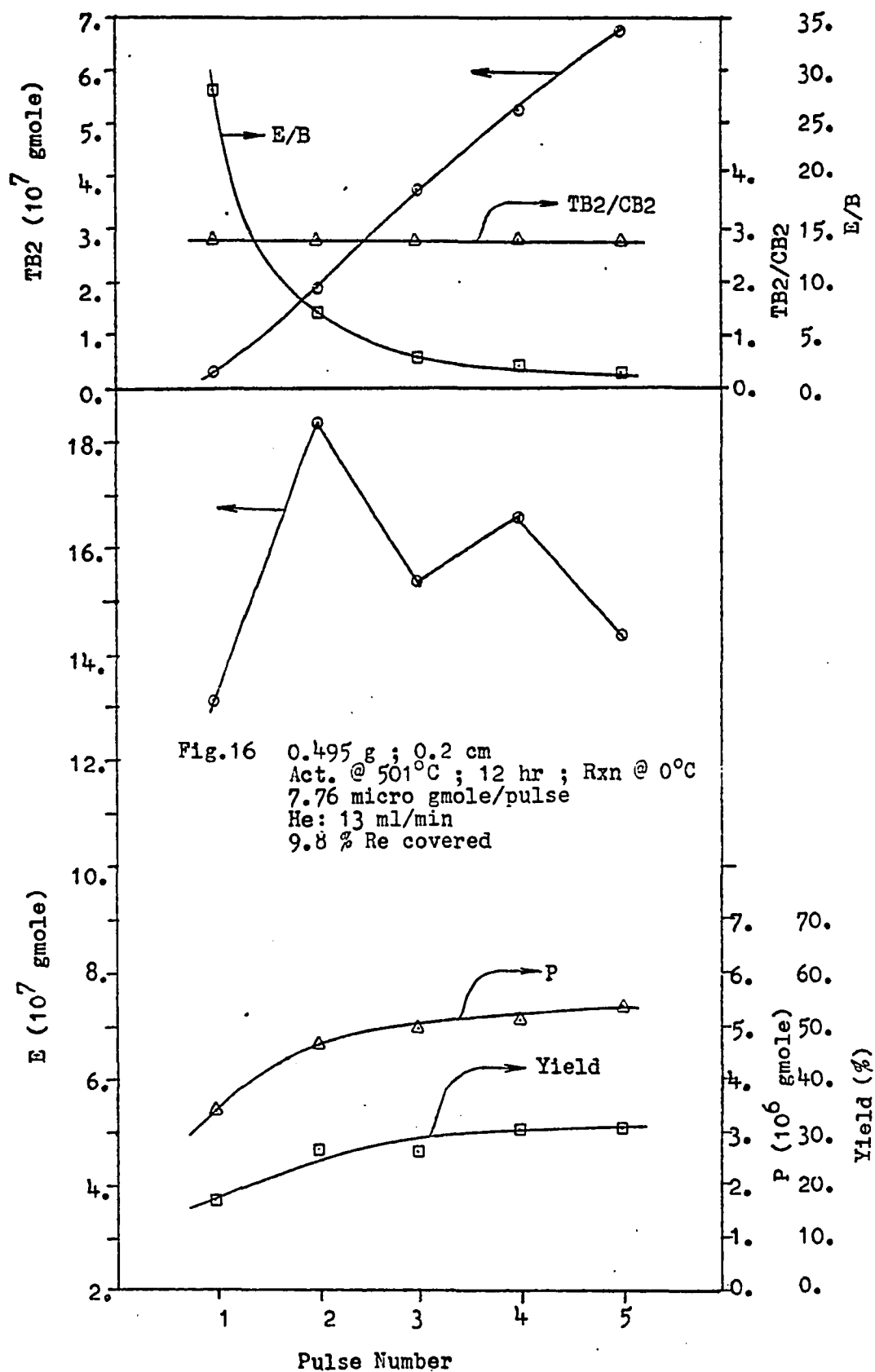
Figure 16 and Table 9 show the same reaction carried out at 0°C and a slower flow rate. Figure 16 indicates some



	<u>Pulse 1</u>	<u>Pulse 2</u>	<u>Pulse 3</u>	<u>Pulse 4</u>	<u>Pulse 5</u>	<u>Flush</u>	<u>TPD</u>
ΔP	2.773E-6	2.714E-6	2.137E-6	2.190E-6	2.183E-6		
C(%)	35.7	28.0	27.53	28.2	28.1		
E/B	20.02	4.632	2.388	1.61	1.37		
TB2/CB2	2.76	2.71	2.79	2.79	2.8		
Y(%)	12.5	18.7	21.3	23.0	24.7		
E	9.235E-7	1.194E-6	1.168E-6	1.104E-6	1.107E-6	1.334E-8	3.665E-8
CO ₂	-----	-----	-----	-----	-----	-----	9.261E-7
P	4.987E-6	5.586E-6	5.623E-6	5.570E-6	5.577E-6	1.926E-7	1.002E-6
1-B	1.713E-9	3.405E-9	7.480E-9	1.480E-8	1.662E-8	1.374E-9	9.010E-8
TB2	3.260E-8	1.858E-7	3.545E-7	4.937E-7	5.830E-7	1.378E-7	1.396E-6
CB2	1.181E-8	6.856E-8	1.271E-7	1.765E-7	2.082E-7	5.000E-8	5.535E-7
P ⁺	-----	-----	8.126E-10	1.078E-9	1.874E-9	-----	1.145E-7
Carbon	<u>1.699E-5</u>	<u>2.018E-5</u>	<u>2.116E-5</u>	<u>2.116E-5</u>	<u>2.218E-5</u>	<u>1.361E-6</u>	<u>1.273E-5</u>
						1.409E-5	
Carbon Loss	6.290E-6	3.100E-6	2.120E-6	1.620E-6	1.090E-6		

Total Loss= 1.422E-5 Deviation= 0.9%
 TPD Carbon/Rhenium= 7.6%

Table 8 0.495 g(0.2 cm) ; He: 34 ml/min
 Act. @ 502°C ; 12 hr ; Rxn @ 0°C
 Reactant: 5P ; 7.76 micro gmole/pulse
 (all values are gmole unless specified)



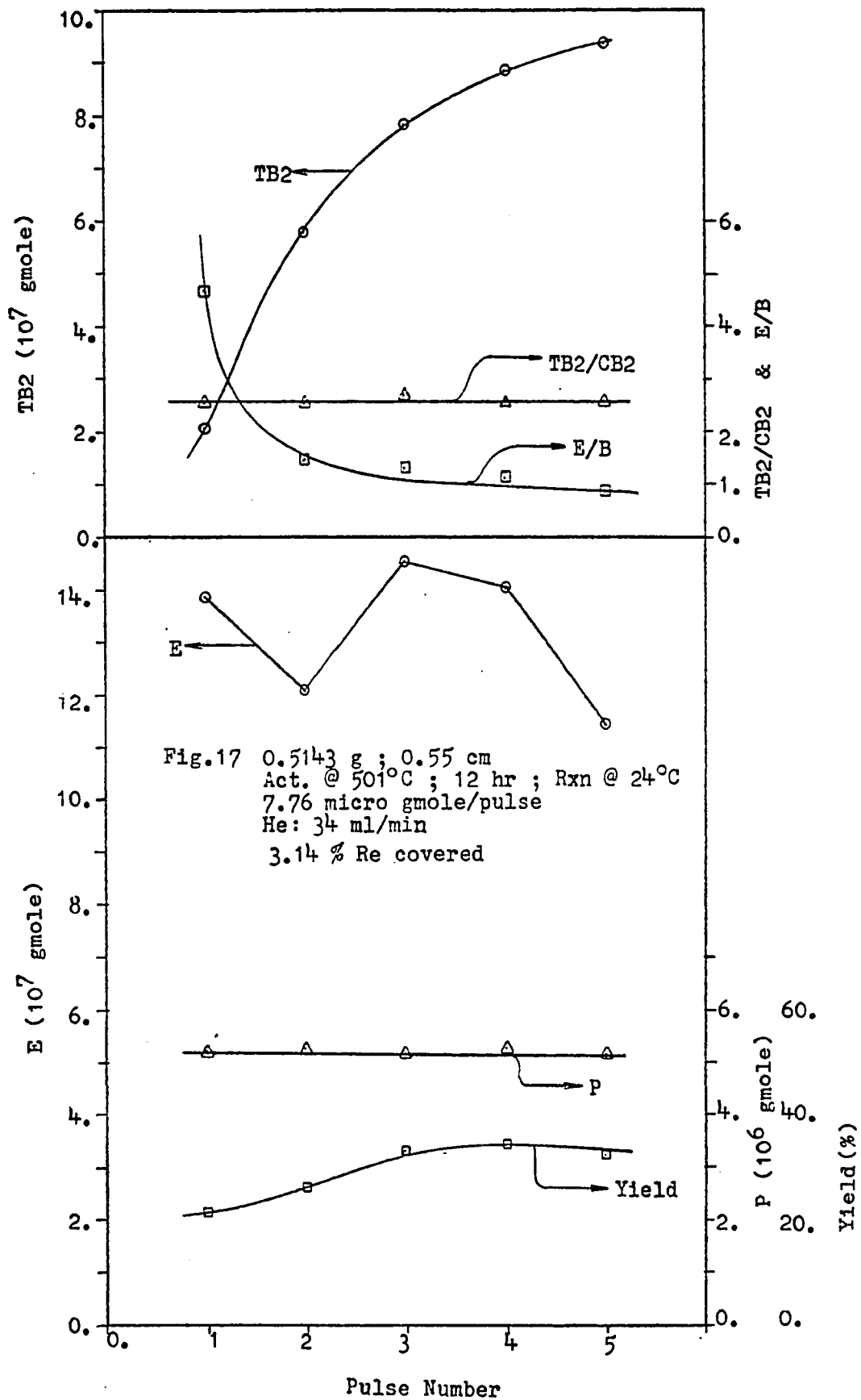
	<u>Pulse 1</u>	<u>Pulse 2</u>	<u>Pulse 3</u>	<u>Pulse 4</u>	<u>Pulse 5</u>	<u>Flush</u>	<u>TPD</u>
-ΔP	4.370E-6	3.100E-6	2.810E-6	2.653E-6	2.423E-6		
C(%)	56.3	39.9	36.2	34.2	31.2		
E/B	28.1	7.06	2.97	2.27	1.52		
TB2/CB2	2.8	2.82	2.77	2.79	2.77		
Y(%)	17.5	27.0	26.5	30.7	30.7		
E	1.316E-6	1.837E-6	1.538E-6	1.654E-6	1.437E-6	4.035E-8	4.927E-8
CO ₂	-----	-----	-----	-----	-----	-----	1.231E-6
P	3.390E-6	4.660E-6	4.950E-6	5.107E-6	5.337E-7	5.770E-7	1.541E-6
1-B	-----	2.842E-9	9.457E-9	1.326E-8	2.220E-8	3.227E-9	1.290E-7
TB2	3.452E-8	1.901E-7	3.732E-7	5.262E-7	6.755E-7	3.207E-7	2.181E-6
CB2	1.232E-8	6.740E-8	1.346E-7	1.887E-7	2.436E-7	1.148E-7	8.167E-8
P ⁺	-----	-----	-----	-----	1.652E-9	1.555E-9	1.723E-7
Carbon	<u>1.389E-5</u>	<u>1.869E-5</u>	<u>1.999E-5</u>	<u>2.154E-5</u>	<u>2.266E-5</u>	<u>3.574E-6</u>	<u>1.638E-5</u>
						1.995E-5	
Carbon Loss	1.029E-5	4.583E-6	3.283E-6	1.738E-6	6.216E-7		

Total Loss= 2.051E-5 Deviation= 2.8%
 TPD Carbon/Rhenium= 9.8%

Table 9 0.495 g(0.2 cm) ; He: 13 ml/min
 Act. @ 501°C ; 12 hr ; Rxn @ 0°C
 Reactant: 5P ; 7.76 micro gmole/pulse
 (all values are gmole unless specified)

interesting points: (1) The tendency of the propylene curve is the same as that in Figure 15. The large adsorption amount at the beginning results in the small amount of propylene in the effluent stream; (2) Because of the higher yield, more TB2 is obtained than was obtained in Figure 15; (3) The TB2's of the first and second pulses are not affected by the flow rate, as seen by comparing them with Figure 15. This fact can again suggest the existence of a critical concentration of the surface active sites for the production of TB2 or even other butenes; (4) The ethylene distribution curve is quite different from that in Figure 15. The drop at the third pulse can suggest a reaction between the surface and the propylene and the original active sites are used up by the first and second pulses; and the slow reduction of the catalyst because of low reaction temperature so new sites can not be produced in time; (5) The high value of E/B of the first pulse is the result of the large adsorption amount of B and/or the existence of a critical value of active sites concentration for producing B.

Figure 17, 18 and Tables 10, 11 demonstrate the results of the same reaction using a thicker bed reactor. A comparison of Figure 17 and 18 with Figures 12 and 13 respectively indicates that the yield and the amount of E and TB2 are higher when the thicker bed reactor is used. Since the thicker bed has more catalyst(3 % more), the longer contact time of the thicker bed reactor may contribute to the increase



	Pulse 1	Pulse 2	Pulse 3	Pulse 4	Pulse 5	Flush	TPD
-ΔP	2.540E-6	2.490E-6	2.590E-6	2.470E-6	2.630E-6		
C(%)	32.7	32.1	33.3	31.8	33.8		
E/B	4.68	1.46	1.3	1.1	0.85		
TB2/CB2	2.53	2.56	2.61	2.54	2.58		
Y(%)	21.7	26.3	33.2	34.5	32.3		
E	1.388E-6	1.210E-6	1.451E-6	1.401E-6	1.144E-6	1.151E-8	1.594E-8
CO ₂	-----	-----	-----	-----	-----	-----	1.013E-6
P	5.220E-6	5.270E-6	5.170E-6	5.290E-6	5.130E-6	6.830E-8	2.878E-7
1-B	4.340E-9	2.231E-8	4.080E-8	4.295E-8	4.730E-8	3.810E-9	5.160E-8
TB2	2.091E-7	5.790E-7	7.805E-7	8.790E-7	9.375E-7	1.077E-7	4.740E-7
CB2	8.278E-8	2.259E-7	2.982E-7	3.467E-7	3.632E-7	4.155E-8	2.090E-7
P ⁺	1.555E-9	5.972E-9	9.778E-9	1.389E-8	1.570E-8	5.664E-9	7.282E-8
Carbon	1.962E-5	2.158E-5	2.293E-5	2.256E-5	2.313E-5	8.687E-7	5.211E-6
						6.079E-6	
Carbon Loss	3.654E-6	1.702E-6	4.370E-7	7.160E-7	1.420E-7		

Total Carbon Loss= 6.560E-6
 TPD Carbon/Rhenium= 3.14%

Deviation= 7.34%

Table 10 0.5143 g(0.55 cm) ; He: 34 ml/min
 Act. @ 501°C ; 12 hr ; Rxn @ 24°C
 Reactant: 5P ; 7.76 micro gmole/pulse
 (all values are gmole unless specified)

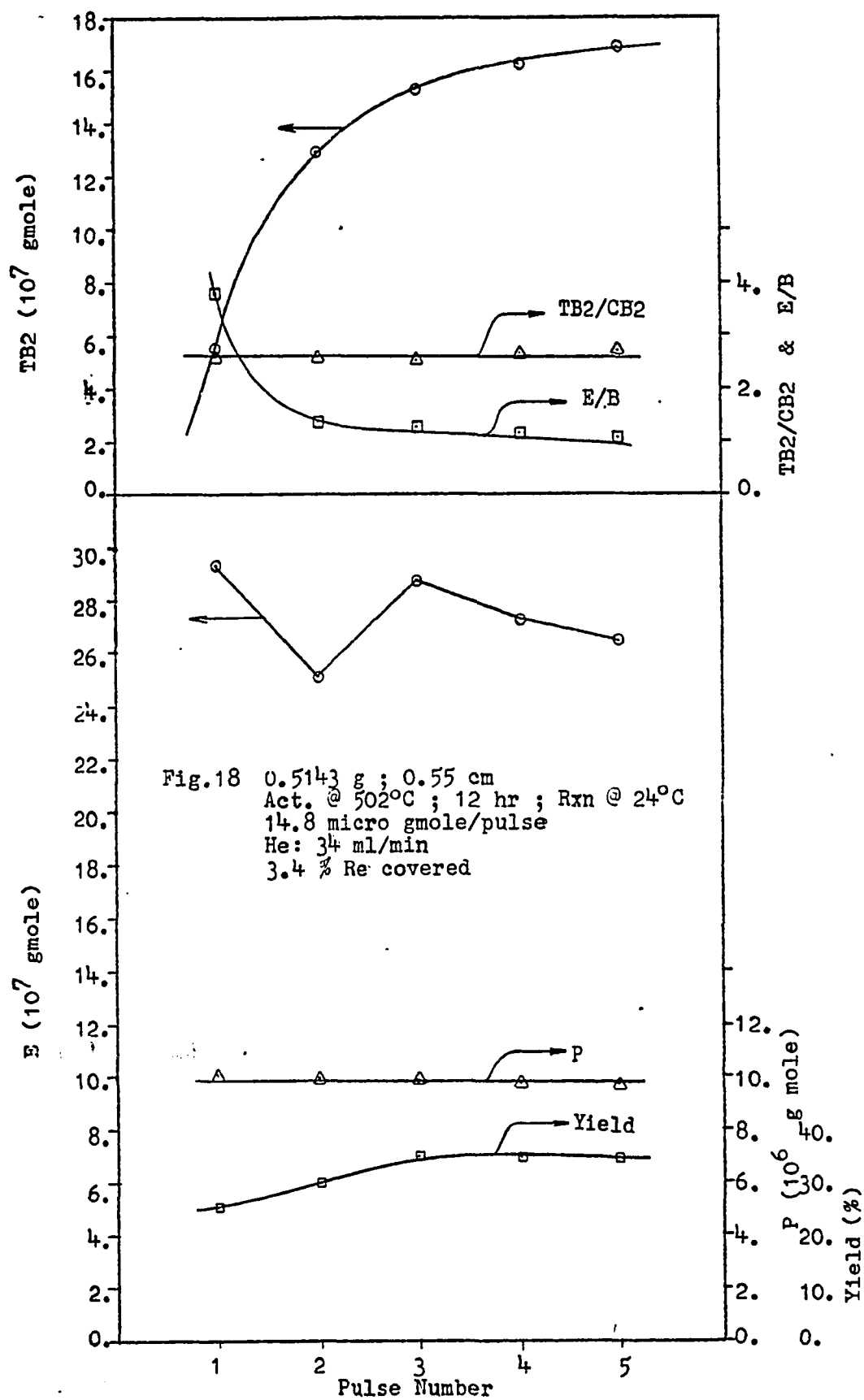


Fig.18 0.5143 g ; 0.55 cm
Act. @ 502°C ; 12 hr ; Rxn @ 24°C
14.8 micro gmole/pulse
He: 34 ml/min
3.4 % Re covered

	Pulse 1	Pulse 2	Pulse 3	Pulse 4	Pulse 5	Flush	TPD
-ΔP	4.740E-6	4.810E-6	4.909E-6	5.033E-6	5.109E-6		
C(%)	32.0	32.5	33.1	34.0	34.5		
E/B	3.78	1.37	1.28	1.16	1.09		
TB2/CB2	2.6	2.61	2.5	2.62	2.72		
Y(%)	25.0	29.5	34.7	34.4	34.3		
E	2.929E-6	2.510E-6	2.873E-6	2.727E-6	2.644E-6	5.233E-9	1.912E-8
CO ₂	-----	-----	-----	-----	-----	-----	1.277E-6
P	1.006E-5	9.990E-6	9.891E-6	9.767E-6	9.691E-6	7.969E-8	3.183E-7
1-B	7.982E-9	5.814E-8	9.350E-8	8.952E-8	1.029E-7	4.925E-9	6.425E-8
TB2	5.553E-7	1.287E-6	1.534E-6	1.631E-6	1.686E-6	1.477E-7	5.766E-7
CB2	2.137E-7	4.925E-7	6.139E-7	6.208E-7	6.180E-7	5.725E-8	2.562E-7
P ⁺	4.356E-9	1.548E-8	2.448E-8	2.991E-8	3.268E-8	7.848E-9	4.335E-9
Carbon	3.916E-5	4.214E-5	4.450E-5	4.427E-5	4.415E-5	<u>1.128E-6</u>	<u>5.880E-6</u>
						7.008E-6	
Carbon Loss	5.240E-6	2.260E-6	-1.00E-7	1.300E-7	2.500E-7		

Total Carbon Loss= 7.780E-6 Deviation= 9.9%
 TPD Carbon/Rhenium= 3.4%

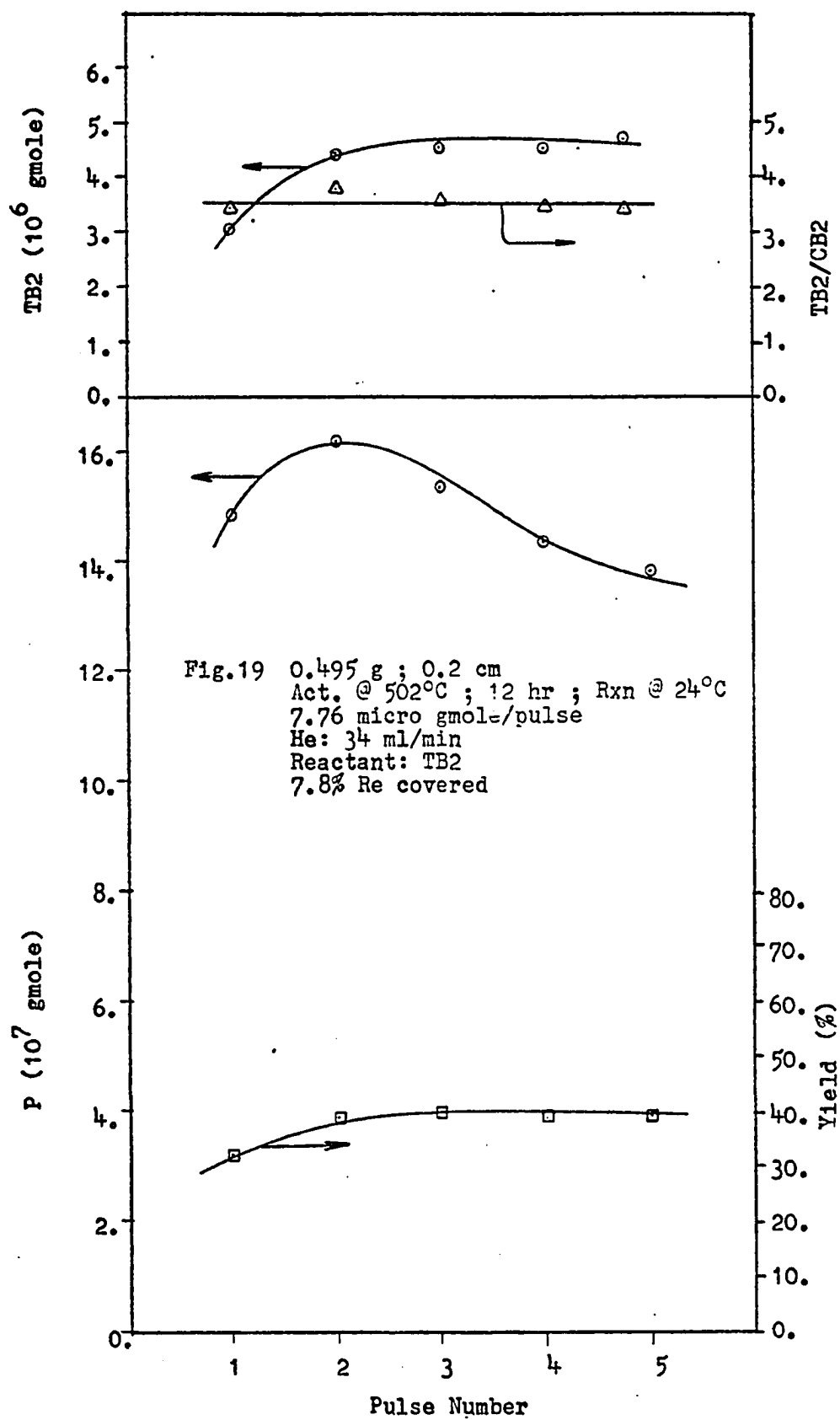
Table 11 0.5143 g (0.55 cm) ; He: 34 ml/min
 Act. @ 502°C ; 12 hr ; Rxn @ 24°C
 Reactant: 5P ; 14.8 micro gmole/pulse
 (all values are gmole unless specified)

of the yield.

The above studies indicate that E/B is always higher than unity initially. Therefore, the Rideal and Langmuir-Hinshelwood models do not seem suitable for the initial reaction, although what is actually occurring is unknown. In order to check whether this observation could be applied to other reactants, TB2 was used as reactant. The results are shown in Figures 19, 20 and Tables 12, 13. These results show that the major product is propylene. Some isomerization products are also observed, i.e., CB2 and 1-B. Therefore, isomerization may be the primary reaction, and followed by metathesis. If metathesis is carried out with 1-B and TB2 or CB2 and if it obeys the Rideal or Langmuir-Hinshelwood model, the initial production of propylene and pentene should have been equal. The tables do not support this prediction.

It is more likely that the initial reaction follows another sequence of steps instead of Rideal and Langmuir-Hinshelwood models, but the Rideal and Langmuir-Hinshelwood models can not be excluded beyond the initiation step because E/B approaches unity after a long reaction time in the flow system study.

In order to determine if the high E/B value at the beginning was due to the adsorption of B or if more E was produced, a one-pulse study was performed. It is discussed in the next section.

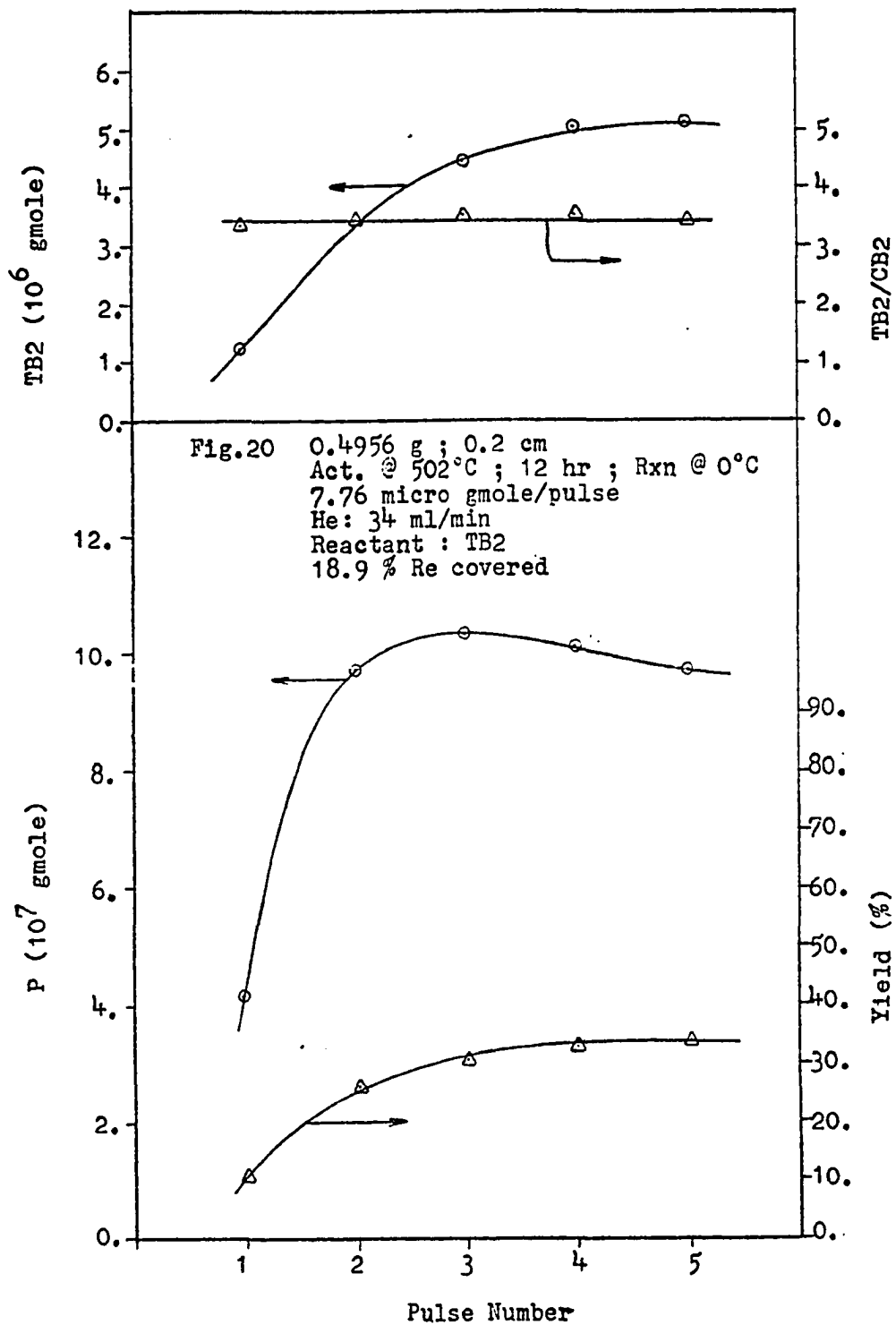


	Pulse 1	Pulse 2	Pulse 3	Pulse 4	Pulse 5	Flush	TPD
-ΔTB2	4.707E-6	3.335E-6	3.217E-6	3.241E-6	3.040E-6		
C(%)	60.0	42.9	41.4	41.7	39.2		
E/B	-----	-----	-----	-----	-----		
TB2/CB2	3.42	3.76	3.59	3.57	3.54		
Y(%)	32.1	39.1	40.1	39.1	39.7		
E	2.171E-8	1.688E-8	1.843E-8	1.162E-8	1.451E-8	1.501E-8	-----
CO ₂	-----	-----	-----	-----	-----	-----	3.739E-6
P	1.481E-6	1.621E-6	1.537E-6	1.439E-6	1.384E-6	8.580E-8	3.428E-7
1-B	3.688E-8	6.795E-8	8.154E-8	8.348E-8	8.736E-8	1.244E-8	1.190E-7
TB2	3.053E-6	4.425E-6	4.544E-6	4.520E-6	4.720E-6	2.608E-7	8.984E-7
CB2	8.909E-7	1.177E-6	1.263E-6	1.263E-6	1.333E-6	9.320E-8	3.695E-7
P ⁺	6.493E-8	1.556E-7	2.137E-7	2.377E-7	2.609E-7	3.792E-8	1.540E-7
Carbon	2.041E-5	2.835E-5	2.926E-5	2.899E-5	3.005E-5	2.429E-6	1.301E-5
						1.544E-5	
Carbon Loss	1.063E-5	2.690E-6	1.780E-6	2.050E-6	9.900E-7		

Total Carbon Loss= 1.814E-5
 TPD Carbon/Rhenium= 7.8%

Deviation= 14.9%

Table 12 0.495 g (0.2 cm) ; He: 34 ml/min
 Act. @ 501°C ; 12 hr ; Rxn @ 24°C
 Reactant: TB2 ; 7.76 micro gmole/pulse
 (all values are gmole unless specified)



	<u>Pulse 1</u>	<u>Pulse 2</u>	<u>Pulse 3</u>	<u>Pulse 4</u>	<u>Pulse 5</u>	<u>Flush</u>	<u>TPD</u>
-ΔTB2	6.545E-6	4.473E-6	3.339E-6	2.739E-6	2.645E-6		
C(%)	84.3	57.6	43.0	35.3	34.1		
E/B	-----	-----	-----	-----	-----		
TB2/CB2	3.35	3.43	3.51	3.55	3.45		
Y(%)	10.7	26.0	30.5	32.7	33.4		
E	-----	-----	-----	-----	-----	-----	-----
CO ₂	-----	-----	-----	-----	-----	-----	3.218E-6
P	4.161E-7	9.765E-7	1.033E-6	1.014E-6	9.741E-7	1.376E-7	1.228E-6
1-B	2.624E-9	9.771E-9	1.571E-8	2.065E-8	2.608E-8	5.898E-9	2.944E-7
TB2	1.249E-6	3.325E-6	4.421E-6	5.021E-6	5.115E-6	5.875E-7	3.908E-6
CB2	3.728E-7	9.693E-7	1.259E-6	1.414E-6	1.480E-6	2.098E-7	1.487E-6
P ⁺	4.675E-9	2.811E-8	6.122E-8	9.286E-8	1.145E-7	2.074E-8	6.793E-7
Carbon	<u>7.768E-6</u>	<u>2.027E-5</u>	<u>2.618E-5</u>	<u>2.932E-5</u>	<u>2.998E-5</u>	<u>3.729E-6</u>	<u>3.305E-5</u>
						3.678E-5	
Carbon Loss	2.327E-5	1.077E-5	4.860E-6	1.720E-6	1.060E-6		

Total Carbon Loss= 4.168E-5 Deviation= 11.7%
 TPD Carbon/Rhenium= 18.9%

Table 13 0.4956 g (0.2 cm) ; He: 34 ml/min
 Act. @ 503°C ; 12 hr ; Rxn @ 0°C
 Reactant: 5TB2 ; 7.76 micro bmole/pulse
 (all values are gmole unless specified)

III-B Study Concerning the E/B Ratio

Since a large adsorption of B may have caused the high value of E/B when propylene was used in the first pulse, a single pulse study followed by TPD may help determine what is really adsorbed on the catalyst and clarify the reason for the high E/B ratio. The procedures were as follows: (1) The catalyst was activated by dry oxygen at 500°C for about 12 hrs. (2) The catalyst was cooled to the reaction temperature in static oxygen. The catalyst was evacuated at reaction temperature for 5 minutes. (3) The carrier gas, oxygen free helium, was introduced to the reactor and the system was purged for half hour. (4) One pulse reactant was injected and the liquid nitrogen trapped product was analyzed. (5) The physically adsorbed hydrocarbons were flushed and followed by TPD at the rate of 11.68°C/min. (6) The liquid nitrogen trapped hydrocarbons obtained from flush and TPD were analyzed. (7) Oxygen was injected pulse by pulse to burn the coke away and the CO₂ was trapped by liquid nitrogen. (8) The material balance for carbon and the ratio of E/B were calculated.

Tables 14, 15, and 16 show in detail the results of this study at different reaction temperatures and bed thicknesses. Independent of the conditions, the ratio of E/B is always greater than unity. The ethylene and butene mentioned here include those obtained from the gas phase product, the amount obtained from flush and the TPD effluent. Accordingly, this study suggests that ethylene and butene are not

	<u>Pulse 1</u>	<u>Flush</u>	<u>TPD</u>
-ΔP	2.347E-6		
C(%)	30.2		
E/B	4.66		
TB2/CB2	2.66		
Y(%)	19.2		
E	1.229E-6	-----	-----
CO ₂	-----	-----	3.535E-7
P	5.413E-6	6.783E-8	3.278E-7
1-B	3.293E-9	-----	1.901E-8
TB2	1.895E-7	2.458E-8	1.976E-7
CB2	7.119E-8	9.758E-9	9.127E-8
P ⁺	9.145E-10	-----	1.807E-8
Carbon	<u>1.976E-5</u>	<u>3.613E-7</u>	<u>2.659E-6</u>
		3.020E-6	
Carbon Loss	3.520E-6		

Total Carbon Loss= 3.520E-6

Deviation= 14%

TPD Carbon/Rhenium= 1.8%

Total E=1.239E-6

Total B=6.062E-7

Total E/B= 2.04

Table 14 0.495 g(0.2 cm) ; He: 34 ml/min
 Act. @ 502°C ; 12 hr ; Rxn @ 24°C
 Reactant: 1P ; 7.76 micro gmole/pulse
 (all values are gmole unless specified)

	<u>Pulse 1</u>	<u>Flush</u>	<u>TPD</u>
-ΔP	2.847E-6		
C(%)	36.7		
E/B	18.67		
TB2/CB2	2.82		
Y(%)	12.4		
E	9.140E-7	4.396E-8	4.334E-8
CO ₂	-----	-----	4.591E-7
P	4.913E-6	1.600E-7	5.730E-7
1-B	-----	-----	3.100E-8
TB2	3.615E-8	1.499E-8	3.905E-7
CB2	1.281E-8	5.195E-9	1.836E-7
P ⁺	-----	-----	2.907E-8
Carbon	<u>1.676E-5</u>	<u>6.489E-7</u>	<u>4.342E-6</u>
		5.451E-6	
Carbon Loss	6.520E-6		

Total Carbon Loss= 6.520E-6
 Deviation= 16.3%
 TPD Carbon/Rhenium= 2.61%

Total E= 1.001E-6
 Total B= 6.742E-7
 Total E/B= 1.48

Table 15 0.495 g(0.2 cm) ; He: 34 ml/min
 Act. @ 502°C ; 12 hr ; Rxn @ 0°C
 Reactant: 1P ; 7.76 micro gmole/pulse
 (all values are gmole unless specified)

	<u>Pulse 1</u>	<u>Flush</u>	<u>TPD</u>
-ΔP	2.524E-6		
C(%)	32.5		
E/B	4.24		
TB2/CB2	2.66		
Y(%)	21.6		
E	1.357E-6	7.365E-9	2.111E-8
CO ₂	-----	-----	6.306E-7
P	5.236E-6	4.224E-8	2.198E-7
1-B	4.930E-9	6.742E-10	2.424E-8
TB2	2.288E-7	3.406E-8	2.425E-7
CB2	8.600E-8	1.250E-8	1.076E-7
P ⁺	1.299E-9	1.042E-9	2.504E-8
Carbon	<u>1.970E-5</u>	<u>3.355E-7</u>	<u>2.955E-6</u>
		3.290E-6	

Carbon
Loss 3.570E-6

Total Carbon Loss= 3.570E-6
Deviation= 8%
TPD Carbon/Rhenium= 1.73%

Total E= 1.385E-6
Total B= 7.413E-7
Total E/B= 1.87

Table 16 0.5143 g (0.55 cm) ; He: 34 ml/min
Act. @ 503°C ; 12 hr ; Rxn @ 24°C
Reactant: 1P ; 7.76 micro gmole/pulse
(all values are gmole unless specified)

produced in equal amounts. The Rideal and Langmuir-Hinshelwood models may not adequately describe the initial reaction.

Table 17 shows the result when TB2 was used as a reactant. This table indicates that propylene is the major product and that the ratio of propylene to pentene is greater than unity, which again illustrates that the metathesis products are not produced in equal amount initially.

Rooney et al. (57) proposed that three moles ethylene produced two moles propylene when ethylene was added to the reactor where propylene had been reacted, and ethylene and butene were observed prior to the injection of ethylene. If this reaction is reversible, it may cause the high E/B value mentioned above, i.e., two moles propylene produce three moles ethylene. In order to test this possibility, the experimental work described in Section III-C was carried out.

III-C Surface Titration Study of Used Catalyst by Ethylene

If the reverse of the reaction proposed by Rooney et al. (57) may be used to explain the high value of E/B, the catalyst can provide active centers for reaction without the involvement of hydrocarbons already adsorbed on the catalyst.

In this section results will be discussed to see if the assumption "no surface hydrocarbons are involved in the production of propylene from ethylene" is true. If the assumption is not true, the reverse reaction will in all likelihood not be true, nor will the high value of E/B be due to

	<u>Pulse 1</u>	<u>Flush</u>	<u>TPD</u>
-ΔTB2	4.643E-6		
C(%)	59.8		
E/B	-----		
TB2/CB2	3.42		
Y(%)	32.2		
E	2.168E-8	-----	-----
CO ₂	-----	-----	1.736E-6
P	1.466E-6	1.000E-7	3.550E-7
1-B	3.750E-8	8.037E-9	7.527E-8
TB2	3.117E-6	2.035E-7	6.842E-7
CB2	9.097E-7	8.357E-8	3.100E-7
P ⁺	6.550E-8	1.390E-8	1.239E-7
Carbon	2.102E-5	<u>1.549E-6</u>	<u>7.696E-6</u>
		9.245E-6	
Carbon Loss	1.002E-5		
Total Carbon Loss=1.002E-5			
Deviation= 8.4%			
TPD Carbon/Rhenium= 4.63%			
		Total E=2.186E-8	
		Total P=1.921E-6	
		Total B=5.428E-6	
		Total P ⁺ =2.033E-7	
Table 17	0.4956 g (0.2 cm) ; He: 34 ml/min		
	Act. @ 501°C ; 12 hr ; Rxn @ 24°C		
	Reactant: 1TB2 ; 7.76 micro gmole/pulse		
	(all values are gmole unless specified)		

the production of three moles ethylene from two moles propylene.

The ethylene reaction on the activated catalyst was tested and the result shows that there is no reaction at all and that the adsorption amount is negligible. Therefore, ethylene may be used as the surface titration agent. The procedures were the same as those mentioned in last section except that ethylene pulses were injected after the injection of propylene pulse(s). Finally, the TPD and oxygen pulses were carried out so that the material balance could be made.

Table 18 shows the result of the injection of one pulse propylene and five pulses ethylene. Note that the carbon loss is negative when ethylene is injected. Such negative loss means that the output is greater than the input, so that some carbon must have been removed from the surface and thus the reaction occurs between ethylene and adsorbed hydrocarbons. Some other relationships drawn from the material balance are also shown: (1) The summation of numbers of moles of P and B is close to the loss of E (compare $P+B$ and $-\Delta R$) when E is used; (2) The summation of one times the number of moles of P and two times the number of moles of B is close to the carbon loss (compare $1xP+2xB$ with carbon loss) when E is used. These observations suggest that the carbene mechanism is responsible for the reaction, but other possibilities can not be excluded without further direct evidence. Another interesting point is that the summation of negative carbon

	<u>Pulse 1</u>	<u>Pulse 2</u>	<u>Pulse 3</u>	<u>Pulse 4</u>	<u>Pulse 5</u>
-ΔR	2.214E-6	5.450E-7	2.950E-7	1.250E-7	3.500E-8
C(%)	28.5	7.0	3.8	1.6	0.83
E/B	3.68	-----	-----	-----	-----
TB2/CB2	2.62	2.65	2.54	2.63	-----
P+B	-----	5.541E-7	2.611E-7	1.373E-7	7.667E-8
1xP+2xB	-----	7.177E-7	2.816E-7	1.425E-7	7.667E-8
E	1.219E-6	7.215E-6	7.465E-6	7.635E-6	7.695E-6
	2.438E-6	1.443E-5	1.493E-5	1.527E-5	1.539E-5
CO ₂	-----	-----	-----	-----	-----
P	5.546E-6	4.906E-7	2.505E-7	1.320E-7	7.667E-8
	1.664E-5	1.472E-6	7.517E-7	3.960E-7	2.300E-7
1-B	5.585E-9	3.327E-9	-----	-----	-----
	2.234E-8	1.331E-8	-----	-----	-----
TB2	2.356E-7	4.372E-8	1.117E-8	3.830E-9	-----
	9.425E-7	1.749E-7	4.468E-8	1.532E-8	-----
CB2	8.972E-8	1.651E-8	4.406E-9	1.453E-9	-----
	3.589E-7	6.607E-8	1.762E-8	5.813E-9	-----
P ⁺	7.804E-10	-----	-----	-----	-----
	3.902E-9	-----	-----	-----	-----
Carbon	2.040E-5	1.615E-5	1.574E-5	1.568E-5	1.562E-5
Carbon	2.880E-6	-6.30E-7	-2.20E-7	-1.60E-7	-1.00E-8
Loss					

Table 18 0.495 g (0.2 cm) ; He: 34 ml/min
 Act. @ 504°C ; 12 hr ; Rxn @ 24°C
 Reactant: 1P-5E ; 7.76 micro gmole/pulse
 (continued on next page)
 (all values are gmole unless specified)

Table 18(continued)

	<u>Pulse 6</u>	<u>Flush</u>	<u>TPD</u>
-ΔR	3.500E-8		
C(%)	0.49		
E/B	-----		
TB2/CB2	-----		
P+B	5.153E-8		
1xP+2xB	5.153E-8		
E	7.725E-6	1.584E-8	1.894E-8
	1.545E-5	3.168E-8	3.788E-8
CO ₂	-----	-----	2.355E-7
	-----	-----	2.355E-7
P	5.153E-8	8.670E-9	1.762E-7
	1.546E-7	2.601E-8	5.286E-7
1-B	-----	-----	1.035E-8
	-----	-----	4.141E-8
TB2	-----	-----	8.086E-8
	-----	-----	3.234E-7
CB2	-----	-----	3.933E-8
	-----	-----	1.573E-7
P ⁺	-----	-----	3.921E-9
	-----	-----	1.960E-8
Carbon	1.560E-5	5.769E-8	1.343E-6
		1.401E-6	
Carbon Loss	-8.00E-8		

Total Carbon Loss= 1.690E-6

Deviation= 15.1%

TPD Carbon/Rhenium= 0.81%

loss and carbon obtained from TPD is close to the carbon number obtained from TPD in Table 14, which again indicates carbon removal from the surface and the tight material balance.

Table 19 shows the result of the injection of one pulse P, five pulses E, and one pulse P at 24°C. The interesting points in Table 18 are also observed in this table. The final pulse of propylene produce similar amount of ethylene to the first pulse and more ethylene than the second pulse of Table 5, which suggest that some kind of surface intermediate, probably a carbene, has the same effect in producing ethylene as the oxygen activated catalyst. The B produced from the final propylene pulse is slightly higher than that of the first pulse and less than that of the second pulse in Table 5. This fact may indicate that some kind of surface species has the effect in producing butenes, and such surface species were partially destroyed by the reaction with ethylene.

Table 20 shows the result of the injection of two pulses P, seven pulses E, and two pulses P at 0°C. Again, the points shown in Table 18 are observed in this table. Furthermore, the most interesting result is the ethylene production of the tenth pulse. A comparison with Table 8 indicates that the ethylene production of the third pulse in Table 8 decreases instead of increasing as shown in the tenth pulse of the Table 20. In addition, the ethylene produced in the tenth pulse is much greater than that in the first

	Pulse 1	Pulse 2	Pulse 3	Pulse 4	Pulse 5	Pulse 6
$-\Delta R$	2.177E-6	5.650E-7	2.250E-7	1.500E-7	7.000E-8	6.000E-8
C(%)	28.1	7.3	2.89	1.93	0.9	0.77
E/B	3.69	-----	-----	-----	-----	-----
TB2/CB2	2.65	2.69	2.48	2.32	-----	-----
P+B	-----	5.948E-7	2.491E-7	1.316E-7	8.346E-8	4.870E-8
1xP+2xB	-----	6.607E-7	2.648E-7	1.365E-7	8.346E-8	4.870E-8
E	1.208E-6	7.195E-6	7.535E-6	7.610E-6	7.690E-6	7.700E-6
	2.417E-6	1.439E-5	1.507E-5	1.522E-5	1.538E-5	1.541E-5
CO ₂	-----	-----	-----	-----	-----	-----
P	5.583E-6	5.290E-7	2.334E-7	1.267E-7	8.346E-8	4.870E-8
	1.675E-5	1.587E-6	7.002E-7	3.801E-7	2.504E-7	1.461E-7
1-B	6.067E-9	3.882E-9	8.050E-10	1.937E-11	-----	-----
	2.427E-8	1.553E-8	3.220E-9	7.750E-11	-----	-----
TB2	2.331E-7	4.520E-8	1.062E-8	3.425E-9	-----	-----
	9.324E-7	1.808E-7	4.251E-8	1.370E-8	-----	-----
CB2	8.785E-8	1.676E-8	4.274E-9	1.477E-9	-----	-----
	3.514E-7	6.707E-8	1.710E-8	5.910E-9	-----	-----
P ⁺	1.600E-11	-----	-----	-----	-----	-----
	8.000E-11	-----	-----	-----	-----	-----
Carbon	2.047E-5	1.624E-5	1.583E-5	1.562E-5	1.563E-5	1.555E-5
Carbon Loss	2.810E-6	-7.20E-7	-3.10E-7	-1.10E-7	-1.10E-7	-3.00E-8

Table 19 0.495 g (0.2 cm) ; He: 34 ml/min
 Act. @ 500°C ; 12 hr ; Rxn @ 24°C
 Reactant: 1P-5E-1P ; 7.76 micro gmole/pulse
 (continued on next page)
 (all values are gmole unless specified)

Table 19(continued)

	<u>Pulse 7</u>	<u>Flush</u>	<u>TPD</u>
-ΔR	2.400E-6		
C(%)	31.0		
E/B	2.61		
TB2/CB2	2.5		
P+B	-----		
1xP+2xB	-----		
E	1.266E-6	8.360E-9	1.750E-8
	2.532E-6	1.672E-8	3.500E-8
CO ₂	-----	-----	7.167E-7
	-----	-----	7.167E-7
P	5.353E-6	4.656E-8	2.126E-7
	1.606E-5	1.397E-7	6.378E-7
1-B	8.662E-9	-----	2.752E-8
	3.465E-8	-----	1.101E-7
TB2	3.407E-7	4.245E-8	2.630E-7
	1.363E-6	1.698E-7	1.052E-6
CB2	1.362E-7	1.585E-8	1.151E-7
	5.451E-7	6.342E-8	4.607E-7
P ⁺	2.068E-8	-----	2.978E-8
	1.034E-8	-----	1.489E-7
Carbon	2.054E-5	<u>3.896E-7</u>	<u>3.161E-6</u>
		3.550E-6	
Carbon Loss	2.740E-6		

Total Carbon Loss= 4.270E-6

Deviation= 16.8%

TPD Carbon/Rhenium= 1.9%

	<u>Pulse 1</u>	<u>Pulse 2</u>	<u>Pulse 3</u>	<u>Pulse 4</u>	<u>Pulse 5</u>	<u>Pulse 5</u>	<u>Pulse 7</u>
-ΔR	2.457E-6	2.151E-6	9.220E-7	5.730E-7	4.330E-7	2.780E-7	2.080E-7
C(%)	31.6	27.7	11.9	7.4	5.5	3.6	2.7
E/B	13.04	3.61	-----	-----	-----	-----	-----
TB2/CB2	2.91	2.84	2.88	2.71	2.82	2.80	2.80
P+B	-----	-----	1.152E-6	6.362E-7	4.204E-7	2.642E-7	1.870E-7
1xP+2xB	-----	-----	1.416E-6	7.679E-7	4.924E-7	2.971E-7	2.105E-7
E	8.945E-7	1.160E-6	6.838E-6	7.187E-6	7.327E-6	7.482E-6	7.552E-6
	1.789E-6	2.321E-6	1.367E-5	1.437E-5	1.465E-5	1.496E-5	1.510E-5
CO ₂	-----	-----	-----	-----	-----	-----	-----
P	5.303E-6	5.609E-6	8.880E-7	5.046E-7	3.484E-7	2.313E-7	1.635E-7
	1.591E-5	1.683E-5	2.664E-6	1.514E-6	1.045E-6	6.939E-7	4.905E-7
1-B	-----	2.704E-9	5.927E-9	5.864E-9	-----	-----	-----
	-----	1.082E-8	2.370E-8	2.345E-8	-----	-----	-----
TB2	5.107E-8	2.149E-7	1.918E-7	9.192E-8	5.315E-8	2.425E-8	1.732E-8
	2.043E-7	8.596E-7	7.673E-7	3.676E-7	2.125E-7	9.700E-8	6.931E-8
CB2	1.751E-8	7.560E-8	6.642E-8	3.388E-8	1.888E-8	8.660E-9	6.188E-9
	7.004E-8	3.024E-7	2.657E-7	1.355E-7	7.552E-8	3.464E-8	2.475E-8
P ⁺	-----	-----	-----	-----	-----	-----	-----
	-----	-----	-----	-----	-----	-----	-----
Carbon	1.797E-5	2.032E-5	1.739E-5	1.641E-5	1.598E-5	1.578E-5	1.568E-5
Carbon Loss	5.306E-6	2.956E-6	-1.87E-6	-8.90E-7	-4.67E-7	-2.65E-7	-1.69E-7

Table 20 0.495 g (0.2 cm) ; He: 34 ml/min
 Act. @ 500°C ; 12 hr ; Rxn @ 0°C
 Reactant: 2P-7E-2P ; 7.76 micro gmole/pulse
 (continued on next page)
 (all values are gmole unless specified)

Table 20
(continued)

	Pulse 8	Pulse 9	Pulse 10	Pulse 11	Flush	TPD
ΔR	1.320E-7	9.000E-8	2.697E-6	2.340E-6		
C(%)	1.7	1.1	34.7	30.1		
E/B	-----	-----	7.04	2.34		
TB2/CB2	-----	-----	3.01	2.84		
P+B	1.144E-7	8.694E-8	-----	-----		
1xP+2xB	1.144E-7	8.694E-8	-----	-----		
E	7.628E-6	7.670E-6	1.293E-6	1.080E-6	1.848E-8	3.315E-8
	1.525E-5	1.534E-5	2.586E-6	2.160E-6	3.697E-8	6.630E-8
CO ₂	-----	-----	-----	-----	-----	7.007E-7
	-----	-----	-----	-----	-----	7.007E-7
P	1.144E-7	8.694E-8	5.063E-6	5.420E-6	1.818E-7	8.452E-7
	3.432E-7	2.608E-7	1.518E-5	1.626E-5	5.454E-7	2.536E-6
1-B	-----	-----	2.101E-9	7.137E-9	-----	6.808E-8
	-----	-----	8.404E-9	2.855E-8	-----	2.723E-7
TB2	-----	-----	1.363E-7	3.361E-7	9.665E-8	1.102E-6
	-----	-----	5.452E-7	1.344E-6	3.866E-7	4.408E-6
CB2	-----	-----	4.520E-8	1.182E-7	3.252E-8	4.578E-7
	-----	-----	1.808E-7	4.728E-7	1.300E-7	1.831E-6
P ⁺	-----	-----	-----	-----	-----	8.375E-8
	-----	-----	-----	-----	-----	4.187E-7
Carbon	1.559E-5	1.560E-5	1.850E-5	2.026E-5	1.099E-6	1.023E-5
Carbon Loss	-7.00E-8	-8.00E-8	4.779E-6	3.014E-6		

Total Carbon Loss= 1.246E-5
 Deviation= 9.0%
 TPD Carbon/Rhenium= 6.16%

pulse. The surface "wash" by ethylene seems to be the only reason for this difference. Accordingly, this ethylene wash may create some kind of active site, probably a carbene, which is suitable for the production of ethylene. The butenes produced by the tenth pulse are more than the amount produced by the first pulse but less than that by the third pulse of Table 8. This result can occur because the wash process does not completely destroy the active site responsible for B production. Similar phenomena are also observed when comparing Table 19 with Table 5.

IV. TEMPERATURE PROGRAMMED DESORPTION STUDY

The temperature programmed desorption (TPD) method is very useful for studying catalyst surface properties, the adsorption state of the adsorbed material(46,47,54), the thermodynamic properties of the desorption process, the function of the adsorption site for reaction(54), and even the reaction mechanism(66). In the preceding section, the TPD combined with the pulse technique was used to determine the reaction route for propylene metathesis. Although this method was applied to desorb the adsorbed olefins so that a material balance could be made, how these olefins adsorbed on the surface is still unknown. In this section, the results from TPD are discussed in relation to this question.

The procedure for doing the TPD study included several

steps: (1) catalyst activation (2) preadsorption of the adsorbate (3) removal of the physically adsorbed gas (4) programmed desorption of the chemically adsorbed residue (5) recording of the TPD chromatogram (6) trapping of the desorbed residue (7) analysis of the trapped material.

All the procedures before the TPD were the same as those described in last section. The TPD was carried out after the injection of five pulses propylene and 15-minute flush with carrier gas.

IV-A Physical or Chemical Adsorption of Residue

TPD technique is only suitable for chemically adsorbed residues. Therefore a check had to be made to see if the residues were chemically or physically adsorbed under the proposed experimental procedures.

Columns 1 and 4 of Table 21 show the results of this check. The result shown in column 1 was obtained using the proposed procedure, while in column 4 an evacuation step was added before the TPD run. The results show that the evacuation does not affect the result of TPD run, so the residues are chemically adsorbed under the proposed procedure.

Accordingly, the evacuation step to remove physically adsorbed residue is not necessary, since the flush with carrier gas has the same function as evacuation.

	<u>5 psia*</u> <u>5 pulses</u>	<u>5 psia</u> <u>9 pulses</u>	<u>5 psia</u> <u>1 pulse</u>	<u>5 psia</u> <u>5 pulses</u> <u>Evac. 30 min</u> <u>before TPD</u>	<u>10 psia*</u> <u>5 pulses</u>	<u>5 psia</u> <u>5 pulses</u> <u>in static He</u> <u>for 65 hr</u>
E	4.054E-8	3.956E-8	4.793E-8	4.619E-8	3.099E-8	4.003E-8
CO ₂	6.730E-7	7.484E-7	2.955E-7	7.304E-7	1.014E-6	9.119E-7
P	1.969E-7	2.102E-7	2.520E-7	2.233E-7	2.664E-7	2.156E-7
1-B	4.258E-8	4.095E-8	2.372E-8	4.193E-8	5.185E-8	3.294E-8
TB2	3.766E-7	3.953E-7	2.430E-7	4.291E-7	4.954E-7	3.979E-7
CB2	1.688E-7	1.732E-7	1.048E-7	1.873E-7	2.057E-7	1.694E-7
∞ P ⁺	6.447E-8	6.823E-8	2.581E-8	6.279E-8	9.246E-8	4.919E-8
Carbon	4.019E-6	4.236E-6	2.762E-6	4.439E-6	5.350E-6	4.285E-6
Carbon/Re	2.34	2.46	1.61	2.57	3.11	2.49

Table 21 Comparison of the hydrocarbons obtained via TPD
with different preadsorption conditions
0.5119 g (0.55 cm) ; He: 34 ml/min for both reaction
and TPD
Act. @ 502°C ; 12 hr ; Rxn @ 24°C
TPD rate @ 5.9°C/min
Reactant: P
*5 psia= 7.299 micro gmole/pulse
10 psia= 14.64 micro gmole/pulse
(all values are gmole unless specified)

IV-B Interaction Between the Adsorbed Residues

A comparison of column 6 in Table 21 with column 1 shows that the residue does not undergo reaction before beginning the TPD run. The increased amount of CO_2 may be caused by the undesorbed P^+ . However, a conclusion that there is absolutely no reaction between the residues can not be drawn, because the reaction may already have occurred and reached equilibrium. Thus, based solely on this comparison, it can not be concluded that the Langmuir-Hinshelwood model does not fit this reaction.

IV-C Effect of Different Preadsorption Conditions

Columns 1,2,3, and 5 of Table 21 demonstrate the effect of different preadsorption conditions. Columns 1 and 2 indicate that after the injection of five pulses, the surface reaches a saturation state under the indicated pulse size. A similar conclusion may also be drawn from the material balance tables in Section III-A. Those tables show that the surface is close to saturation state after the third pulse, if the carbon loss is considered.

Columns 1 and 3 show that the surface is not at a saturation state after one injection pulse. Columns 1 and 5 show that the adsorption amount depends on the partial pressure.

IV-D TPD Chromatogram and T_M

The TPD chromatogram may be recorded by the thermistor set 1 (Figure 1) when the desorbed residue passes through.

Figure 21 gives an example of the chromatogram. At least five distinguishable peaks are observed, but the last three are very small so they can not always be accurately recorded. Because of the temperature change, the carrier gas flow rate may be affected. Therefore, the small peaks, if any, at higher desorption temperatures are hard to record due to the base line change. The fact that CO_2 is always observed in the trapped material suggests that the oxygen comes from the catalyst instead of from the oxygen free helium.

The presence of five peaks indicate five different activation energies of desorption or heats of desorption. Therefore the catalyst surface is energetically heterogeneous. However, surface migration of the residue and the complexity caused by adsorption of a mixture may complicate this desorption process.

Table 22 gives the T_M 's of different peaks with different preadsorption conditions and different carrier gas flow rates. Columns 1 and 2 show that the T_M 's are shifted to higher values, except for peaks IV and V, when the ratio of Carbon/Re(surface coverage) is higher. Columns 1 and 3 show that the T_M 's are shifted to lower values, except for peaks IV and V, when the ratio of Carbon/Re is lower. These comparisons suggest that the individual adsorption sites are

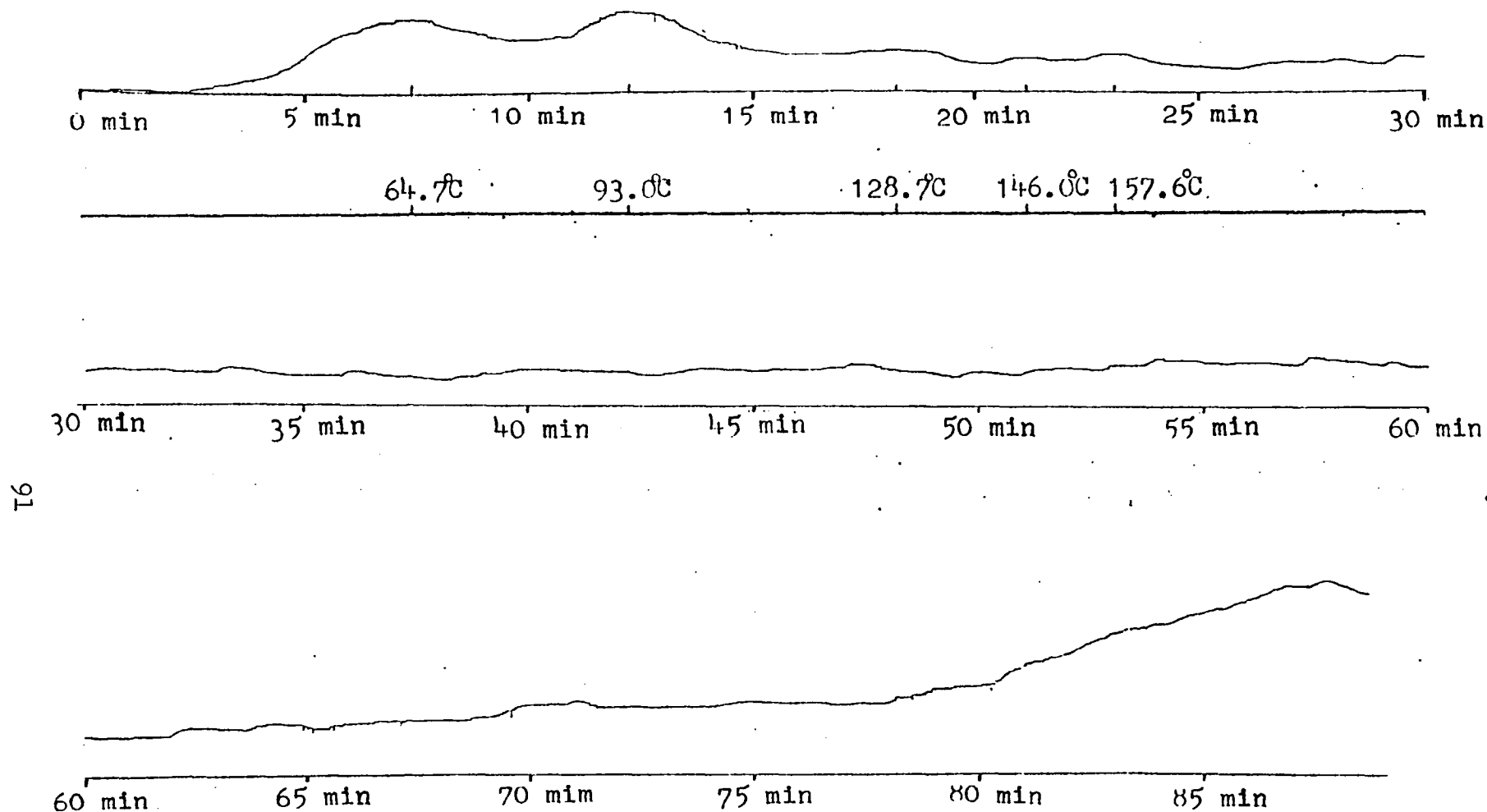


Fig. 21 TPD chromatogram after the injection of 5 pulses P
 7.299 micro gmole/pulse
 Act. @ 502°C ; Rxn @ 24°C ; He @ 34 ml/min
 TPD rate @ 5.9°C/min ; He @ 34 ml/min ; surface coverage: 2.34%
 Catalyst: 0.5119 g (0.55 cm)

	<u>5 psia[*]</u> <u>5 pulses</u>	<u>10 psia[*]</u> <u>5 pulses</u>	<u>5 psia</u> <u>1 pulse</u>	<u>5 psia</u> <u>9 pulses</u>	<u>5 psia</u> <u>5 pulses</u> <u>He: 154 ml/min for TPD</u>
Carbon/Re	2.34	3.11	1.61	2.46	-----
Peak I	64.7°C	69.2°C	58.2°C	64.4°C	55.3°C
Peak II	93.0°C	99.7°C	89.8°C	92.3°C	88.1°C
Peak III	128.7°C	131.3°C	120.6°C	125.3°C	115.0°C
Peak IV	146.0°C	145.2°C	148.6°C	-----	140.2°C
Peak V	157.6°C	157.2°C	160.1°C	-----	157.9°C

Table 22 Comparison of T_M with different preadsorption and TPD conditions

0.5119 g (0.55 cm) ; He: 34 ml/min for both reaction and TPD

Act. @ 502°C ; 12 hr ; Rxn @ 24°C

TPD rate 5.9°C /min

Reactant: P

* 5 psia= 7.299 micro gmole/pulse

10 psia=14.64 micro gmole/pulse

likely to be heterogeneous, since otherwise the T_M 's should appear at the same values. The shift of T_M 's to lower values with less adsorption may be caused by the different binding energies of various species on the catalyst.

Columns 1 and 5 of Table 22 show that the T_M 's are shifted to lower values, except for peak V, when a higher carrier gas flow rate is used. This phenomenon indicates the occurrence of readsorption during the TPD when a lower flow rate is used. Because of the high flow rate the residue can not be trapped by the liquid nitrogen and the value of Carbon/Re is not shown in the table.

The desorption corresponding to peaks IV and V, especially peak V, of Table 22 is likely to have been controlled by mass transfer effects or caused by experimental error since these peaks are too small to be accurately measured.

IV-E Effect of TPD Rate and Surface Migration

Table 23 expresses the effect of TPD rate on the desorbed materials. The table indicates that different rates do not have an effect on the composition, although readsorption and re-reaction may occur during the TPD. Note that ethylene is not observed when a thin bed is used, but is when a thick bed is used (Table 21). This result may again suggest the occurrence of readsorption and re-reaction during the TPD.

Figure 22 demonstrates the presence of surface migra-

	<u>5.9°C/min</u>	<u>8.82°C/min</u>	<u>11.68°C/min</u>
E	-----	-----	-----
CO ₂	1.785E-7	1.781E-7	1.712E-7
P	2.385E-7	2.153E-7	2.365E-7
1-B	3.390E-8	3.104E-8	3.312E-8
TB2	3.242E-7	3.080E-7	3.162E-7
CB2	1.604E-7	1.721E-7	1.563E-7
P ⁺	5.794E-8	4.148E-8	5.685E-8
CO ₂ [*]	7.417E-7	7.372E-7	7.595E-7
Carbon/Re	2.42	2.34	2.39

Table 23 Comparison of the desorbed hydrocarbon(via TPD)
with different TPD rates

0.4924 g (0.2 cm) ; He: 34 ml/min for both reaction and TPD
Act. @ 502°C ; 12 hr ; Rxn @ 24°C
Reactant: P
* obtained via the injection of O₂
(all values are gmole unless specified)

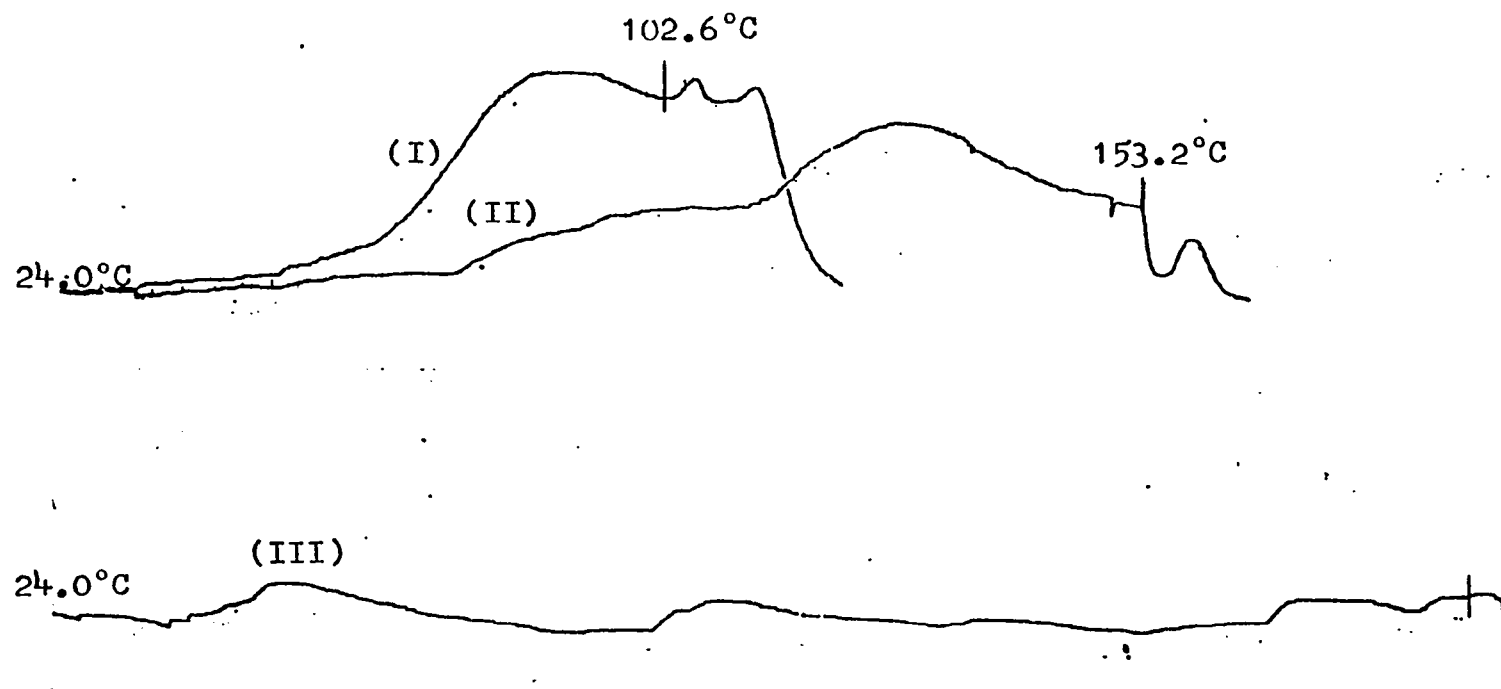


Fig. 22 TPD chromatogram of the adsorbed P (5 pulses)
 7.299 micro gmole/pulse ; He @ 34 ml/min
 Catalyst: 0.4924 g (0.2 cm)
 Act. @ 501°C ; 12 hr ; Rxn @ 24°C
 TPD rate @ 11.68°C/min ; He @ 34 ml/min
 This chromatogram reveals the migration of adsorbed
 hydrocarbon during TPD

tion during the TPD run. The TPD was carried out with four steps. The figure shows the first three steps represented as (I), (II), and (III). The first step started from 24°C and stopped at 102.6°C, followed by a quench to 24°C. The second step started from 24°C and stopped at 153.2°C, followed by a quench to 24°C. The third and fourth steps followed the same procedures but stopped at 200°C and 500°C respectively. The fourth step was followed by an injection of oxygen instead of a quench so that the total material balance could be made.

Table 24 presents the results from Figure 22. This table shows that the olefins are desorbed below 200°C. Above 200°C only CO₂ is desorbed, and the oxygen is from the catalyst while the carbon is from the coke and/or the cracked residue.

IV-F Heat of Desorption

Cvetanovic et al. (46,47) proposed that the activation energy of desorption or the heat of desorption may be calculated from the T_M 's if the individual site is homogeneous. In Section IV-D the presence of heterogeneous individual sites and readsorption during TPD run were suggested, so Cvetanovic's method can not be used to calculate the exact value of activation energy of desorption or the heat of desorption. However, an estimate of the approximate heat of desorption can be made instead of the exact calculation.

	<u>102.6°C</u>	<u>153.3°C</u>	<u>200.0°C</u>	<u>500.0°C</u>	<u>Total</u>
E	-----	-----	-----	-----	-----
CO ₂	-----	-----	-----	1.678E-7	9.710E-7*
P	1.396E-7	8.301E-8	2.149E-8	-----	8.032E-7
1-B	1.184E-8	1.224E-8	3.940E-9	-----	2.441E-7
TB2	1.860E-7	1.216E-7	2.560E-8	-----	2.802E-8
CB2	7.773E-8	5.503E-8	1.329E-8	-----	3.332E-7
P ⁺	2.280E-8	2.569E-8	7.597E-9	-----	1.460E-7
Carbon/Re	0.99	0.69	0.17	0.1	5.608E-8
					2.43

Table 24 Comparison of hydrocarbon desorbed with different upper limit temperatures

0.4924 g (0.2 cm) ; He: 34 ml/min for reaction and TPD

Act. @ 502°C ; 12 hr ; Rxn @ 24°C

TPD rate @ 11.68°C/min

Reactant: P ; 5 pulses injected ; 7.299 micro gmole/pulse

* obtained via the injection of O₂

Table 25 illustrates the dependence of T_M on bed thickness and the approximate value of heat of desorption. The T_M 's of the thick bed are always higher than those of the thin bed. This fact indicates the occurrence of readsorption during TPD run when a thick bed is used. Theoretically, the second peak should have a higher value of heat of desorption, but in fact the opposite is true. The possible reasons for this unexpected result are: (1) residue migration on the surface; (2) the occurrence of readsorption and re-reaction; (3) the compensation effect of the preexponential factor(67).

IV-G Adsorption and TPD Chromatogram of CO_2

Figure 21 demonstrates the presence of a heterogeneous surface. The TPD chromatogram of preadsorbed CO_2 proves this as well.

Figure 23 illustrates the TPD chromatogram of CO_2 . There are four distinguishable peaks and a small amount of CO_2 still coming off at a higher temperature. Accordingly, there is no doubt that the surface is energetic heterogeneous although readsorption and migration can still occur.

In order to check if the adsorbed CO_2 is totally desorbed below $200^\circ C$ as observed in the olefin desorption (Table 24), the TPD run was divided into two sections. The result is shown in Table 26. Apparently, the CO_2 is still adsorbed above $200^\circ C$, but the amount is only about 10% of

	0.5119 g (0.55 cm) Act. @ 502°C; 12 hr; Rxn @ 24°C 5 pulses P 7.299 micro gmole/pulse He: 34 ml/min for reaction and TPD Reactant: P Carbon/Re: 2.34%-2.57%		0.4924 g (0.2 cm) Act. @ 502°C; 12 hr; Rxn @ 24°C 5 pulses 7.299 micro gmole/pulse He: 34 ml/min for reaction and TPD Reactant: P Carbon/Re: 2.34%-2.57%	
	<u>Peak I</u>	<u>Peak II</u>	<u>Peak I</u>	<u>Peak II</u>
Heat of desorption (Kcal/gmole)	8.7	3.0	8.1	4.7
5.9°C/min	64.7°C	93.0°C	67.2°C	87.3°C
8.82°C/min	73.6°C	116.6°C	73.5°C	105.9°C
11.68°C/min	80.8°C	138.2°C	84.1°C	117.2°C

Table 25 Comparison of T_M and heat of desorption
with different bed thickness

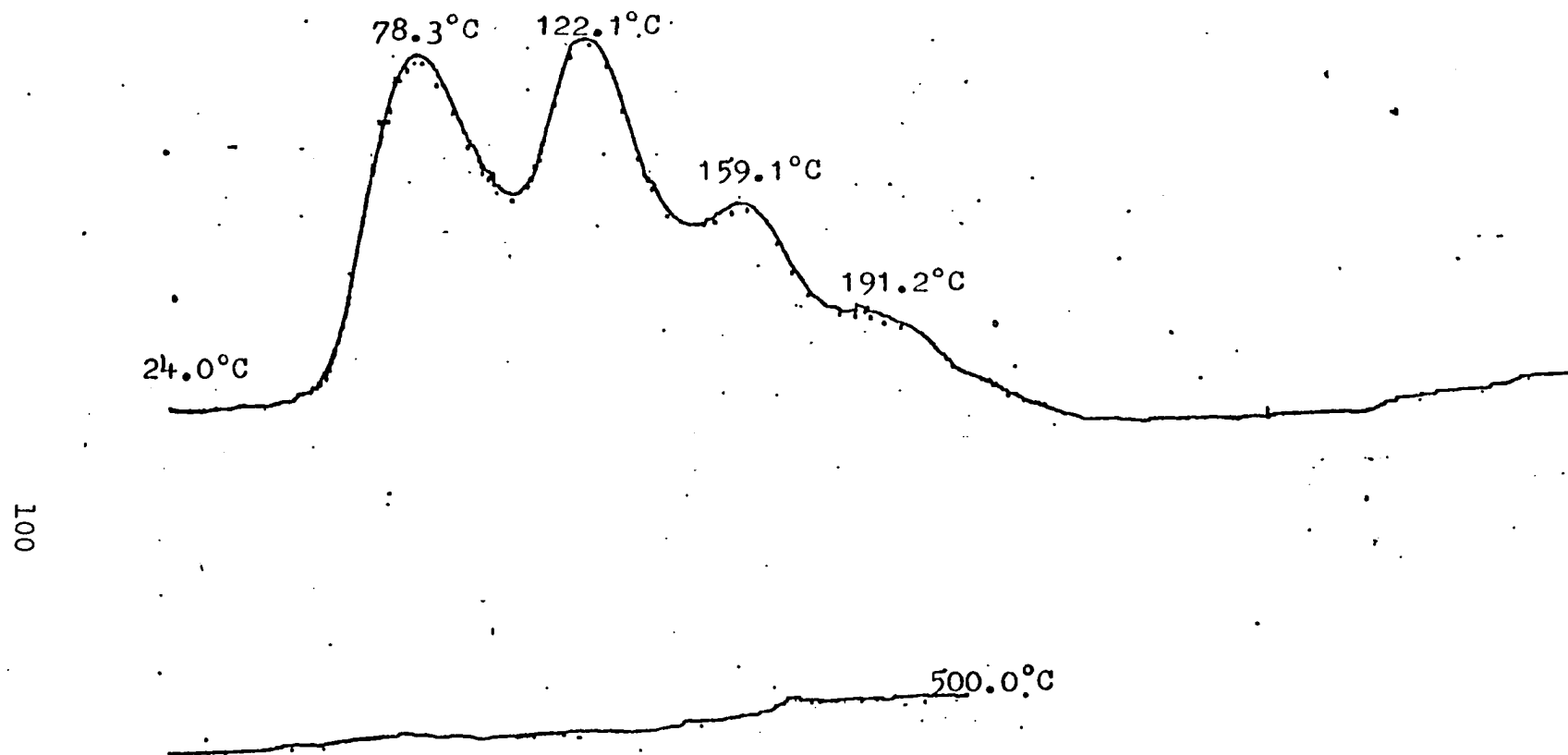


Fig. 23 TPD chromatogram of the adsorbed CO₂
Act. @ 502°C ; 12 hr ; CO₂ in static for 10 hr @ 24°C
TPD rate @ 11.68°C/min ; He @ 34 ml/min
Catalyst: 0.4956 g (0.2 cm)

24°C to 208°C:	4.069E-6
208°C to 500°C:	<u>4.821E-7</u>
Total:	4.551E-6

Table 26 CO₂ adsorption amount
 0.495 g (0.2 cm)
 Act. @ 502°C ; 12 hr
 CO₂ in static for 12 hr @ 24°C
 (values are in gmole)

the total adsorption amount.

IV-H Effect of TPD on Reaction

Figure 24 shows a case where TPD was carried out after the injection of four pulses of propylene, followed by the fifth pulse injection of propylene. The TPD was carried out to a temperature not more than 200°C to avoid coking and cracking (Table 24). The amount of ethylene produced by the fifth pulse increased substantially, while the trans-2-butene decreased. Furthermore, the higher the final temperature of the TPD, the more ethylene produced by the fifth pulse; correspondingly, the higher the temperature, the less trans-2-butene produced. Accordingly, the TPD produces some type of active site suitable for the production of ethylene, but not for trans-2-butene. This result supports the idea that the production of E and B follow different routes.

V. SPECIFIC POISON BY CO₂ AND NH₃

Section IV-G showed the TPD run of CO₂, while this section shows the reaction on the catalyst pretreated with CO₂. The catalyst was activated then treated by static CO₂ for 10 hrs, followed by pumping the bulk CO₂ out of the reactor and reaction of propylene.

The results are shown in Table 27 and 28, and Figures

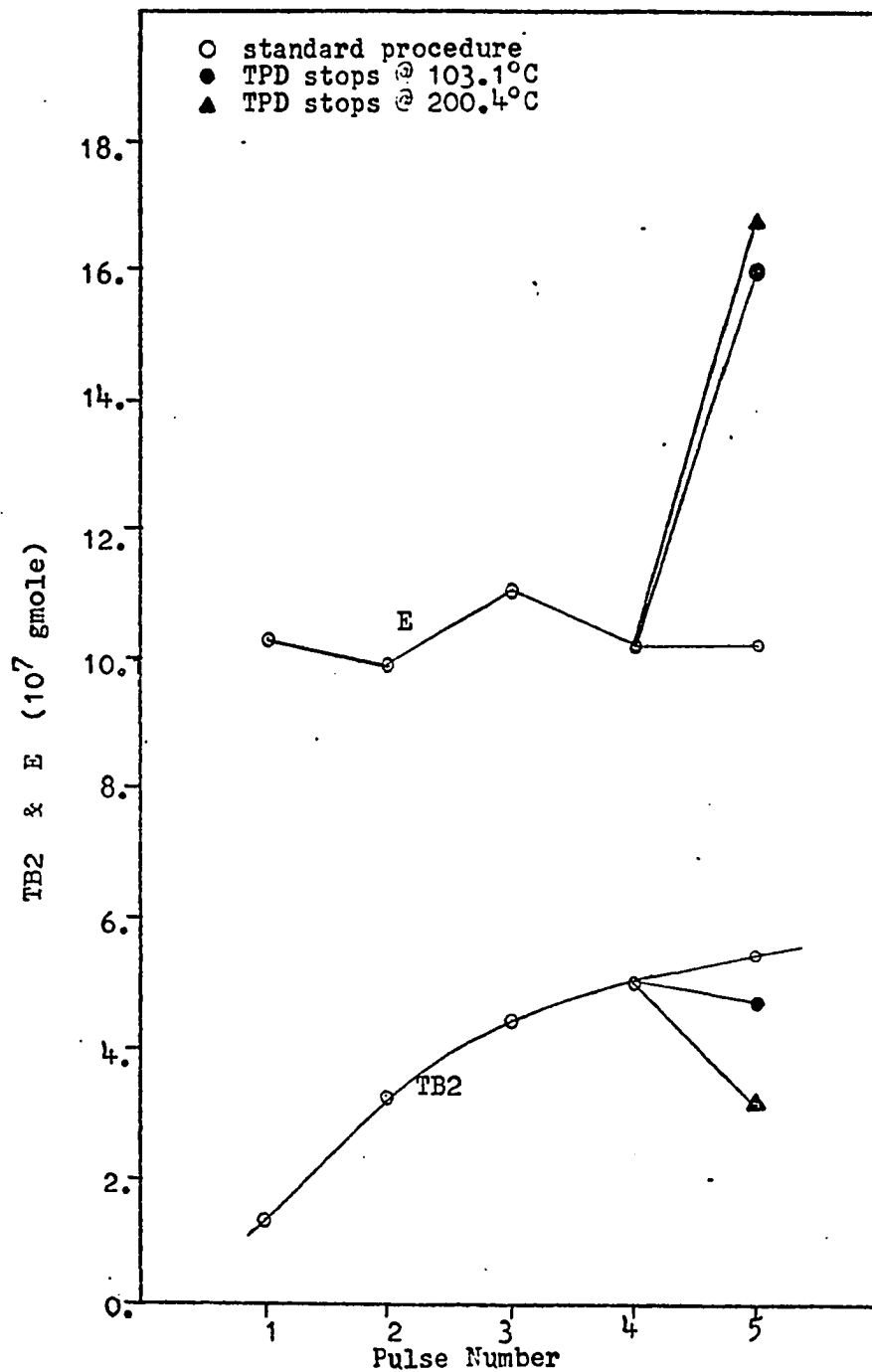


Fig.24 0.4924 g ; 0.2 cm
 Act. @ 501°C ; 12 hr ; Rxn @ 24°C
 7.3 micro gmole/pulse
 He: 34 ml/min
 TPD performed in between 4th and 5th pulses

	Pulse 1	Pulse 2	Pulse 3	Pulse 4	Pulse 5	Flush	TPD
ΔP	2.710E-6	2.720E-6	2.600E-6	2.710E-6	2.670E-6		
C(%)	34.9	35.0	33.5	34.9	34.2		
E/B	3.75	1.5	1.13	1.08	0.83		
TB2/CB2	2.6	2.5	2.64	2.65	2.66		
Y(%)	24.3	29.0	32.1	35.2	33.1		
E	1.489E-6	1.353E-6	1.315E-6	1.430E-6	1.150E-6	2.086E-8	-----
CO ₂	6.052E-7	2.988E-7	2.289E-7	2.090E-7	2.102E-7	2.350E-8	3.904E-6* 8.783E-7
P	5.050E-6	5.040E-6	5.060E-6	5.050E-6	5.093E-6	5.986E-8	3.320E-7
1-B	5.517E-9	1.969E-8	3.747E-8	3.920E-8	4.440E-8	2.572E-9	4.330E-8
TB2	2.830E-7	6.297E-7	8.177E-7	9.060E-7	9.847E-7	9.107E-8	4.417E-7
CB2	1.087E-7	2.522E-7	3.092E-7	3.416E-7	3.695E-7	3.542E-8	1.865E-7
P ⁺	8.932E-10	6.264E-10	1.058E-8	1.617E-8	1.637E-8	4.120E-9	6.388E-8
Carbon	1.971E-5	2.144E-5	2.252E-5	2.323E-5	2.325E-5	7.583E-7	4.879E-6 *
						5.637E-6	
Carbon Loss	3.570E-6	1.840E-6	7.570E-7	4.230E-8	2.255E-8		

Total Carbon Loss= 6.232E-6 Deviation= 9.5%
 TPD Carbon/Rhenium= 3.09%
 *contributed by hydrocarbon not by the originally
 adsorbed CO₂

Table 27 0.495 g (0.2 cm) ; He: 34 ml/min ; Reactant: P
 Act. @ 501°C ; 12 hr ; in static CO₂ for 12 hr @ 24°C;
 Rxn @ 24°C
 (all values are gmole unless specified)

	Pulse 1	Pulse 2	Pulse 3	Pulse 4	Pulse 5	Flush	TPD
-ΔP	3.168E-6	2.647E-6	2.388E-6	2.428E-6	2.395E-6		
C(%)	40.8	34.1	30.7	31.2	30.8		
E/B	14.97	4.21	2.11	1.47	1.23		
TB2/CB2	2.57	2.61	2.49	2.59	2.59		
Y(%)	18.8	23.8	25.6	26.4	28.0		
E	1.370E-6	1.492E-6	1.352E-6	1.218E-6	1.198E-6	-----	3.412E-8
CO ₂	6.100E-7	3.214E-7	2.369E-7	1.979E-7	1.666E-7	2.345E-8	4.602E-6*
P	4.592E-6	5.113E-6	5.372E-6	5.332E-6	5.365E-6	8.506E-8	9.261E-7
1-B	1.649E-9	2.756E-9	9.166E-9	1.312E-8	1.836E-8	-----	1.006E-6
TB2	6.470E-8	2.540E-7	4.495E-7	5.882E-7	6.885E-7	1.488E-7	9.071E-8
CB2	2.517E-8	9.733E-8	1.805E-7	2.273E-7	2.659E-7	5.510E-8	1.478E-6
P ⁺	-----	-----	-----	1.294E-9	2.161E-9	7.825E-10	5.549E-7
Carbon	1.688E-5	1.974E-5	2.137E-5	2.175E-5	2.239E-5	1.074E-6	1.309E-5*
Carbon Loss	6.400E-6	3.540E-6	1.910E-6	1.530E-6	8.900E-7	1.416E-5	

Total Carbon Loss= 1.427E-5 Deviation= 0.7%

TPD Carbon/Rhenium= 7.8%

* contributed by hydrocarbon not by the originally adsorbed CO₂

Table 28 0.495 g (0.2 cm) ; He: 34 ml/min ; Rxn @ 24°C
 Act. @ 501°C ; 12 hr ; in static CO₂ for 10 hr @ 24°C
 Reactant: 5P ; 7.76 micro gmole/pulse
 (all values are gmole unless specified)

12 and 15. The figures indicate that the adsorption of CO_2 has a positive effect on the reaction, although the ethylene production curve has been changed slightly. This change in the ethylene curve will be discussed later. Table 27 shows that the adsorbed CO_2 may be displaced on the injection of propylene and the material balance shows that the amount of olefins adsorbed is similar to that in Table 5. The same results are obtained from Table 28 and 8. Therefore, the adsorbed CO_2 increases the reaction rate. This rate increase may be ascribed to the acidity change of sites adjacent to the active site because of the adsorption of CO_2 (68,69).

If the proposed effect of acidity on the reaction is correct the elimination of the acidity may kill the catalyst activity. NH_3 is a good poison to both Lewis and Bronsted acids because NH_3 has a pair of unshared electrons (69) which may react with acidic sites. Introducing 67.51 micro-gmole NH_3 (0.75% of Re plus Al atoms) to the activated catalyst kills the activity completely. Therefore, acidity, to which both the Lewis and Bronsted acid sites may contribute, is important to the reaction. Unfortunately, the poison only to the Bronsted acid can not be found, so the exact effect of Bronsted acid is still unknown.

CHAPTER IV

DISCUSSION

I. RATE EQUATIONS OF THE KINETIC STUDY

As discussed by Hsu(30), the rate of metathesis reaction in a heterogeneous catalysis system is not just a function of reactant concentration but also a function of the number of surface active sites. He proposed a model for the changes of the site density and derived the rate expression with respect to the surface active site concentration. This rate expression was

$$R = k_m P^a L \quad (9)$$

where k_m , P , and L are rate constant, reactant partial pressure, and active site density respectively. In addition, since the reactant partial pressure was fixed at 1 atm, the expression was simplified as

$$R = k_c L \quad (10)$$

Expressions for L as a function of time were derived for both the break-in and deactivation periods. Some sim-

plified rate expressions are shown in Table 2.

Hsu(30) correlated his kinetic data with equation (10), and concluded that the break-in rate was second order with respect to the adsorption active site density, and that deactivation rate was between 1 and 2 order with respect to L (active site density).

In fact, the rate expression should be written as

$$R = k_c L^b \quad (11)$$

instead of equation (10). A correlation of the kinetic data obtained in the present work with equation (11) and L shows that the correlation does not converge unless b is equal to unity. Therefore, the reaction rate is first order with respect to the active site density. The discussion and the result shown in Table 2 are based on the case where $b=1$.

In contrast to Hsu's(30) correlation, Table 2(Part B) shows that first order with respect to the adsorption active site density and surface active site density(L) may adequately describe the break-in and deactivation rates. A close look at Table 2(Part A) shows that the expression of 1-B and 1-D have the same meaning as that of 2-B and 2-D because the exponential term may be expanded into a series. This fact may explain why Hsu(30) proposed that both first and second order deactivation rates adequately correlated with his kinetic data. However, the break-in rate was second order instead of first order in the present study with respect to the adsorp-

tion active site density. This difference is still not adequately understood.

Since the deactivation rate may be correlated with first order formula, the deactivation rate constants are shown in Table 2(Part C). The smallest deactivation rate constant occurs when the reaction is carried out at 50°C. This result is consistent with Figure 7.

Table 29 shows the rate equation obtained from the correlation. The high deviation at 203°C and 303°C may be due to experimental error.

Figure 25 represents the proposed superimposition effect and correspond to Table 3. The amount of CO₂ should decrease with decreasing temperature if it represents the amount of high molecular weight product and coke. The amount of hydrocarbon should decrease with increasing temperature if it represents the equilibrium adsorption amount. However, deviation is observed at the low temperature end of CO₂ curve and high temperature end of hydrocarbon curve, because of the re-reaction occurring during the TPD run. Because of the high concentration of hydrocarbon on the catalyst surface and the occurrence of readsorption during the TPD run(see Table 22), re-reaction may occur, such as cracking and reactions to produce higher molecular weight hydrocarbons. The cracking reaction can cause the deviation of the hydrocarbon curve, while the production of higher molecular weight product and coke causes the deviation of the CO₂ curve. However, the

Reaction Temperature (°C)	Order		R(t)	Dev.(%)
	B	D		
0.0	2	1	$0.005827(1-(1+27.94t)^{-1}) \times \exp(-0.06783t)$	1.34
	2	2	$0.005887(1-(1+27.09t)^{-1})/(1+0.07973t)$	1.32
	1	1	$0.00542(1-\exp(-18.637t)) \times \exp(-0.04736t)$	2.00
	1	2	$0.005432(1-\exp(-18.563t))/(1+0.05166t)$	2.06
25.0		1	$0.01568 \times \exp(-0.118t)$	3.32
50.0		1	$0.02837 \times \exp(-0.0432t)$	2.46
103.0		1	$0.04544 \times \exp(-0.114t)$	1.78
203.0		1	$0.0511 \times \exp(-0.692t)$	11.3
303.0		1	$0.001452 \times \exp(-0.576t)$	13.5

Table 29 Result of the Correlation of the Kinetic Data

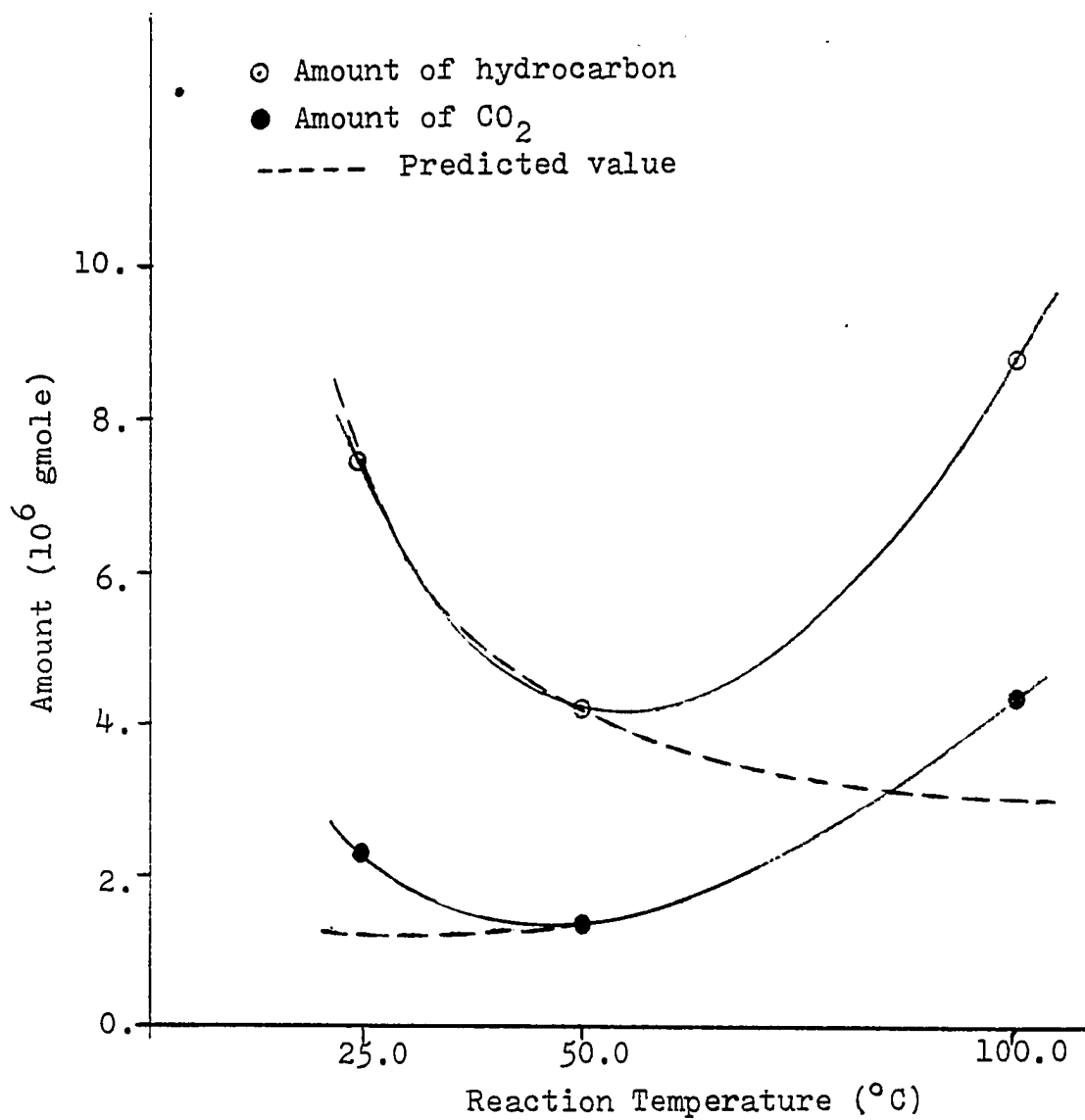


Figure 25 The Result of TPD After Flow System Kinetic Study

minimum point of this superimposition effect is still around 50°C. Therefore, the most stable reaction occurs at 50°C and is due to the lower amount of adsorption compared to that at a lower temperature, and the lower molecular weight product produced compared with that at a higher temperature.

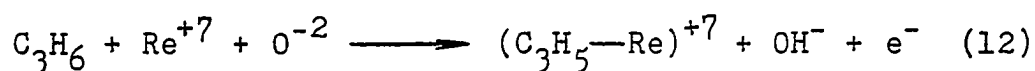
II. BREAK-IN AND DEACTIVATION

Wills et al.(5) studied propylene metathesis using tungsten oxide/silica as the catalyst. They found the break-in period and color change. The color was yellow initially and changed to blue, $WO_{2.9}$, at steady state. However, when the catalyst was prereduced to $WO_{2.9}$ by hydrogen at 400°C, the break-in period was still observed. Accordingly, the formation of a certain type of organometallic structure was proposed during the break-in period along with the reduction.

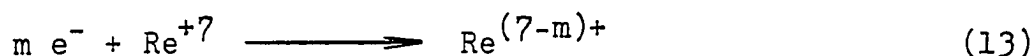
Andreev et al.(16) observed Re(+6) from reflectance spectra after contacting the Re_2O_7/Al_2O_3 catalyst with propylene. They proposed the formation of mesoperrhenate structure with the participation of rhenium and alumina after heating the catalyst above 360°C and having the rhenium in the ReO_5^{-3} state. They also proposed that the presence of Re(VI) and anion vacancy formed the F-center which were responsible for the reaction.

Boelhouwer et al.(64,65) concluded that the metathesis activity was generated by the reduction of the catalyst by olefins(propylene and higher alkenes). Simultaneously, water

was generated, detected by IR, and the greater part were associatively adsorbed at room temperature. Furthermore, the production of methylene along with the reduction was detected by IR. The initial reduction of the catalyst(Re^{+7}) by olefins was proposed by Peacock(70), although the exact process is still unknown, as follows:



and the neighboring Re^{+7} was reduced by the free electrons as follows:



Therefore, it is generally accepted that the break-in, observed at 0°C , period is partially due to the reduction of the catalyst by reactant to create new active sites. The break-in period not observed in Figures 3, 4, 5, and 6 at higher reaction temperatures may be ascribed to the faster rate of reduction because of the higher temperatures. In addition, surface oxygen may also play a role in the break-in period since evacuation of the bulk oxygen at different temperatures may leave different amounts of oxygen on the catalyst. Thus, when the reaction is carried out at 0°C some of the oxygen can need to be replaced by the olefin or some kind of reaction can even occur between the olefin and oxygen.

The deactivation period may be ascribed to the poison by impurity in the reactant, to reactant, to coke, and to

high molecular weight products(30).

III. EFFECT OF SOURCES FOR SUPPORT AND PROMOTER

Fridman et al.(17) studied the $\text{ReO}_7/\text{Al}_2\text{O}_3$ catalyst with the differential thermal analysis method and concluded that the rhenium must be present as a tightly bound surface compound, mesoperrhenate structure, that is thermally stable in air up to 1120°K . This conclusion was consistent with LeRoy and Johnson's(19) conclusion.

The present study(Table 4) indicates that the proposed formation of mesoperrhenate structure is possible and depends on the materials for the support and promoter. For example, $\text{NH}_4\text{ReO}_4/\text{Al}_2\text{O}_3$, $\text{NaReO}_4/\text{Al}_2\text{O}_3$, $\text{NH}_4\text{ReO}_4/13\text{X}$, and $\text{NH}_4\text{ReO}_4/13\text{X}(\text{Ca})$ may form some kind of mesoperrhenate structure because rhenium loss was not observed during the high temperature activation. Therefore, the participation of both the support and promoter to form some mesoperrhenate structure may contribute to the stability of the promoter, which also affects the activity of the catalyst. The factors, however, affecting the formation of the mesoperrhenate structure are still in doubt, although the present study shows that the surface area and pore size of the support may be two factors.

In addition to the mesoperrhenate structure, several other factors may affect the activity:

(1) According to Swift and Kobylinski's study(22), the addition of Ia and IIa group metal ions may depress the

catalyst acidity to increase the selectivity with the cost of decreasing conversion. The present study is partially consistent with the results proposed by Swift et al.(22), because the sodium and potassium containing catalysts($\text{NaReO}_4/\text{Al}_2\text{O}_3$, $\text{NH}_4\text{ReO}_4/13\text{X}$, and $\text{NH}_4\text{ReO}_4/3\text{A}$) have lower activities compared to the standard catalyst($\text{NH}_4\text{ReO}_4/\text{Al}_2\text{O}_3$). In addition, the decreasing conversion of the sodium and potassium containing catalysts may suggest that the proper amount of acidity is necessary for this reaction. The effect of Bronsted acid will be discussed later.

(2) The catalyst has higher activity when calcium is substituted for sodium or potassium with the ion exchange technique. For instance, $\text{NH}_4\text{ReO}_4/3\text{A}(\text{Ca})$ and $\text{NH}_4\text{ReO}_4/13\text{X}(\text{Ca})$ (see Table 4) have higher activities than $\text{NH}_4\text{ReO}_4/3\text{A}(\text{K})$ and $\text{NH}_4\text{ReO}_4/13\text{X}(\text{Na})$ respectively. Since K, Na, and Ca all depress the acidity, such results may suggest the effect of electrostatic field. In order to keep the electronic neutrality of the catalyst, every Ca ion must replace two Na or K ions and generate different electronstatic fields, which are result of different distributions of electrons. Different electronstatic fields may have effect on the activity and on the formation of mesoperrhenate structure, although it is not yet certain. Tung et al.(61) studied the hexane cracking with Y type zeolite and found that when Na was replaced by Ca, the activity was better. They proposed that this difference was due to the different electronstatic field. Therefore, it

seems that the calcium containing zeolite is better than the sodium and potassium containing zeolites when used in both cracking and metathesis reactions.

(3) Ward et al.(62) studied the surface areas of Y zeolites with different extents of ion exchange of sodium by ammonium. They found that the surface area changes with different contents of sodium, although no definite relationship between sodium content and surface area was drawn. Thus, the catalyst structure may be affected by such ion exchange and cause different activity per unit area.

Moreover, Ward(73) found that the acidity of the Y zeolite depends on the cation size. He concluded that the larger the cation size the lower the acidity and activity. Since the cation radii of Ca, K and Na are 0.99\AA , 1.33\AA , and 0.95\AA , the $\text{NH}_4\text{ReO}_4/13\text{X}(\text{Ca})$ should have lower activity than $\text{NH}_4\text{ReO}_4/13\text{X}(\text{Na})$ and the $\text{NH}_4\text{ReO}_4/3\text{A}(\text{Ca})$ should have higher activity than $\text{NH}_4\text{ReO}_4/3\text{A}(\text{K})$ if the acidity were the factor controlling the activity. However, different results are seen in Table 4. Thus, when ion exchange is carried out for zeolite, the acidity, the different activity per unit area, the electrostatic field may affect the activity or the formation of mesoperrhenate structure which affects the activity.

(4) Lin et al.(11,55) showed that $\text{NH}_4\text{ReO}_4/\text{SiO}_2$ needed a higher reaction temperature than $\text{NH}_4\text{ReO}_4/\text{Al}_2\text{O}_3$. Table 4 shows that the support with higher ratio of Al_2O_3 to SiO_2 has a higher activity when zeolite was used as support(compare

$\text{NH}_4\text{ReO}_4/3\text{A}(\text{Ca})$ with $\text{NH}_4\text{ReO}_4/13\text{X}(\text{Ca})$). Accordingly, although a detailed interpretation would be more complicated, the different ratio of Al_2O_3 to SiO_2 may be a factor for the metathesis reaction when zeolite is used as support.

From the above discussions the following conclusions may be drawn: (1) The presence of sodium and potassium have a negative effect on the activity; (2) The activity of the catalyst depends on the formation of mesoperrhenate structure, the activity per unit area, the acidity, the electrostatic field, the ratio of Al_2O_3 to SiO_2 if zeolite is used as support and some other unknown factors caused by the application of different sources.

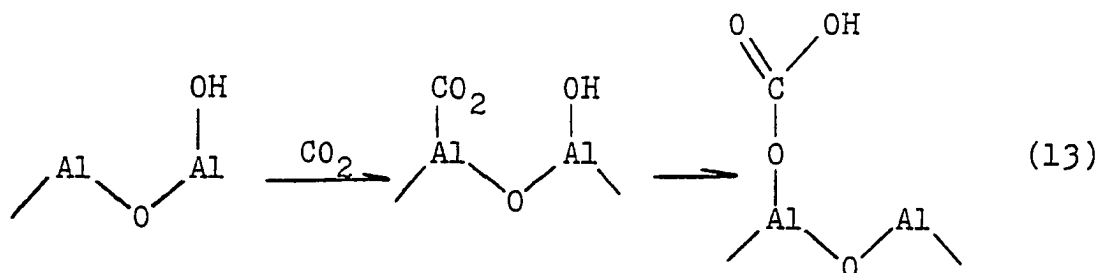
IV. THE EFFECT OF BRONSTED ACID

Kimura et al.(23) studied 1-butene isomerization and concluded that both Bronsted acid and Lewis acid contributed to double bond isomerization. Bronsted acid served as proton donor directly while the formation of a carbonium ion was necessary in order to provide proton via Lewis acid. Hall et al.(74) studied cyclopropane reactions over a molybdena/alumina catalyst and concluded that the isomerization reaction correlated linearly with the sum of the concentrations of anion vacancy and hydroxyl group appearing as Mo-OH . However, the metathesis was correlated with anion vacancy. Hsu (30) studied the evacuation temperature effect on the meta-

thesis reaction and concluded that the anion vacancy created by evacuation was partially responsible for the reaction. Accordingly, it is generally accepted that Lewis acid directly contribute to the metathesis reaction.

The present study suggests that Bronsted acid is also a factor in the metathesis reaction. The results during the initial reaction study with pulse technique show that the yields are 6% higher if the catalyst has been pretreated in static CO₂ for 10 hours(see Figures 12, 15 and Tables 5, 8, 27, 28).

The adsorption of CO₂ on a metal oxide was proposed as follows(69):



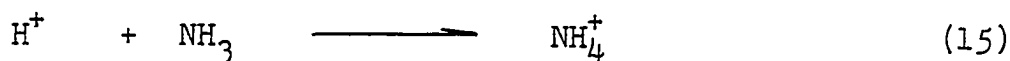
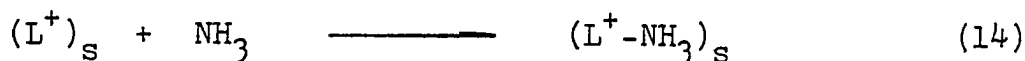
Thus, the structure of Bronsted acid may be changed because of the adsorption of CO₂. This structure difference is the only explanation for the higher yield obtained with the CO₂ pretreated catalyst.

A comparison of Tables 5 and 27 shows that part of the adsorbed CO₂ is replaced by olefins when propylene is injected into the reactor. These tables also show that the

desorbed species obtained from TPD have no apparent difference. These observations may suggest that the adsorption site of olefins and the Bronsted acid site are not the same.

From the above discussions it is reasonable to say that the increased yield results from the different form of Bronsted acid. Bronsted acid is not just a factor for isomerization but also for the metathesis reaction, and its effect depends on its structure. Moreover, the metathesis reaction is enhanced by Bronsted acid adjacent to the adsorption site. Otherwise the adsorption amount of the hydrocarbons would not be the same when compared to that obtained without CO₂ pretreatment. The parallel increase of the yield along the pulse number can suggest that Bronsted acids adjacent to the adsorption site are involved in both initiation and propagation reactions, or only involved in the initiation reaction to create more chain carriers which cause higher propagation rate if the carbene mechanism is applied.

The specific poison of the activity by NH₃ may also partially prove the effect of Lewis and Bronsted acids. Because of the unshared pair of electrons in the NH₃ molecule, the poison of Lewis and Bronsted acids by NH₃ was proposed as follows(69):



When 67.51 micro-gmole NH_3 is injected into the reactor containing the oxygen regenerated catalyst, the activity of metathesis is zero. This result explains the role of these two acids in the metathesis reaction.

A combination of the discussion in this section with the source effect discussed and the Kimura's(23) study indicates that Bronsted acid has an effect on both isomerization and metathesis reaction. In addition, since water was proved as a poison to the metathesis(30) and a poison to Lewis acid (69) only, the author would like to suggest that Lewis acid is the major factor for the metathesis and Bronsted acid adjacent to Lewis acid may enhance the reaction rate. The present study shows that such enhancement depends on the form of Bronsted acid.

V. TEMPERATURE PROGRAMMED DESORPTION STUDIES

Figures 21 and 23 show that the adsorbed species are desorbed at different temperatures, so the overall catalyst surface is energetic heterogeneous. Otherwise only one peak would be observed.

Figure 22 shows that migration of the adsorbed species during the TPD run does occur. This phenomenon makes the desorption process more complicated. Table 24, corresponding to Figure 22, shows that the molecular olefins are desorbed at temperatures below 200°C , while CO_2 is desorbed between 200°C and 500°C . Since the carrier gas is oxygen free helium,

the source of oxygen must be the catalyst itself. After the regeneration of the catalyst by flow oxygen, the oxygen can be restored on the catalyst.

Since the peak maximum temperature changes with different adsorption amounts of olefins (Table 22), the individual adsorption site is also energetic heterogeneous. Otherwise, the peak maximum temperature would be independent of the adsorption amount. If the adsorption site is heterogeneous, the adsorption must start from the place with higher activation energy of desorption. Thus, the peak maximum temperature should shift to a higher value with a lower amount of adsorption. However, this is not the case in Table 22. This unexpected result may be explained by the complicated binding between the olefin mixture and the catalyst, since the theory of TPD is based on the adsorption of one component. The constant values of the peak maximum temperatures of the fourth and fifth peaks (Table 22) are probably due to the mass transfer effect or experimental error and the later is more reasonable since mass transfer effect will be proved to be negligible.

Based on the assumptions that desorption is first order, the mass transfer effect is negligible, at steady state, and homogeneous surface, Cvetanovic et al. (47) made the material balance of a single component and obtained two equations as follows:

$$2\log T_M - \log \beta = E_d / 2.303RT_M + \log(E_d/AR) \quad (16)$$

when readsorption does not occur during TPD and

$$2\log T_M - \log \beta = \Delta H / 2.303RT_M + \log((1-\theta_M)^2 V_S \Delta H / FA^* R) \quad (17)$$

when readsorption occurs freely. Where β is the temperature increasing rate, E_d is the activation energy of desorption, ΔH is the heat of desorption, R is the universal gas constant, F is the carrier gas flow rate, θ_M is the surface coverage at peak maximum, V_S is the volume of the catalyst solid phase, and A and A^* are the preexponential factors of the desorption rate constants.

By varying the carrier gas flow rate the readsorption is found at a lower flow rate (34 ml/min), so only the heat of desorption may be obtained (see Table 22). Since the heterogeneous individual adsorption site has been proven (Table 22), the exact value of the heat of desorption can not be obtained. However, the rough average value of the heat of desorption may be estimated for this particular adsorption situation by plotting the $(2 \log T_M - \log \beta)$ term with respect to $1/T_M$ if some temperature increasing rates are applied.

The heats of desorption are illustrated in Table 25. Usually the adsorption site with higher T_M value would have a higher value of heat of desorption, but the opposite result is seen in Table 25. This discrepancy may result from the complicated readsorption, re-reaction, and from the compensation effect of the preexponential factor of the desorption rate constant (67).

In summary, because of the complicated adsorption state and desorption process, the exact quantitative data are hard to obtain from the TPD technique in this study.

VI. MASS TRANSFER EFFECT

In order to interpret the experimental data the mass transfer effect must first be checked to see if it controls the reaction.

Lin(55) applied different particle size catalysts to prove that the intraparticle mass transfer effect was negligible.

Hsu(30) doubled the amount of catalyst at the same space velocity to prove that the interphase mass transfer effect was negligible.

Therefore, both the interphase and intraparticle mass transfer effects are negligible in the flow system kinetic study. Detailed calculations to check these two mass transfer effects for the pulse technique are discussed below

VI-(A) Interphase Mass Transfer Effect

Some available data are listed as follows:

- (1) Particle diameter(if spherical particle is assumed): 50 mesh or 0.0508 cm.
- (2) Porosity of the catalyst: 30%.
- (3) Flow rate at 25°C: $0.5 \text{ cm}^3/\text{sec}$ or $2.04 \times 10^{-5} \text{ gmole/sec}$
or $3.0 \times 10^{-4} \text{ g/sec-cm}^2$.

(5) Viscosity of propylene at 25°C: 86×10^{-6} p.

(6) Catalyst density: 0.85 g/cm^3 .

Based on the calculation method proposed in Satterfield's book(72), the bed thickness required when interphase mass transfer effect controls the reaction may be calculated as follows:

The diffusion flux is

$$N = k_g(p_o - p_s) = k_c(C_o - C_s) \quad (18)$$

where $k_g (=) \text{ gmole/sec-cm}^2\text{-atm}$, $k_g = k_c/(RT)$, p_o and p_s are the partial pressures of the reactant in the gas phase and on the catalyst surface, and C_o and C_s are the concentrations of the reactant in the gas phase and on the catalyst surface.

The factor j_D is defined as

$$j_D = k_g P Sc^{2/3} / G_M \quad (19)$$

where P is the total pressure, Sc is the Schmidt number, and $G_M (=) \text{ gmole/sec-cm}^2$.

An empirical expression of j_D was proposed as

$$j_D = 0.357 / (\alpha Re^{0.359}) \quad (20)$$

where α is the porosity of the catalyst.

If steady state may be assumed and the overall reaction is controlled by interphase mass transfer, the mole fractions of the reactant at the inlet and outlet of the bed have a relationship which may be written as

$$\ln(Y_1/Y_2) = (k_g a P z)/G_M \quad (21)$$

where Y_1 and Y_2 are the mole fractions at inlet and outlet of the bed, a is the surface area per unit volume, and z is the bed thickness.

The Reynolds number may be calculated as

$$Re = DG/\mu = (0.0508) \times (3 \times 10^{-4}) / (86 \times 10^{-6}) = 0.1772 \quad (22)$$

and the factor j_D may be calculated from equation(20)

$$j_D = 0.357 / (0.3 \times 0.1772^{0.359}) = 2.215 \quad (23)$$

The ϵ/K values for helium and propylene are 10.22 and 298.9. The σ values for helium and propylene are 2.551 and 4.678. Therefore

$$\sigma_{AB} = (\sigma_A + \sigma_B)/2 = 3.614 \quad \text{and}$$

$$\epsilon_{AB} = ((\epsilon_A/K)(\epsilon_B/K))^{0.5} = 55.27.$$

Moreover, the value of KT/ϵ_{AB} at 25°C is 5.37, which gives a value of 0.8311 to the collision integral Ω . Then the diffusion coefficient can be calculated as

$$\begin{aligned} D_{AB} &= 0.001858 T^{1.5} ((M_A + M_B)/(M_A M_B))^{0.5} / P \sigma^2 \Omega \\ &= 0.458 \text{ cm}^2/\text{sec} \end{aligned} \quad (24)$$

and

$$D_{AB, \text{eff}} = D_{AB}^\alpha = 0.153 \text{ cm}^2/\text{sec} \quad (25)$$

The density of propylene in the gas phase is calculated

as

$$\rho = PM/RT = 1.717 \times 10^{-3} \text{ g/cm}^3. \quad (26)$$

The Schmidt number is calculated as

$$Sc = \mu / \rho D_{AB, \text{eff}} = 0.327 \quad (27)$$

By substituting equations 23, 27, and the flow rate into equation 19, the k_g may be obtained as 3.333×10^{-5} gmole/sec-cm²-atm.

Since the surface area of the catalyst is known as about 100 m²/g, the surface area per unit volume is about 85 m²/cm³. By substituting k_g , a , and flow rate into equation (21) and assuming 30% conversion, the bed thickness may be estimated as about 8.84×10^{-8} cm.

The ratio of the actual bed thickness (0.2 cm) to the thickness calculated here is about 2.26×10^6 .

Satterfield stated that when the ratio of actual bed thickness to the calculated thickness is larger than 100, the concentration difference between the gas phase and catalyst surface is negligible. In the present case the ratio is 2.26×10^6 , so the overall reaction is not controlled by inter-phase mass transfer.

VI-(B) Intraparticle Mass Transfer Effect

Some available data are listed as follows:

- (1) All the available data in last section.

(2) Tortuosity factor(if cylindrical pore is assumed)
is 3.0.

The intraparticle mass transfer effect may be checked from the effectiveness factor, which is a function of the Thiele modulus.

For a spherical particle, the Thiele modulus is defined as

$$\phi_s = r(k_v C_s^{m-1}/D_{\text{eff}})^{1/2} \quad (28)$$

where k_v is the intrinsic reaction rate constant per unit volume, \bar{r} is the particle radius, C_s is the catalyst surface concentration, and D_{eff} is the effective diffusion coefficient. For a spherical particle, the effectiveness factor is defined as

$$\begin{aligned} \eta_s &= \text{real rate/intrinsic rate} \\ &= (3/\phi_s)(1/\tanh\phi_s - 1/\phi_s) \end{aligned} \quad (29)$$

where the intrinsic rate is the rate without diffusional effect.

The k_v , however, is usually hard to obtain so Satterfield proposed a new dimensionless relationship for the Thiele modulus as

$$\bar{\Phi} = \frac{r^2}{D_{\text{eff}}} \left(-\frac{1}{V_c} \frac{dn}{dt} \right) \frac{1}{C_s} \quad (30)$$

where r is the radius of the particle, and V_c is the volume of the catalyst per unit mass.

From data obtained in the last section, the diffusion coefficient is $0.458 \text{ cm}^2/\text{sec}$. When the Knudsen effect is not important, then

$$D_{AB, \text{eff}} = D_{AB} \alpha / \tau = 0.458 \times 0.3 / 3.0 = 0.0458 \text{ cm}^2/\text{sec} \quad (31)$$

When the Knudsen effect predominates, then

$$\begin{aligned} D_{K, \text{eff}} &= 19400 (\alpha^2 / \tau S \rho) (T/M) \\ &= 1.82 \times 10^{-3} \text{ cm}^2/\text{sec} \end{aligned} \quad (32)$$

where τ is the tortuosity factor, S is the surface area cm^2/g . The overall diffusion coefficient is the combination of the two coefficients above and is expressed as

$$\frac{1}{D_{\text{eff}}} = \frac{1}{D_{AB, \text{eff}}} + \frac{1}{D_{K, \text{eff}}} \quad (33)$$

Thus, D_{eff} is calculated as $1.75 \times 10^{-3} \text{ cm}^2/\text{sec}$.

If 30% conversion is assumed, the concentrations of the reactant at inlet and outlet may be calculated from the ideal gas law and the average value taken as $3.485 \times 10^{-5} \text{ gmole/cm}^3$. The parentheses term in equation (30) may be calculated as

$$- \frac{1}{V_c} \frac{dn}{dt} = \frac{6.75}{3600} \times \frac{1}{42} \times 0.3 \times \frac{1}{1.2} = 1.12 \times 10^{-5} \text{ gmole/sec/cm}^3$$

By substituting $r(0.0254 \text{ cm})$, $D_{\text{eff}}(1.75 \times 10^{-3} \text{ cm}^2/\text{sec})$, $C_s(3.485 \times 10^{-5} \text{ gmole/cm}^3)$, and the parentheses term into equation (30), the Thiele modulus is obtained as 0.12. From the

attached figures(72), the effectiveness factor corresponding to this Thiele modulus is seen as almost equal to unity, so the intraparticle mass transfer effect may be neglected.

VII. REACTION MECHANISM

Since the interphase and intraparticle mass transfer effect are proven negligible in the last section, these effects will not alter the following discussion of the mechanism and other interpretation of the experimental results.

VII-(A)

The ratio of TB2 to CB2 changes with reaction time at 0°C reaction temperature(Figure 2), but a constant value is obtained from the pulse technique(Figure 15). This constant value is close to the maximum value in Figure 2. The above difference can suggest that CB2 is the initial product and the production of TB2 follows the cis-trans isomerization activity. This isomerization activity can be affected by steric effect and is a function of CB2 concentration because the TB2/CB2 increases with time to reach a maximum value in the flow system study. The ratio of TB2/CB2 is always less than equilibrium value(e.g. 3.92 at 0°C) for both flow and pulse studies is a fact which again suggests that CB2 is the initial product.

The 1-B is observed at every pulse in the pulse study,

but not observed in the flow system study until 203°C. This difference suggests the possible steric effect for the production of 1-B in addition to the theoretically small equilibrium amount, which is due to the high surface concentration in the flow study.

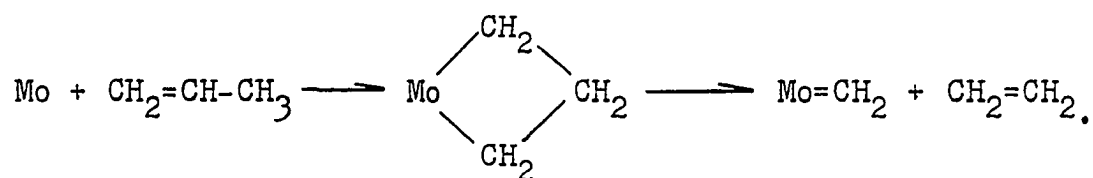
The induction period of TB2/CB2 at 0°C in the flow system study is not observed at higher reaction temperatures. This fact may indicate that the steric effect is partially overcome by higher temperature or the surface concentration of CB2 increases with increasing temperature. Furthermore, the ratio of TB2/CB2 is a function of reaction temperature which is caused by thermodynamic constraint. The higher the reaction temperature the more CB2 produced, so TB2/CB2 decreases with increasing reaction temperature. The decreasing value of TB2/CB2 with respect to the reaction time at 203°C is due to the steric effect resulting from the adsorption of high molecular weight product or coke. This result can again suggest that CB2 is the initial product.

VII-(B)

The ratio of E/B is higher than unity at 0°C at the beginning in the flow study, then decreases to a constant value smaller than unity(Figure 2). This decrease is less obvious with increasing reaction temperature(Figures 3, 4, 5, and 6). The high value of E/B at the beginning is also

observed in the pulse study at both 0°C and 25°C (Figures 12 and 15). Two possible reasons for the high E/B value at the beginning are the following: (1) more B is adsorbed on the catalyst; (2) the production of E and B follow different routes.

Ethylene adsorbs only slightly on the catalyst, but butenes adsorb more readily. Therefore, the high ratio of E/B may be caused by the different adsorption ability of ethylene and butenes. However, the one pulse studies (Table 14, and 15) show that the ratio of E to B is between 1.5 and 2.0 when considering the adsorbed species all together. Accordingly, it is unlikely that the high ratio at the beginning is due to different adsorption ability. Burwell Jr. et al. (58) obtained the same result of the ratio of E/B using $\text{Mo(CO)}_6/\text{Al}_2\text{O}_3$ as catalyst. The reaction was carried out at 53°C with pulse technique, and the E/B decreases from 2.5 of the first pulse to 1.0 of the third pulse. Furthermore, they proposed a mechanism for generating carbene as



The effect of the carrier gas flow rate on the production of E and TB2 (Figure 12 vs. Figure 14 and Figure 15 vs. Figure 16), indicates that the production of E is much more sensitive to the flow rate than that of TB2. This flow rate effect, along with the different shapes of the E and TB2

curves, suggest that the production of E and TB2 follow different routes.

Since the production of TB2 is not sensitive to the carrier gas flow rate (Figures 12, 14, 15, and 16), a critical active site concentration for the production of TB2 can exist (can also exist for CB2 and 1-B). When the active site concentration for the production of TB2 is less than the critical value, the production of TB2 is not affected by the carrier gas flow rate. The production of TB2 with respect to the active site concentration may be illustrated by the following figure:

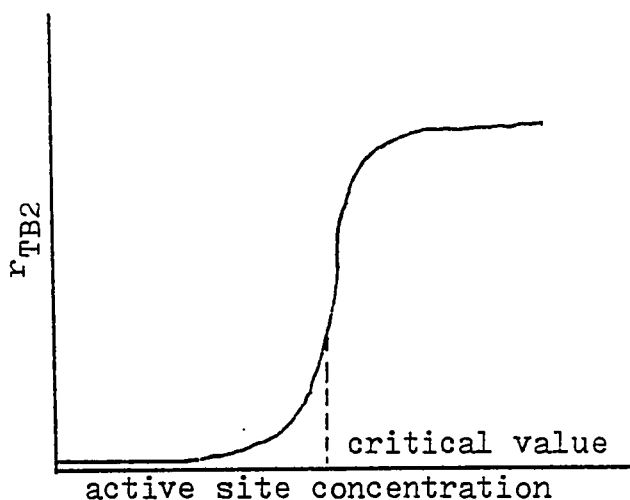


Fig. 26 Illustration of the critical active site concentration in the TB2 production

The value of E/B in the pulse study (Figures 12, 14, 15, and 16) is higher than that in the flow system study (Figure 2 and 3). This fact may be explained by the further reaction of E in the flow study because of the high surface

concentration on the catalyst, although the exact nature of this reaction is not yet known.

The irregular shape of the ethylene production curve in the pulse study (Figures 12, 14, 15, and 16) can be interpreted using the following factors: (1) Some kind of active site is generated after the oxygen regeneration. This active site better fits the production of ethylene; (2) Some surface oxygen may be replaced by olefins upon the injection of the reactant. This replacement depends on the temperature; (3) The catalyst is reduced by olefins to generate new active sites; (4) The adsorption of CO_2 may change the form of Bronsted acid to enhance catalyst activity while retarding the reduction process of the catalyst by olefins; (5) The produced ethylene may undergo further reaction; (6) The active sites generated by the reduction of the catalyst with olefins superimpose on the original active sites generated by oxygen activation and is illustrated in the following figure:

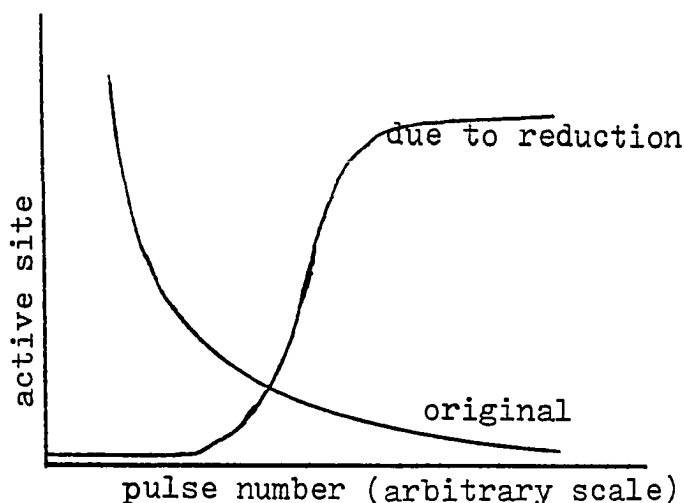


Fig. 27 The superimposition of active sites produced by oxygen regeneration and olefin reduction

The ethylene production curve in Figure 12 demonstrates the superimposition of the original active sites and the active sites generated by reduction. The E at the second pulse is less than that of the first pulse because the active sites generated by reduction can not make up for the consumption of the original active sites in time. After the reduction is completed, the E increases (pulses 3, 4, and 5 of the E curve in Figure 12). A comparison of the E curve in Figures 12 and 14 shows that the E produced decreases again at the fourth and fifth pulses in Figure 14. This decrease can be ascribed to the further reaction of E because of the slow flow rate. The decrease of E does not indicate the deactivation of the catalyst because the TB2 curve does not show a decrease.

Since the adsorption of CO_2 may change the structure of Bronsted acid to increase the activity, both the amount of E and TB2 produced increase with CO_2 pretreated catalyst as seen in Figure 12. However, the second maximum of the E curve shifts to the fourth pulse, which may be attributed to the slower reduction rate because of the adsorption of CO_2 .

The TB2 curve, unlike the irregular shape of the E curve, is a smooth curve in Figures 12 and 14 and is probably due to the existence of the critical value of the active site concentration for producing TB2. Since E predominates over TB2 at the beginning, the carbene mechanism more reasonably describes the reaction at the beginning. A carbene, left on

the catalyst after producing E, may be responsible for producing TB2. Therefore, the accumulated amount of carbene and the critical value of active site concentration produce a smooth curve for TB2.

The E curves in Figures 15 and 16 are similar to those in Figures 12 and 14 respectively. The major difference is in the first pulse. It is believed that the pumping of bulk phase oxygen before introducing the carrier gas leaves different amount of oxygen on the catalyst if the oxygen is pumped at different temperatures, and the lower the temperature the more oxygen left. Thus, if the reaction is carried out at 0°C, some portion of the first pulse will be spent in replacing certain types of surface oxygen as compared with the first pulse at 25°C. Such replacement causes the low production of E at the first pulse when the reaction is carried out at 0°C. After the first pulse, the shapes of the E curves are similar to those in Figures 12 and 14 (especially at slow flow rate) and may be explained as discussed in the last paragraph. The superimposition effect is not clear in Figure 15 because of the low activity at low temperature and high flow rate, which leaves some original active sites for the third pulse. Therefore, the amount of E produced at the third pulse does not drop sharply. In contrast to Figure 15, Figure 16 is the result of a slower flow rate, so more original active sites are spent at the second pulse causing a sharp drop of the E curve at the third pulse. Moreover, the slower flow rate

causes further reaction of the produced E of the fifth pulse.

VII-(C)

Based on the transalkylidenation type reaction, three reaction mechanisms were proposed(29): pairwise concerted, pairwise nonconcerted, and carbene. Furthermore, based on the transalkylidenation type reaction, four kinetic models were proposed(31): the Rideal model, the Langmuir-Hinshelwood one site model, the Langmuir-Hinshelwood two site model, and the carbene complex model.

Begley and Wilson(36) tested these models with experimental data and concluded that the Rideal model described their data better than the others. However, Wills et al.(37,38) concluded that the Langmuir-Hinshelwood two site model described their data best.

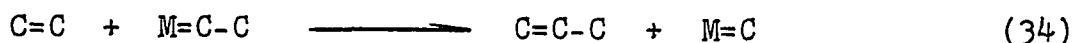
When propylene is used as a reactant, the amounts of produced ethylene and butenes should be equal if the reaction follows any one of the Rideal, Langmuir-Hinshelwood one site, or Langmuir-Hinshelwood two site models. If the reaction follows the carbene mechanism, the ethylene and butenes do not have to be equal. Although Wilson et al.(36) and Wills et al.(37,38) correlated their kinetic data with Rideal and Langmuir-Hinshelwood two site models respectively, it seems that they missed the initiation step if the reaction follows the carbene mechanism and this step is a fast reaction.

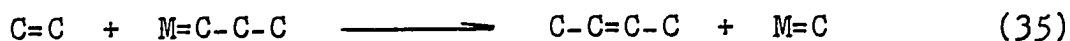
In the present work, the study using pulse technique

shows that the ratio of E to B is between 1.5 and 2.0 (Table 14, 15 and 16) in the first pulse, which suggests the existence of an initiation step which does not follow the Rideal model or the Langmuir-Hinshelwood models.

Further evidence for this fact is obtained from the surface titration study. This study proves that the reaction proposed by Rooney et al.(57) is not quite right. The reverse reaction can not occur because some species are taken away from the catalyst surface when an ethylene pulse is injected (Table 18), which is in contrast to what Rooney et al.(57) had proposed. Moreover, this reverse reaction is not thermodynamically allowed. Because the Gibbs free energy of formation of E and P are 16.282 Kcal/mole and 14.99 Kcal/mole(75) respectively, which cause a Gibbs free energy change of 6.29 Kcal per mole E produced and an equilibrium constant of 2.4×10^{-5} . Therefore, the high E/B value is not due to the production of three moles E from two moles P.

The surface titration study also resulted in two interesting relationships: (1) the number of moles of ethylene consumed is equal to the number of moles of propylene and butenes produced; (2) one times the number of moles of propylene plus two times the number of moles of butenes is approximately equal to the number of carbon atoms taken out of the catalyst. These relationships imply the carbene mechanism, which is illustrated as





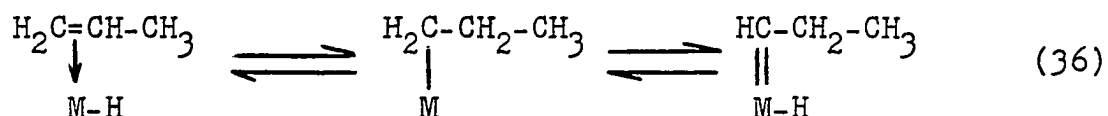
However, other possibilities can not be excluded without direct evidence for these reactions. The injection of the propylene pulse following the surface titration produces more ethylene than it should (pulse 7 of Table 19 vs. pulse 2 of Table 5 and pulse 10 of Table 20 vs. pulse 3 of Table 8). This fact may partially prove the existence of M=C on the catalyst after surface titration.

Figure 24 shows the TPD after the injection of four pulses of propylene and followed by the fifth pulse injection of propylene. The productions of E and TB2 of the fifth pulse are in opposite directions, i.e., E increases while TB2 decreases. This interesting result can again suggest that the productions of E and TB2 follow different routes and some kind of material left on the catalyst after TPD promotes the production of E. Probably, this left over material is M=C.

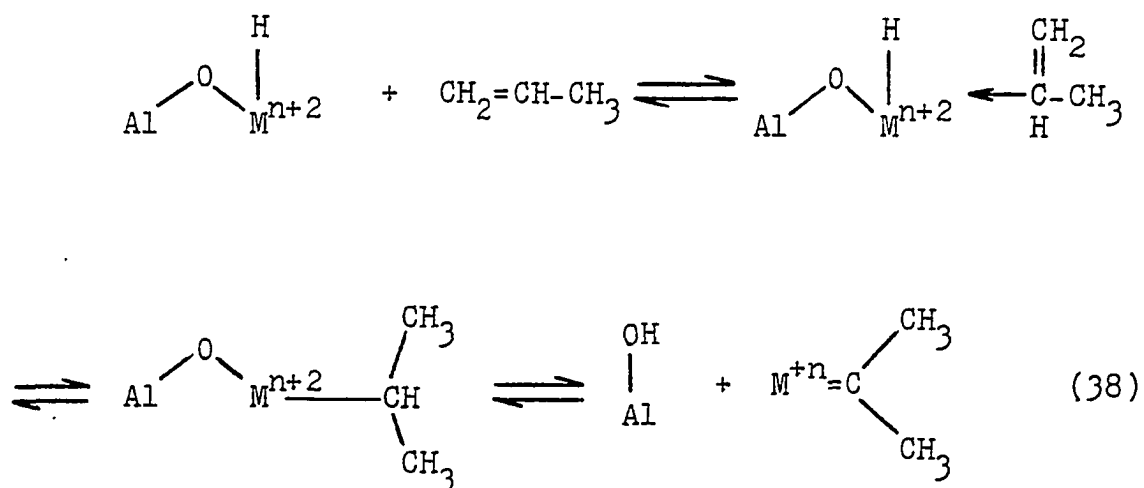
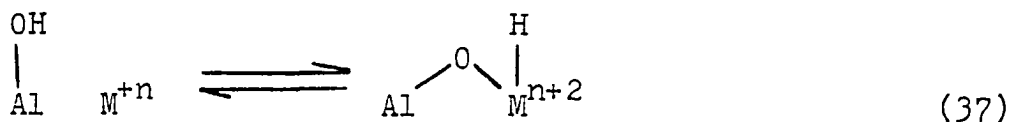
TB2 is also used as the reactant and the result shows that the major product is propylene. This fact is possible if the isomerization reaction occurs first to produce 1-B, followed by the metathesis reaction which occurs between 1-B and TB2 or CB2. However, if this assumption is correct, the amount of propylene and pentene produced should be equal, but this predicted result is not observed (Table 12 and 13). Therefore, the reaction must follow another mechanism although it is not yet certain.

The above discussions indicate that the metathesis reaction is better described by the carbene mechanism, although the mechanism for producing carbene is still in doubt.

Rooney et al.(35) proposed such a mechanism, when metal hydride is involved, as



Shmidt et al.(76) studied the metathesis with Tungsten-Alumina catalyst and proposed another mechanism for producing carbene as



The Bronsted acid adjacent to the active site is necessary for both of these two mechanisms. The present

work shows such effect by pretreating the catalyst with CO_2 . Therefore, consistent conclusions have been obtained regarding the importance of the Bronsted acid to the reaction.

According to the initiation step proposed by Burwell et al.(58)(see page 131), E is the major initial product and a carbene ($\text{M}=\text{C}$) is left on catalyst. The reaction of P with $\text{M}=\text{C}$ produces E and $\text{M}=\text{C}-\text{C}$, and next reaction of P with $\text{M}=\text{C}-\text{C}$ produces B and $\text{M}=\text{C}$. Thus, the productions of $\text{M}=\text{C}-\text{C}$ and $\text{M}=\text{C}$ are in a cyclic process and may explain the unity of E/B after a long reaction time in the flow study. The author would like to suggest that Bronsted acid is involved in the initiation step in addition to what Burwell et al.(58) proposed.

The other two mechanisms can not explain the product concentrations obtained in the present work, because the major products should be butenes and pentenes if the initiation step follows the mechanism proposed by Rooney; and the initial product should be iso-pentene and iso-butene if the initiation step obeys the mechanism proposed by Shmidt et al. Nevertheless, without direct evidence the mechanism generating carbene as chain carrier is still in doubt although Boelhouwer et al.(64) observed methylene from IR after $\text{Re}_2\text{O}_7/\text{Al}_2\text{O}_3$ was contacted with butene.

Comparing the result in the present work and the initiation mechanisms proposed by Burwell et al.(58), Rooney et al.(35), and Shmidt et al.(76), the author would like to suggest that the mechanism proposed by Burwell et al.(58)

along with the Bronsted acid effect is a reasonable one.

VIII. DETERMINATION OF KINETIC PARAMETERS FROM PULSE STUDY

Although it is difficult to obtain kinetic parameters from pulse study, it is possible to solve some simplified cases. This section discusses a simplified case with the following assumptions:

- (1) Mass transfer effects are negligible.
- (2) The axial dispersion is negligible.
- (3) The adsorption isotherm is a linear isotherm.
- (4) The adsorption reaches equilibrium rapidly.
- (5) The reaction rate is controlled by the surface reaction.
- (6) The reaction is first order and irreversible with respect to the reactant concentration.
- (7) The pulse is a delta function.

The material balance of the reactant A on the catalyst surface is derived as

$$(1-\alpha) \frac{\partial q_A}{\partial t} = Q_A - R_A \quad (39)$$

where α is the porosity, q_A is the concentration of reactant A per unit volume of the solid, R_A is the reaction rate, and Q_A is the rate of net input of A to the solid phase.

The material balance of the reactant A in the gas phase is derived as

$$v \frac{\partial C_A}{\partial x} + \alpha \frac{\partial C_A}{\partial t} + Q_A = 0 \quad (40)$$

where v is the carrier gas flow rate, x is the axial direction of the catalyst bed.

Since the adsorption isotherm is linear, Q_A may be written as

$$Q_A = k_A' C_A - k_A'' q_A = k_A' \left(C_A - \frac{q_A}{K_A} \right) \quad (41)$$

where k_A' , k_A'' , and K_A are adsorption, desorption and equilibrium rate constants respectively.

Substituting equation (41) into equations (39)(40) and obtain

$$(1-\alpha) \frac{\partial q_A}{\partial t} = k_A' \left(C_A - \frac{q_A}{K_A} \right) - R_A \quad (42)$$

$$v \frac{\partial C_A}{\partial x} + \alpha \frac{\partial C_A}{\partial t} + k_A' \left(C_A - \frac{q_A}{K_A} \right) = 0 \quad (43)$$

Substituting equation(42) into equation(43) and obtain

$$v \frac{\partial C_A}{\partial x} + \alpha \frac{\partial C_A}{\partial t} + (1-\alpha) \frac{\partial q_A}{\partial t} + R_A = 0 \quad (44)$$

The equilibrium constant may also be defined as

$$K_A = q_A / C_A. \quad (45)$$

Substituting equation(45) into equation(44) may

obtain

$$v \frac{\partial C_A}{\partial x} + \alpha \frac{\partial C_A}{\partial t} + (1 - \alpha) K_A \frac{\partial C_A}{\partial t} + R_A = 0 \quad (46)$$

Since the reaction is first order, equation (46) may be written as

$$v \frac{\partial C_A}{\partial x} + (\alpha + (1 - \alpha) K_A) \frac{\partial C_A}{\partial t} + k C_A = 0 \quad (47)$$

Furthermore, equation (47) may be written as

$$v_A \frac{\partial C_A}{\partial x} + \frac{\partial C_A}{\partial t} + \frac{k}{w_A} C_A = 0 \quad (48)$$

where w_A is $\alpha + (1 - \alpha) K_A$, and v_A is v/w_A .

Equation(48), along with the following initial and boundary conditions, may be solved by taking the Laplace transform.

$$\text{I.C.} \quad C_A(0, x) = 0 \quad (49)$$

$$\text{B.C.1} \quad C_A(t, 0) = C_A^0 \psi(t) \quad (50)$$

$$2 \quad C_A(t, L) \longrightarrow (\partial C_A / \partial x)_{x=L} = 0 \quad (51)$$

The solution of equation (48) is

$$\bar{C}_A = C_A^0 \exp\left(-\frac{kx}{v}\right) \exp\left(-\frac{sx(\alpha + (1 - \alpha) K_A)}{v}\right) \quad (52)$$

Equation(52) contains the reaction rate constant and the adsorption equilibrium constant, and these two constants

may be solved by using the Moment Analysis Method.

The nth moment in Laplace and time domain are defined as

$$M_n = (-1)^n \lim_{s \rightarrow 0} \left(\frac{d^n}{ds^n} \bar{C}_A \right) \quad (53)$$

$$M_n = \int_0^{\infty} C_A t^n dt \quad (54)$$

The nth moment in the Laplace domain may be calculated by substituting equation(52) into equation(53). The nth moment in the time domain may be calculated by substituting the breakthrough curve, which is recorded by mass spectrometer, into equation(54). Therefore, these two constants may be obtained by setting $M_n(\text{time domain}) = M_n(\text{Laplace domain})$ at two different times.

If the reaction is a second order irreversible reaction then equation(48) becomes

$$v_A \frac{\partial C_A}{\partial x} + \frac{\partial C_A}{\partial t} + \frac{k}{w_A} C_A^2 = 0. \quad (55)$$

This is a quasi-linear partial differential equation and can be solved with the characteristic method.

If the reaction is a first order irreversible reaction with axial dispersion then equation(48) becomes

$$\frac{1}{Pe} \frac{\partial^2 Y}{\partial \eta^2} = \frac{\partial Y}{\partial \eta} + \frac{\partial Y}{\partial \tau} + \beta Y, \quad (56)$$

where $Y = C_A/C_A^0$, $\eta = x/L$, $\tau = v_A t/L$, $\theta = L/v$, $\beta = \theta k$, and $Pe = Lv/D$.

Equation(56), along with the following initial and boundary conditions, can be solved by taking the Laplace transform.

$$\text{I.C. } \tau=0 \quad Y(0,\eta)=0 \quad (57)$$

$$\text{B.C.1 } \eta=0 \quad Y(\tau,0)=\psi(t) + \frac{1}{Pe} \left. \frac{\partial Y}{\partial \eta} \right|_{\eta=0} \quad (58)$$

$$2 \quad \eta=1 \quad \left. \frac{\partial Y}{\partial \eta} \right|_{\eta=1} = 0 \quad (59)$$

If the reaction is a second order irreversible reaction with axial dispersion then equation(48) becomes

$$D \frac{\partial^2 C_A}{\partial x^2} = v \frac{\partial C_A}{\partial x} + w_A \frac{\partial C_A}{\partial t} + k C_A^2. \quad (60)$$

This equation can be solved with the similarity method and the following conditions

$$\text{I.C. } t=0 \quad C_A(0,x)=0 \quad (61)$$

$$\text{B.C.1 } x=0 \quad C_A(t,0)=C_A^0\psi(t) + \frac{D}{v} \left. \frac{\partial C_A}{\partial x} \right|_{x=0} \quad (62)$$

$$2 \quad x=L \quad \frac{\partial C_A}{\partial x} = 0. \quad (63)$$

The advantage of the moment analysis method is to skip the step which takes the Laplace inverse, and it is an efficient method when the Laplace inverse is difficult to take.

The advantage of using the pulse technique to determine

the kinetic parameters is that only one experimental work is enough, but the disadvantage is that the order of the reaction and the rate determining step must be known. This disadvantage makes this application almost impossible.

CHAPTER V

CONCLUSION

The flow system kinetic study shows that the most stable activity occurs at 50°C reaction temperature and the highest activity at 100°C reaction temperature, if the catalyst ($\text{NH}_4\text{ReO}_4/\text{Al}_2\text{O}_3$) is regenerated by flowing oxygen for about 12 hours at about 500°C. CB2 is the initial product and the production of TB2 is restricted by the isomerization activity and steric effect. The produced ethylene reacts further more easily than butenes. The break-in period is observed at 0°C and probably will also be observed below 8°C. The break-in is due to the reduction by olefins and the formation of organometallic structure and the deactivation is due to poison by impurities, high molecular weight product, and coke. The deactivation and reaction rates are first order of the active site density. The break-in rate is first order of the adsorption active site density.

The standard catalyst, $\text{NH}_4\text{ReO}_4/\text{Al}_2\text{O}_3$, has the highest activity among the seven catalysts studied: $\text{NH}_4\text{ReO}_4/\text{Al}_2\text{O}_3$; $\text{NH}_4\text{ReO}_4/\text{TiO}_2$; $\text{NaReO}_4/\text{Al}_2\text{O}_3$; $\text{NH}_4\text{ReO}_4/13\text{X}(\text{Na})$ zeolite; $\text{NH}_4\text{ReO}_4/13\text{X}(\text{Ca})$ zeolite; $\text{NH}_4\text{ReO}_4/3\text{A}(\text{K})$ zeolite; and $\text{NH}_4\text{ReO}_4/3\text{A}(\text{Ca})$

zeolite. The sodium and potassium metals have a negative effect on the activity, regardless of whether NaReO_4 is used as promoter or the sodium or potassium containing zeolite is used as support. The catalyst has a better activity if the sodium and potassium in the zeolite are exchanged by calcium.

The formation of a mesoperrhenate structure with the participation of the promoter and support is important in stabilizing the catalyst and preventing loss of the promoter. The activity of a catalyst is a function of the acidity, the electrostatic field, the activity per unit area, the adsorption ability, the ratio of Al_2O_3 to SiO_2 when zeolite is used, and the formation of a mesoperrhenate structure. It is believed that the detailed explanation is more complicated than just considering these factors.

The activity of the studied catalysts is in the following order: $\text{NH}_4\text{ReO}_4/\text{Al}_2\text{O}_3 > \text{NH}_4\text{ReO}_4/3\text{A}(\text{Ca}) \text{ zeolite} > \text{NH}_4\text{ReO}_4/\text{TiO}_2 > \text{NH}_4\text{ReO}_4/13(\text{Ca}) \text{ zeolite} > \text{NaReO}_4/\text{Al}_2\text{O}_3 > \text{NH}_4\text{ReO}_4/13\text{X}(\text{Na}) \text{ zeolite}$. Although the catalysts with zeolite as support have lower activities than the standard catalyst, further study would be of value because the ratio of Al_2O_3 to SiO_2 can be changed and the electrostatic field and acidity can be adjusted by applying the ion exchange technique.

Since the ratio of E to B is higher than unity at the beginning and the reverse reaction of that proposed by Rooney et al.(57) is excluded, the carbene mechanism is more reasonable for describing the metathesis reaction, although the

mechanism for producing the chain carrier is still in doubt. The E/B value approaches unity after a long reaction time can be attributed to the cyclic production of the carbenes responsible for the productions of E and B. The other reactant, TB2, has also been tested by the pulse technique and the result shows that none of the Rideal, Langmuir-Hinshelwood one site, and Langmuir-Hinshelwood two site models can explain the product distribution, so the carbene mechanism is a more reasonable explanation.

Bronsted acid plays an important role in affecting the activity, because the yield is 6% higher if the catalyst is pretreated with CO_2 . The adsorption of CO_2 changes the structure of Bronsted acid and perhaps the acidity as well, and enhance the reaction. The mass balance indicates that the Bronsted acid affecting the reaction is adjacent to the adsorption site but not at the adsorption site. It is known that water is a poison to Lewis acid(anion vacancy) and NH_3 is a poison to both Lewis and Bronsted acids. Since water kills the activity completely, it is believed that Lewis acid is the major active site for metathesis and Bronsted acid adjacent to Lewis acid has promotion effect.

According to the three initiation mechanisms proposed by Burwell et al.(58), Rooney et al.(35), and Shmidt et al.(76) and the present study, the author would like to suggest that the mechanism proposed by Burwell et al.(58) along with the involvement of Bronsted acid is a reasonable explanation

for the initiation step.

The TPD chromatogram shows that the catalyst as well as the individual adsorption site are energetically heterogeneous. The TPD result also shows that oxygen on the catalyst is involved in the burning process of coke, so it is possible that some catalyst oxygen can be involved in reaction, although no evidence can support this postulate. Because of the complicated adsorption of a mixture, readsorption during TPD run, and migration of residue during TPD run, the exact value of the heat of desorption is difficult to obtain.

BIBLIOGRAPHY

1. Banks, R.L., and Bailey, G.C.; Ind.Eng.Chem., Prod. Res.Develop., 3, 170 (1964)
2. Bradshaw, C.P.C., Howman, E.J., and Turner, L.; J. Cat., 7, 269 (1967)
3. Calderon, N., Ofstead, E.A., Ward, J.P., Judy, W.A., and Scott, K.W.; J. Am. Chem. Soc., 90:15, 4133 (1968)
4. Bailey, G.C.; Cat. Rev. 3(1), 37 (1969)
5. Luckner, R.C., and Wills, G.B.; J. Cat. 28, 83 (1973)
6. Kobylinski, T.P., and Swift, H.E.; J. Cat. 33, 83 (1974)
7. Davie, E.S., Whan, D.A., and Kemball, C.; J. Cat. 24, 272 (1972)
8. Davenport, W.H., Kollonitsch, V., and Kline, C.H.; Ind. & Eng. Chem. 60(11), 10 (1968)
9. Yao, H.C., and Shelef, M.; J. Cat. 44, 392 (1976)
10. Moffat, A.J., Clark, A., and Johnson, M.M.; J. Cat. 22, 379 (1971)
11. Lin, C.J., Aldag, A.W., and Clark, A.; J. Cat. 45, 287 (1976)
12. Moffat, A.J., and Clark, A.; J. Cat. 17, 264 (1970)
13. Edreve-Kardjieva, R., and Andreev, A.; React. Kinet. Catal. Lett. 5(4), 465 (1976)
14. Pennella, F., and Banks, R.L.; J. Cat. 31, 304 (1973)
15. Giordano, N., Padovan, M., Vaghi, A., Bart, J.C.J., and Castellan, A.; J. Cat. 38, 1 (1975)
16. Andreev, A.A., Edreva-Kardjieva, R.M., and Neshev, N.M.; J. Roy. Neth. Chem. Soc., 96, M23 (1977)
17. Nechitailo, A.E., and Fridman, R.A.; J. Cat. 45, 114 (1976)

18. Shirpo, E.S., Avaev, V.I., Antoshin, G.V., Ryashentseva, M.A., and Minachev, K.M.; J. Cat. 55, 402 (1978)
19. Marvin, F.L., and Leroy, V.M.; J. Cat. 35, 434 (1974)
20. Nakamura, R., and Echigoya, E.; J. Roy. Neth. Chem. Soc. 96, M31 (1977)
21. Giordano, N., Bart, J.C.J., Vaghi, A., Castellan, A., and Martinotti, G.; J. Cat. 36, 81 (1975)
22. Kobylinski, T.P., and Swift, H.E.; J. Cat. 26, 416 (1972)
23. Ozaki, A., and Kimura, K.; J. Cat. 3, 395 (1964)
24. Brouwer, D.M.; J. Cat. 1, 22 (1962)
25. Engelhardt, J.; J. Roy. Neth. Chem. Soc. 96, M101 (1977)
26. Lombardo, E.A., Jacono, M.L., and Hall, W.K.; J. Cat. 51, 243 (1978)
27. Vannice, M.A., Garten, R.L.; J. Cat. 56, 236 (1979)
28. DeVries, J.L.K.F., and Pott, G.T.; J. Roy. Neth. Chem. Soc. 96, M115 (1977)
29. Mol, J.C., and Moulijn, J.A.; Adv. Cat. 24, 131 (1975)
30. Hsu, J.C.; Ph.D. Dissertation The Effect of Catalyst Pretreatment on the Olefin Metathesis Catalyzed by Alumina Supported Rhenium Oxide, University of Oklahoma (1979)
31. VanRijn, F.H.M., and Mol, J.C.; J. Roy. Neth. Chem. Soc. 96, M96 (1977)
32. Clark, A., and Cook, C.; J. Cat. 15, 420 (1969)
33. Grubbs, R.H., and Brunck, T.K.; J. Am. Chem. Soc. 94:7 2538 (1972)
34. Grubbs, R.H., Carr, D.D., Hoppin, C., and Burk, P.L.; J. Am. Chem. Soc. 98:12, 3478 (1976)
35. Laverty, D.T., Rooney, J.T., and Stewart, A.; J. Cat. 45, 110 (1976)
36. Begley, J.W., and Wilson, R.T.; J. Cat. 9, 375 (1967)
37. Luckner, R.C., McConchie, G.E., and Wills, G.B.; J. Cat. 28, 63 (1973)

38. Lewis, M.J., and Wills, G.B.; J. Cat. 15, 140 (1969)
39. Furusawa, T., Suzuki, M., and Smith, J.M.; Cat. Rev. 13(1), 43 (1976)
40. Hattore, T., and Murakami, Y.; Cana. J. Chem. Eng. 52, 601 (1974)
41. Hattori, T., and Murakami, Y., J. Cat. 10, 114 (1968)
42. Murakami, Y., Hattori, T., and Hattori, T.; J. Cat. 10, 123 (1968)
43. Hattori, T., and Murakami, Y.; J. Cat. 12, 166 (1968)
44. Hattori, T., and Murakami, Y.; J. Cat. 31, 127 (1973)
45. Hattori, T., and Murakami, Y.; J. Cat. 33, 365 (1974)
46. Amenomiya, Y., and Cvetanovic, R.J.; Cat. Rev. 6(1), 21 (1972)
47. Amenomiya, Y., and Cvetanovic, R.J.; Adv. Cat. 17, 103 (1967)
48. Grant, W.A., and Carter, G.; Vacuum 15, 13 (1965)
49. Tokoro, Y., Uchijima, T., and Yoneda, Y.; J. Cat. 56, 110 (1979)
50. Amenomiya, Y., and Cvetanovic, R.J.; J. Phys. Chem. 67, 144 (1963)
51. Amenomiya, Y., and Cvetanovic, R.J.; J. Phys. Chem. 67, 2705 (1963)
52. Amenomiya, Y., and Cvetanovic, R.J.; J. Phys. Chem. 67, 2046 (1963)
53. Munuera, G.; J. Cat. 18, 19 (1970)
54. Amenomiya, Y., and Cvetanovic, R.J.; J. Cat. 18, 329 (1970)
55. Lin, C.J., Ph.D. Dissertation Kinetics and Mechanism of the Olefin Disproportionation Reaction Over Supported Rhenium Oxide Catalysts, University of Oklahoma (1975)
56. Ismayel-Milarovic, A., Basset, J.M., Praliand, H., Dufaux, M., and DeMourgues, L.; J. Cat. 31, 408 (1973)

57. O'Neill, P.P., and Rooney, J.J.; J. Am. Chem. Soc. 94:12, 4383 (1972)
58. Brenner, A., and Burwell, L. Jr.; J. Cat. 52, 364 (1978)
59. Sodesawa, T., Ogata, E., and Kamiya, Y.; Bull. Chem. Soc. Japan, 50(4), 998(1977)
60. Turkevich, J.; Cat. Rev. 1(1), 1 (1967)
61. Tung, S.E., and McIninch, E.; J. Cat. 10, 166 (1968)
62. Ward, J.W., and Hansford, R.C.; J. Cat. 13, 363 (1969)
63. Moscou, L., and Lakeman, M.; J. Cat. 16, 173 (1970)
64. Olsthoorn, A.A., and Boelhouwer, C.; J. Cat. 44, 197 (1976)
65. Olsthoorn, A.A., and Boelhouwer, C.; J. Cat. 44, 207 (1976)
66. McCarth, J., and Madix, R.J.; J. Cat. 38, 402 (1975)
67. Boudart, M.; Kinetics of Chemical Processes, Prentice-Hall, Inc., (1968)
68. Parkyns, N.D.; J. Phys. Chem. 75, 526 (1971)
69. Knozinger, H.; Adv. Cat. 25, 184 (1976)
70. Peacock, J.M., Sharp, M.J., Parker, A.J., Ashmore, P.G., and Hockey, J.A.; J. Cat. 15, 379 (1969)
71. Aris, R.; Chem. Eng. Sci. 6, 262 (1957)
72. Satterfield, C.N.; Mass Transfer in Heterogeneous Catalysis, M.I.T. Press (1970)
73. Ward, J.W.; J. Cat. 10, 34 (1968)
74. Hall, W.K., and Jacono, M.L.; J. Colloid and Interface Sci. 58, No.1 (1977)
75. Daniels, F., Alberty, R.A.; Physical Chemistry, John Wiley & Sons, Inc. 2nd ed. (1963)
76. Shnidt, F.K., Grechkina, YE.A., Levkovskii, Yu.S., Shmidt, O.I., and Lavrent'yeva, V.B.; Petro. Chem. USSR 18, 1 (1979)